Republic of Iraq
Ministry of Higher Education and Scientific Research
University of Misan/College of Engineering
The Department of Civil Engineering

MOMENT REDISTRIBUTION ASSESSMENT IN CONTINUOUS REINFORCED CONCRETE BEAMS OF HYBRID SECTION

By

Dhuha Kareem Hassan

A thesis submitted in partial fulfillment
of the requirements for the Master of Science
degree in Civil Engineering
University of Misan

April2022

Thesis Supervisors: Prof. Dr. Saad Fahad Resan
Assist. Prof. Dr. Hayder Al-Khazraji

﴿ وَلَقَدْ آتَيْنَا دَاوُودَ وَسُلَيْمَانَ عِلْمًا ۖ وَقَالَا الْحَمْدُ لِلَّهِ الَّذِي فَضَّلَنَا عَلَىٰ كَثِيرٍ مِنْ عِبَادِهِ الْمُؤْمِنِينَ ﴾

سورة النمل الآية 15

صدق الله العلي العظيم

DEDICATION

I dedicate my research to whom no one can compare them at universe,

To whom GOD has commanded us to honor them,

To those who have given a lot,

And who have put forward what cannot be returned

My patents

To my brothers and sister,

To everyone who gave me a support in my scientific journey

ACKNOWLEDGEMENTS

In the Name of Allah…

First, I would thank my GOD for granting me success to finish this work, which is a dream for me and my family.

The path towards this thesis has been circuitous. For its completion thanks go to the special people who challenged, supported, and stuck with me along the way.

Foremost, I want to offer this endeavor to our GOD who helped me and enabled me to complete this research.
I would like to express my special gratitude and thanks to my supervisors Prof. Dr. Saad Fahad Resan and Assis. Prof. Dr. Hayder Al-Khazraji for help, encouragement and extend their support during the work.

I would like to extend my thanks to Professor Dr. Abbas O. Dawood Dean of the college of engineering and Assistant Professor Dr. Samir Mohammed Chasib; head of Civil Engineering Department and to all my teachers in my college.

Much gratitude to my father how didn't leave me all the time of the work.

Special thanks and gratitude are due to my family for enduring me throughout the years of my studies, to love and support them for the rest of my life. Also special thanks to my closer friends.

ABSTRACT

The concept of moment redistribution is utilized by the design of statically indeterminate structures to reduce the absolute magnitudes of moments in critical areas, completely use the capacity of non-critical cross sections, and simplify detailing by allowing a reduction in reinforcement ratios.

The current study intends to use moment redistribution concept besides the smart utilization of concrete strength to develop the continuous reinforced concrete beams which used by hybrid concrete of normal (lower and upper) limit strength grades (20 and 60) MPa in addition to investigates the effectiveness of introduced hybrid modes upon moment redistribution and related issues such as strength capacity, flexural stiffness, flexural ductility, section rotation capacity, plastic hinge formation and mechanism.

This research presents an experimental investigation, consisting of developing and testing twelve rectangular continuous reinforced concrete beams of 3000 mm length and cross-section (120×200). Four of tested beams are control beams, two of them were homogeneous cross-section with compressive strength (20 and 60) MPa respectively, and the other adopted as developed beams of hybrid strength (two layers) with compressive strength fashions (60/20 and 20/60) respectively. Other beams got changing strength capacity to be compatible with the actual moment redistribution. Three section enhancement strength rates (R) within beam midspan are considered which are 0%, 15% and 30%, the rates are corresponding with section reduction rates within middle support.

The results clearly show that, for both modes, the moment capacity tends to increase with enhancement rate increasing and the best improving is corresponding to those of hybrid mode II as the comparing rates of Mode I in respect to Mode II are vary between 1.06 to 0.869. The enhancement ratio affects the load–deflect response for both adopted hybrid modes. The specimens of R=0 do not get difference while the

significant divergence indicated for R=30. The same observation is indicated for the mid span and at the inner quarter of the span. The results depict that the hybrid specimens of Mode II get better than the corresponding specimens of Mode I in scope of flexural stiffness, while the flexural ductility is improved as enhancement rating increased with relative more improving for specimens of mode II, while the improving rating tends to be matched for higher enhancement rate (30%). Besides, the increasing of enhancement ratio companied with significant plastic rotation capacity improving. The hybrid specimens of Mode II, extremely better than the corresponding specimens of Mode I, in scope of provided plastic rotation capacity, the comparing rates vary between 0.353 and 0.329.

Generally, the merging of moment-redistribution trend in R.C. continuous beams, with the fully hybrid strength section could be considered as a technique to reduce the overall design cost without scrapped the required structural characteristics. And the hybrid strength modes in RC beams which based on reducing the strength in some region and increasing it in other region could be also useful likewise steel reinforcement re-assigning.

TABLE OF CONTENTS

LIST OF TABLES

LIST OF FIGURES

LIST OF SYMBOLES

$f_{c`}$ Cylinder concrete compressive strength in MPa

f_{cu} Cube Compressive Strength in MPa

ϵ_c Concrete strain

$\emptyset$ Diameter of reinforcement mm

C Depth of crack block mm

D Ductility index

θ Enhancement or reducing moment resistance ratio

R Enhancement or reducing moment resistance ratio

T Energy dissipation j/cm^3

λ Flexural stiffness

q_m Improving moment redistribution at mid span

f_r Modulus of rupture in MPa

q Moment redistribution ratio

L_P Plastic hinge length mm

M_{Pm} Plastic moment at mid span kN.m

M_{Ps} Plastic moment at middle support kN.m

q_s Reducing moment redistribution at middle support

f_t Tensile strength in MPa

$\mathcal{E}_P$ The increase in strain in the concrete measured from the initial yielding of steel reinforcement in the section

M_{um} Ultimate moment at mid span kN.m

M_{us} Ultimate moment at middle support kN.m

Δ_u Ultimate deflection in mm

f_y Yield strength in MPa

Δ_y Yield deflection in mm

ABBRIVATION

ASTM	American Society for Testing and Materials
BS	British Standard
BFRP	Basalt fiber reinforced polymer
CTLB	Continuous two-layer beam
CFRP	Carbon Fiber Reinforced Polymer
HSC	High Strength Concrete
HYSC	Hybrid strength concrete
GFRP	Glass Fiber Reinforced Polymer
NSC	Normal strength concrete
R.O	Reverse Osmosis
RC	Reinforced Concrete
RPC	Reactive powder concrete
SP	Superplasticizer
TLB	Two-layer beam
UHPFRC	Ultra-high performance fiber reinforced concrete
W/C	Water to Cement ratio

CHAPTER ONE: INTRODUCTION

1.1 General

Smart section area distribution and appropriate strength selection are the key parts in the design philosophy for cost-effective structural members. The main elements for the success of any project are durability, cost, and construction time, as well as understanding the factors of complexity. The use of these features in each part of the project reduces the cost of construction while also reducing the time it takes to complete. Additionally, the concrete members are the most essential components of the construction project, and enhancing their properties, increasing their strength, using additives certain, and simple construction methods contribute effectively to the project's success [1].

Concrete is produced in average of 10 billion tons a year, and demand for the product is expected to increase to 18 billion tons by 2050 [2]. Among many methods of improving the properties of concrete are those that related to increasing its strength by using additives [3] as well as implementing them in certain forms that are appropriate to the facility on the other hand, which contributes to the increase durability in general, while the use of hybrid concrete contributes effectively to reduce the constructions cost [4].

The fundamental drawback of simply supported reinforced concrete beams, is the relative large moments in the span, which result in large deflections and extensive cracking [5]. Furthermore, because there is no internal moment redistribution in simple statically determinate reinforced concrete structures, the load bearing capacity of the structure is determined by the section where the moment is maximum. A solution to this problem is the use of continuous (statically indeterminate) RC structures that allow reduction of the maximum moment and

deflection. In continuous beams, the moments above the supports and those in the span are redistributed, permitting the use of typical longitudinal reinforcement.

1.2 Continuous Concrete Beams

Continuous beam is a beam that is supported by more than two supports, these beams are statistically indeterminate and are known as Redundant or Indeterminate Structures as they cannot be analyzed by making use of basic equilibrium which give continuity in the different elements Figure 1.1. The advantage of continuous beams that had more vertical load capacity can support a very heavy loads and deflection at the middle of the span is minimal as opposed to simple supported beams [6].

Slabs, beams, columns, and footings are examples of structural members used in reinforced concrete structures. These structural elements may be produced in separate units as precast concrete slabs, beams, and columns. Unless some form of continuity is given at their ends, precast units are intended as building elements on simple supports. Beams are structural elements that sustain loads that are applied transversely to the beam axis, causing shear and bending stresses. Concrete beams are usually continuous, meaning they span many supports and act as a single structural element. Because the rebars are located continuously through the supports, they provide a mechanism for stress transmission between adjacent spans. For continuous member, it prefers to using principal of moment redistribution in regions of maximum bending moment. Figures 1.2 show continuous concrete structure and continuous beam.

Figure 1.1 Continuous member [6]

Figure 1.2 Structural members of reinforced continuous concrete buildings [7]

1.3 Moment Redistribution in Continuous Concrete Beams

Moment redistribution is a particular behavior observed in statically indeterminate reinforced concrete structures as a result of structural redundancy and nonlinear reinforced concrete characteristics. Consideration of moment redistribution in practical design is an efficient approach to complete use the reserve capacity of the materials and also providing convenience for construction [8]. The objective of moment redistribution is to distribute bending moments away from peak moment regions, such as beam column joints or continuous member supports. This decreases the congestion of reinforcing bars in such regions and makes structural members easier to construct and detail. Equilibrium must be maintained, that's mean if the bending moments are reduced in certain portions, they must be raised in other sections [9]. To prevent an excessive demand on the ductility of a structural member, 15% moment redistribution is normally to be taken as a reasonable limit, though certainly BS 8110 permits up to 30% moment redistribution.

The ability of a reinforced concrete flexural member to redistribute moment is the most basic application of member ductility. Even for this relatively simple problem,

national standards (BSI, 1995; CSA, 1994; German Institute of Standardisation, 1997; International System of Unified Standard Codes of Practice for Structures, 1990; Standards Australia, 1994) resort to what appears to be empirical solutions for deriving the percentage moment redistribution. These are based on the neutral axis depth factor k_u (the depth to the neutral axis as a proportion of the effective depth) as shown in Figure 1.3 (where K_{MR} is the moment redistributed as a proportion of its original value) and which themselves vary widely [10].

The difficulty of quantify moment redistribution originates from a highly complicated problem that has been recognized for over 40 years [11]. The fundamental concept of moment redistribution shown in Figure 1.4.

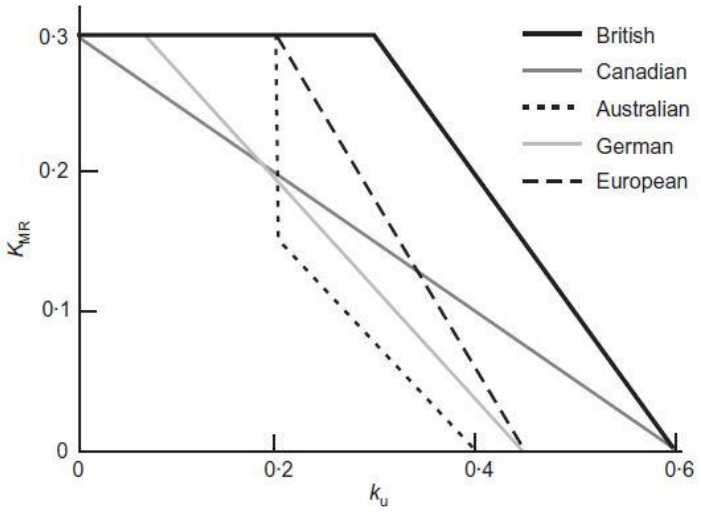

Figure 1.3 Allowable moment redistribution in codes worldwide [10]

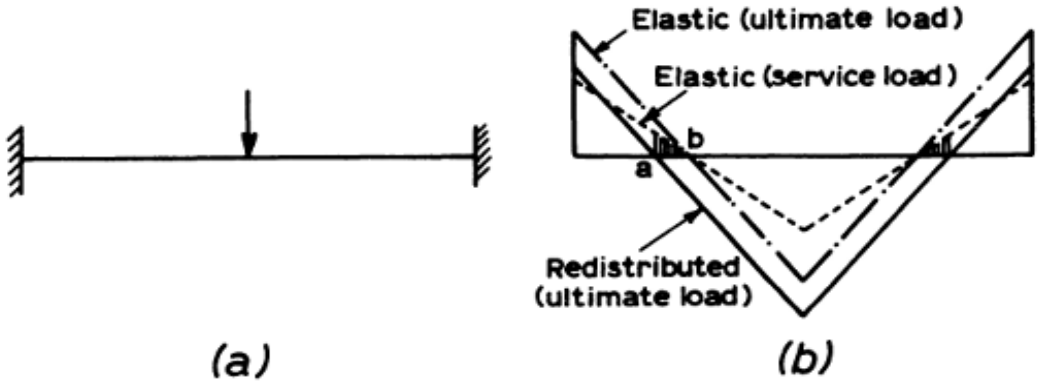

Figure 1.4 The fundamental concepts of moment redistribution [9]

While the limitation of moment redistribution according to ACI code were:

Moment redistribution of maximum positive or negative moments in continuous flexural members is based on the net tensile strain, ε_t, for both;

- Reinforced concrete members.
- Prestressed concrete members

2- The shown Figure shows the permissible limits on moment redistribution. It indicates that the percentage, q', calculated by the elastic theory, must not exceed (1000 ε_t) %, with maximum of 20%, as shown in Figure 1.5

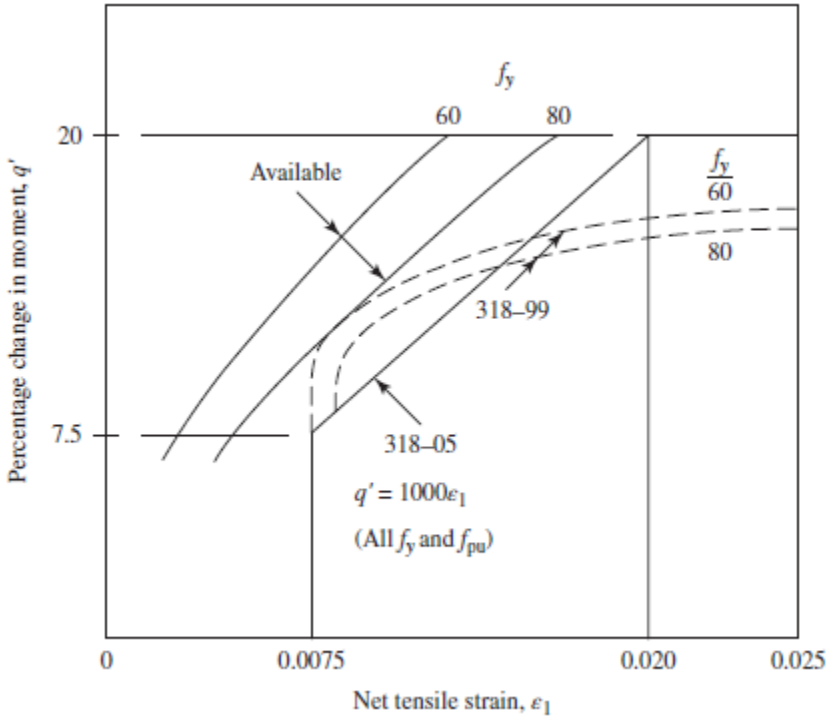

Figure 1.5 Permissible moment redistribution for minimum rotation capacity courtesy of ACI-PCA [17]

3- Moment redistribution is allowed only when $\varepsilon_t \geq 0.0075$, indicating adequate ductility is available at the section at which moment is reduced.

4- When $\varepsilon_t < 0.0075$, no moment redistribution is allowed.

5- The modified negative moments must be used to calculate the modified positive moments within the span, ACI Code, Section 6.6.5.1.

6- Moment redistribution does not apply to members designed by the direct design method for slab systems [17].

In summary, the percentage of decrease in maximum negative or positive moments in continuous beams (q`) is as Equation 1.1 and as the follows:

1. When $\varepsilon_t \geq 0.0075$, moment redistribution is allowed ($\rho/\rho_b > 0.476$)
2. When $\varepsilon_t = 0.0075$, the percentage of moment redistribution is 75% ($\rho/\rho_b = 0.476$)
3. When $\varepsilon_t = 0.020$, the percentage of moment redistribution is 20% ($\rho/\rho_b = 0.217$)
4. When $0.0075 < \varepsilon_t < 0.020$, the percentage of moment redistribution is

$$q` = 1000\ \varepsilon_t \qquad 1.1$$

For example, if $\varepsilon_t = 0.010$, then the percentage of moment redistribution is 10%.

The relationship between the steel percentage, ρ, in the section and the net tensile strain, ε_t shown in Equation 1.2:

$$\varepsilon_t = \frac{0.003 + {f_y}/{E_s}}{{\rho}/{\rho_b}} - 0.003 \qquad 1.2$$

Moment redistribution factor, q, based on the ACI Code 318-02 is calculated as shown in Equation 1.3

$$q = 20\left(1 - \frac{\rho - \rho`}{\rho_b}\right) \qquad 1.3$$

In above eq., the code limits the steel ratio ρ or ρ –ρ' at the section where the moment is reduced to a maximum ratio of 0.5 ρ_b.

1.4 Hybrid Strength Reinforced Concrete Beam

A concrete made up of more than one type of concrete is known as (hybrid concrete strength). Hybrid concrete beams have multiple concrete strength layers to increase resistance and improve performance [12]. Many research has focused on them, using a variety of concrete types or the same concrete type with a variety of additions, such as steel fiber. The usage of hybrid concrete is motivated by the need to reduce building costs. Figure 1.5 shown hybrid section of beam of high and normal strength [13].

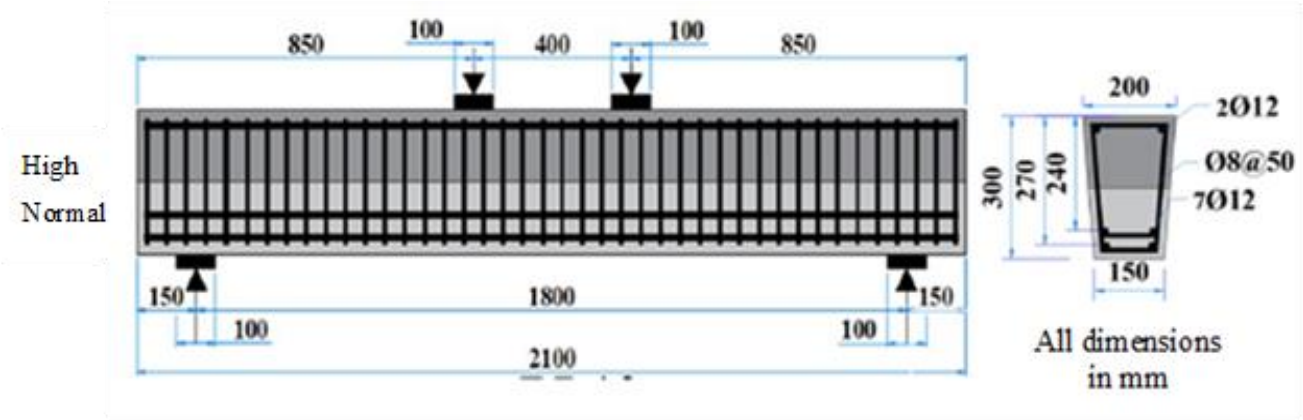

Figure 1.6 Hybrid section of tested specimen [13]

A hybrid section is a structural concrete section that consists of both new and old concrete layers. The expansion of the hybrid concept of composite concrete member as well as concrete technology advancements have allowed the production of composite section showing high compressive strength, high ductility, high absorption, and high tensile strength.

Multiple concrete layers of various types have been integrated in such away that they all contribute the optimal usage to achieve the above-mentioned properties [14]. Engineers have recently become interested in hybrid reinforced concrete buildings because of its lower cost and superior performance under load.

1.5 Plastic Hinge

It is well established that the inelastic behavior of Reinforced Concrete (RC) sections leads to a redistribution of moments and forces, resulting in an increased load carrying capacity of the members and the indeterminate structure [15]. As the applied load is increased, hinges start forming in succession at locations where the hinge moment capacity is reached; with further increase in the applied load, these hinges continue to rotate until the last hinge forms converting the structure into a mechanism resulting in failure.

As a result, structural experts and designers have been fascinated by this zone for decades. The length of the plastic hinge zone is a critical design parameter where strong confinement must be supplied to increase member ductility in order to endure extreme occurrences such as earthquakes [16]. Quantifying the moment-rotation capacity of a hinge in a reinforced concrete member such as that shown in Figure 1.6 [17].

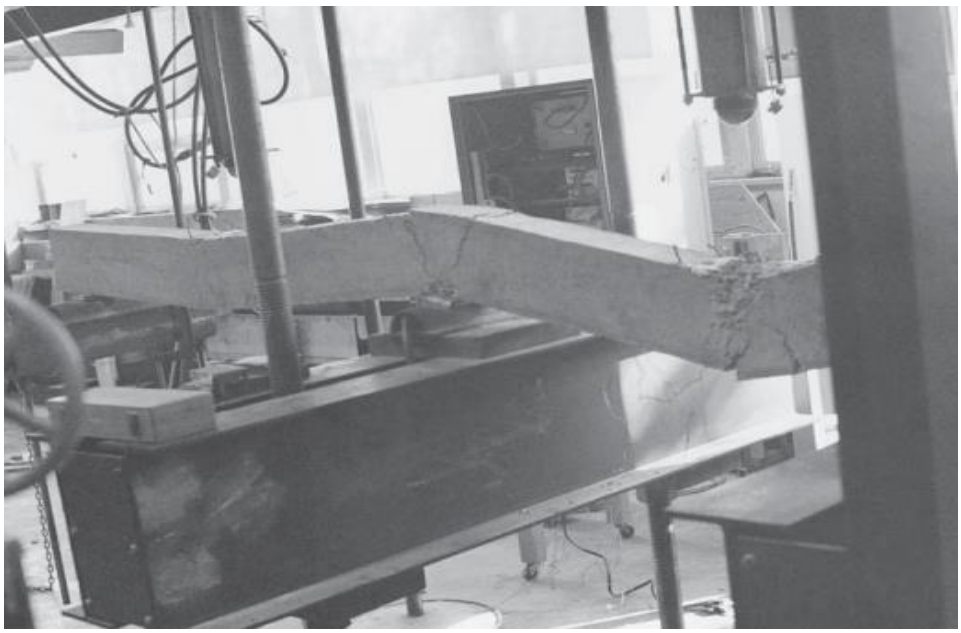

Figure 1.7 Plastic hinges developed in the positive and negative maximum moment regions [17]

Plastic hinge within the beam and at the support with the diagram of stress strain shown in Figure 1.7 [17]. The mechanism of the beam as shown in Figure 1.8 where illustrate the development of the plastic hinge [17].

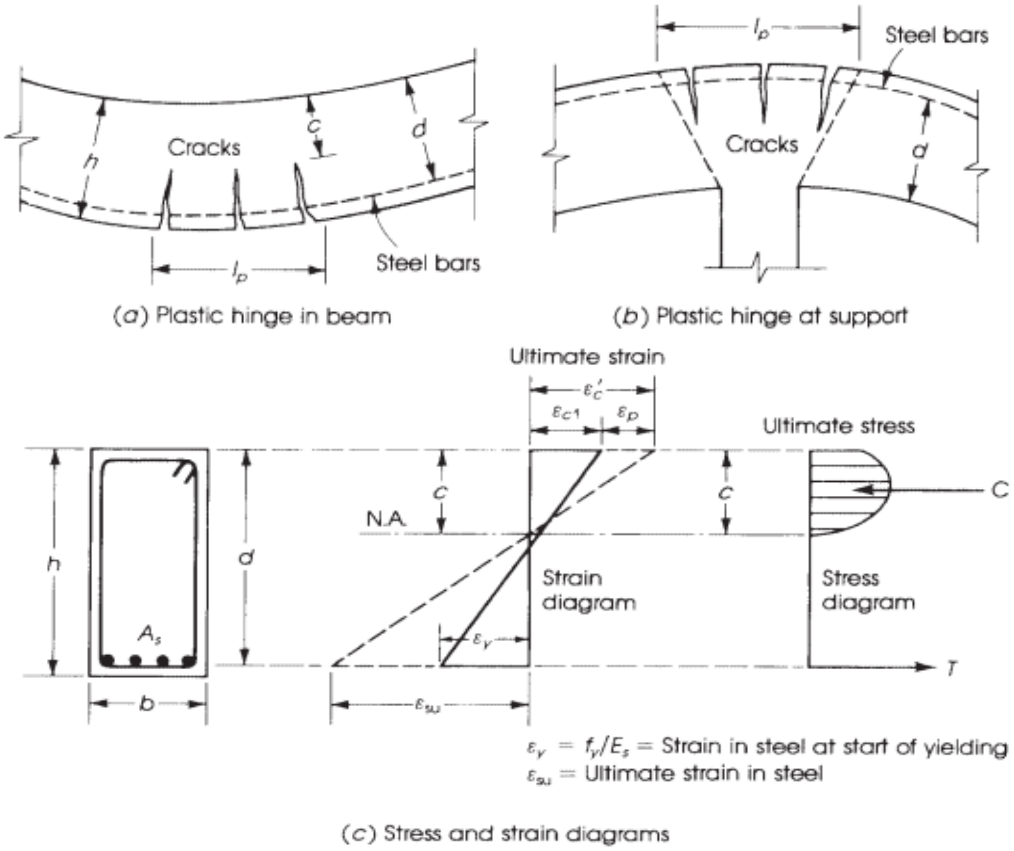

Figure 1.8 Plastic hinge and typical stress and strain distribution [17]

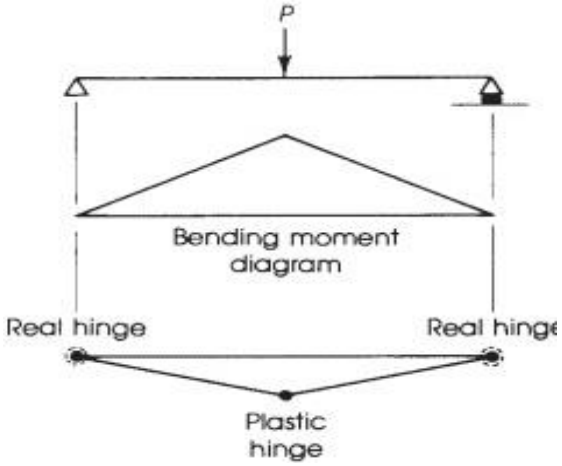

Figure 1.9 Development of plastic hinges [17]

1.6 Objectives of the Study

The thesis aims to:

1. Strength capacity and moment redistribution regards continues reinforced concrete beams of developed hybrid section strength are investigated. Normal compressive concrete strength are utilized within various hybrid section fashions which are complained by mid span section strength enhancement besides section strength reduction in middle support region so as to investigate moment redistribution.
2. Experimenting to improve overall understanding of the behavior of a structure made up of two types of concrete and then verifying the hybrid concrete for its applicability as a structural concrete beam.

1.7 Layout of the Thesis

This thesis is divided into five chapters which can be clarified as follows:

1. **Chapter one:** It is the introduction chapter that including the introduction of moment redistribution in continuous concrete beams, the hybrid strength concrete beams and high strength concrete.
2. **Chapter Two**: It concerns with the literatures review that present the theories of moment redistribution in continuous concrete beams of rectangular section, as well as, the impotence of hybrid beams.
3. **Chapter Three:** It is the experimental work chapter that comprises a brief description about the tests carried out during the investigations of the materials in the laboratory along with the detailed procedures.
4. **Chapter Four:** It deals with the experimental results and discussion chapter, and the comparing results of hybrid beams with the conventional concrete beams.

5. **Chapter Five:** It is the conclusions and recommendations chapter that summarized the overall outcome of the experimental work of this thesis and the several suggestions for further studies.

CHAPTER TWO: LITERATURE REVIEW

2.1 Introduction

The experimental investigation of moment redistribution in continuous concrete beams of hybrid strength rectangular section beams was the core of this research. This chapter summarizes the previous research on moment redistribution in continuous concrete beams and hybrid compressive strength beams.

2.2 Redistribution Moment in Continuous Concrete Beam

Lin and Chien in 2000 [18] introduced the effect of section ductility on moment redistribution of continuous concrete beams as shown in Figure 2.1. Both analytical and experimental methods were employed. The major factors used in this study were the amount of transverse reinforcement, the amount of tensile reinforcement, the amount of reinforcement of the compression and the strength of concrete. It's based on a total of twenty-six beam specimens in his experimental work where dimensions are (6400×200×300) mm. The comparison of analytical and experimental results showed that the analytical results acceptable to that of experimental. It indicates that decrease of tensile reinforcement and increase of compression reinforcement will increase ductility and cause more moment redistribution. The findings also revealed that transverse reinforcement has better confining effects and causes considerable redistribution of the moment.

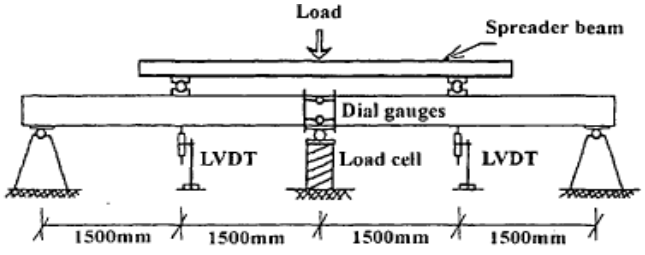

Figure 2.1 Test setup [18]

Maghsoudi and Bengar in 2009 [19] investigated moment redistribution and ductility of reinforced high strength concrete RHSC continuous beams strengthened with carbon fiber reinforced polymer CFRP. In terms of enhancement of moment and load capacity, moment redistribution, and various forms of ductility, the study examined the responses of RHSC continuous beams. Experimental work based on tested five reinforced concrete two span beams with overall dimensions equal to (250×150×6000) mm. One as a control beam and four high strength reinforced concrete beams strengthened with externally bonded carbon fiber reinforced polymer sheets on the tension face. The main parameters investigated were the thickness of carbon FRP (CFRP) sheets, strengthening of both the hogging and sagging field and the end of anchorage technique. Ultimate strength increased by increasing the number of CFRP sheet layers. While ductility, moment redistribution, and ultimate strain on CFRP sheets decreased. In addition, ultimate strength and moment redistribution was improved by using end anchorage. The moment redistribution ratio significantly decreased from 16.06 to 1.51 by increasing the number of CFRP layers.

Oehlers et al. in 2010 [10] studied moment redistribution in reinforced concrete beams. The significance of ductility in the construction of reinforced concrete structures and as a result, the importance of ductility has long been recognized by structural engineers. The value of a reinforced concrete member's ability to redistribute moment to give prior warning of failure, adjust the structural response to allow changes in applied load and column drift, and absorbed energy during earthquake, blast and other dynamic loadings. By applying the model of moment-redistribution capacity, this research has shown that with increasing bar diameter, concrete confinement and bar fracture strain, the moment-redistribution capacity increases and decreases with increasing bond strength.

Akbarzadeh and Maghsoudi in 2010 [20] in experimental and analytical investigation of reinforced high strength concrete continuous beams strengthened with fiber reinforced polymer discussed the flexural behavior and moment redistribution of reinforced high strength continuous concrete beams strengthened with carbon fiber reinforced polymer and glass fiber reinforced polymer sheets. Five wide continuous two span beams of dimensions (150×250×6000) mm were tested up to failure on the control beam and four strengthened reinforced high strength concrete beams with externally bonded carbon fiber CFRP and glass fiber GFRP reinforced polymer sheets on the concrete tension faces, a concentrated load was applied to the beams in the middle of each span. The result showed that the ultimate strength of CFRP sheets increases as the number of layers increases, while ductility, moment redistribution, and ultimate strain of CFRP sheets decrease. In addition, using the GFRP sheet for strengthen the continuous beam reduced ductility loss and moment redistribution, but it did not substantially increase the beam's ultimate strength. The moment enhancement ratio of the strengthened continuous beams was even greater than the ultimate load enhancement ratio of the same beam.

El-Mogy et al. in 2011 [21] investigated effect of transverse reinforcement on the flexural behavior of continuous concrete beams reinforced with fiber reinforced polymer FRP. Six beams were reinforced with longitudinal glass fiber-reinforced polymer (GFRP) bars, although one was reinforced with steel as a control. The beams were continuous over two spans of 2800 mm each and have a rectangular cross section of (200×300) mm. As transverse reinforcement, steel and GFRP stirrups were used. The primary investigated parameters in this study were the material, spacing, and amount of transverse reinforcement. In addition, the ultimate capacity was calculated by comparing the experimental results to the code equations. The results of the experiments showed that moment redistribution in FRP-reinforced continuous concrete beams was possible and that increasing the amount of transverse

reinforcement improves the results. In addition, when GFRP stirrups were used to reinforce beams, they performed similarly to their steel-reinforced counterparts.

Akiel et al. in 2018 [22] an experimental studied about serviceability and moment redistribution of continuous concrete members reinforced with hybrid steel basalt fiber reinforced polymer -BFRP bars. Test results were published in this research of 12 two-span concrete specimens internally-reinforced with basalt fiber-reinforced polymer (BFRP) (group A) or hybrid steel-BFRP bars (group D), the specimen's dimensions are (5000×500×200) mm. Six specimens were under-reinforced, although the remaining six specimens were designed to be over-reinforced. The specimens had various reinforcement ratios for hogging-to-sagging. The specimens were subjected to two-point loads, each one of them was located at a distance of 0.4L from the middle of support. The behavior of the specimens reinforced by BFRP bars only deviated from the elastic effect. By decreasing the hogging-to-sagging reinforcement ratio, this deviation appeared to increase. Compared to their counterparts reinforced with BFRP bars only, specimens reinforced with hybrid steel-BFRP bars exhibited less deviation from the elastic response. The hybrid steel-BFRP bar reinforced specimens exhibited less deflections and smaller crack widths at service load than those of their counterparts reinforced only with BFRP bars. The hybrid-reinforced specimens appeared to show lower moment redistribution ratios than those reinforced with BFRP bars only for their counterparts. Figure 2.2 shows the specimens after failure.

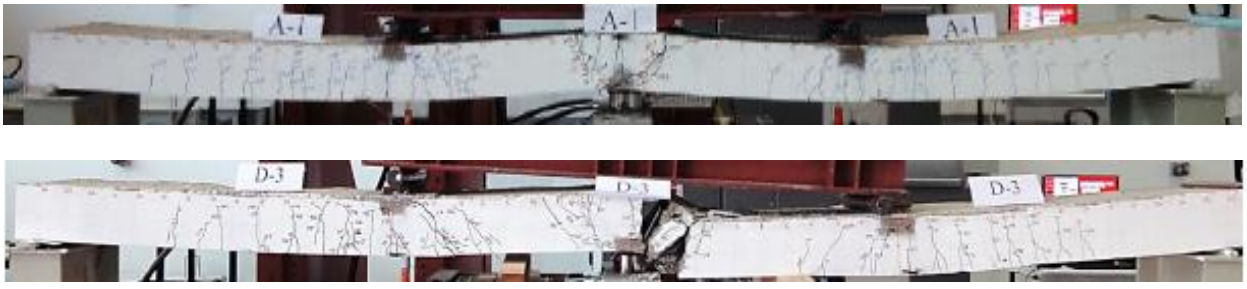

Figure 2.2 Photos of over reinforced specimen A1 and under reinforced specimen B1 at failure [22]

Visintin et al. in 2018 [23] studied experimental investigation of moment redistribution in ultra-high-performance fiber reinforced concrete beams. This research was presented the findings of an experimental study of the moment redistribution capacity of four continuous beams constructed in two spans of dimensions (5500×200×220) mm made of ultra-high performance fiber reinforced concrete (UHPFRC) with different reinforcement ratios, in order to know if existing empirical design approaches can be extended to UHPFRC. The results of the experimental investigation show that the observed moment redistribution was greater than the code predictions for beams where the hinge formed at the support as showed in Figure 2.3. However, for the beam where the hinge formed under the load points, the redistribution of the moment observed was significantly less than the predictions of the codes. Hence, current design guidelines do not always provide a conservative prediction of moment redistribution in UHPFRC beams in the results of this study.

Figure 2.3 Typical beam after failure [23]

2.3 Reinforced Concrete Beams of Hybrid Compressive Strength

Kheder et al. in 2010 [24] introduced flexural strength and cracking patterns of hybrid strength concrete beams. This experimental investigation was focused on the flexural tests of the twelve normal strengths concrete NSC, high strength concrete HSC and hybrid strength concrete HYSC simply supported beams of (3000×175×275) mm dimensions under point loading. Hybrid strength concrete beams cast with two concrete compressive strengths of 20 and 70 MPa were

compared to their flexural and cracking behavior with normal 20 MPa and high-strength 70 MPa beams. As compared to normal strength beams, the hybrid beams showed an increase in the load carrying capacity at cracking, yielding and ultimate loading. The load carrying capacity increase was between (1.80 and 70.8%) higher than normal strength beams and only (3.3-9.8%) lower than the corresponding beams of high compressive strength. The crack width in the hybrid beams at all loading stages was narrower than both types of beams. The crack width at service and ultimate loading stages were (19.5-26) % and (9.2-15.1) % narrower than those of the corresponding normal and high strength beams respectively. The use of HYSC beams with 70 MPa concrete in the compression zone of the beam allowed an increase in the beam's balanced steel ratio, which was close to that of the high-strength concrete used (70 MPa). Figure 2.4 shows the crack mode of different strengthen beams.

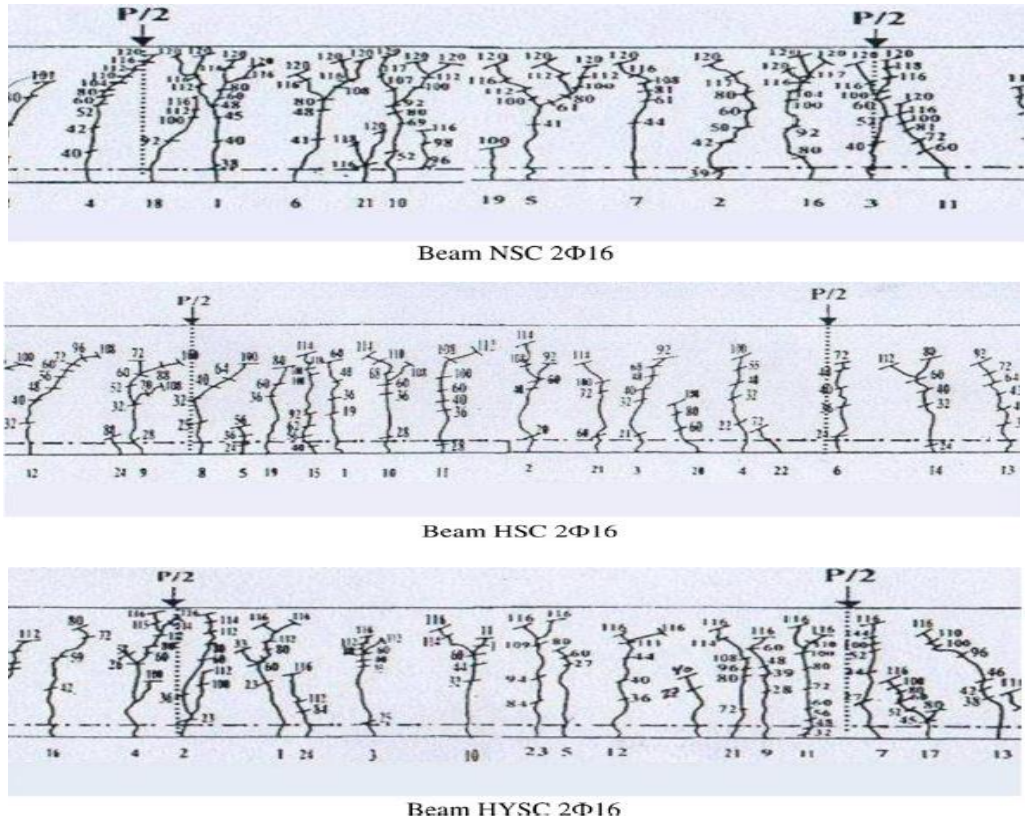

Figure 2.4 Cracking patterns at middle third of beams (2Ø 16) [24]

Abbas and Abd in 2015 [25] studied the behavior of hybrid concrete beams containing two types of (HSC) and conventional concrete was investigated. It was an experimental investigation for twelve test beams with a dimension of (100×200×1100) mm was divided into four groups, each one of them consisting of three sample, beams same in size and gross section but different in concrete type and steel bar, as shown in Figure 2.5.

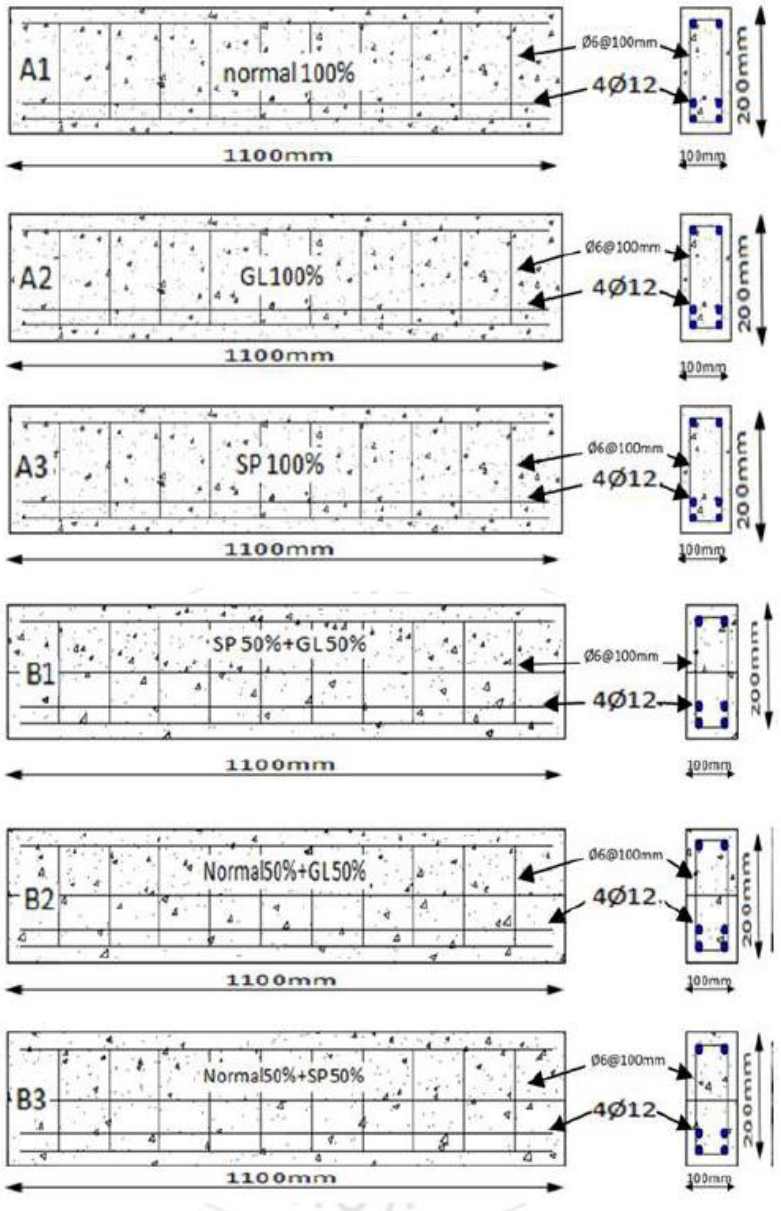

Figure 2.5 Homogenous and hybrid specimens [25]

The additive of the first type HCS was superplastizer (SP) and the second one glass fiber (GL) reinforced polymer. All beams were tested to fail under two-point loading to analyze the structural behavior. As a result, in comparison with normal concrete, the failure perimeter increased significantly with specimens made of high-strength concrete and hybrid concrete compared to normal concrete.

Al-Hassani et al. in 2015 [26] studied flexural behavior of hybrid T beams (made of reactive powder concrete and normal strength concrete). The research shown an experimental study to investigate the flexural behavior of hybrid T beams and to study the ability to use normal concrete strength together with Reactive Powder Concrete (RPC) in the same section to find the advantages of these two materials in optimal way**.**

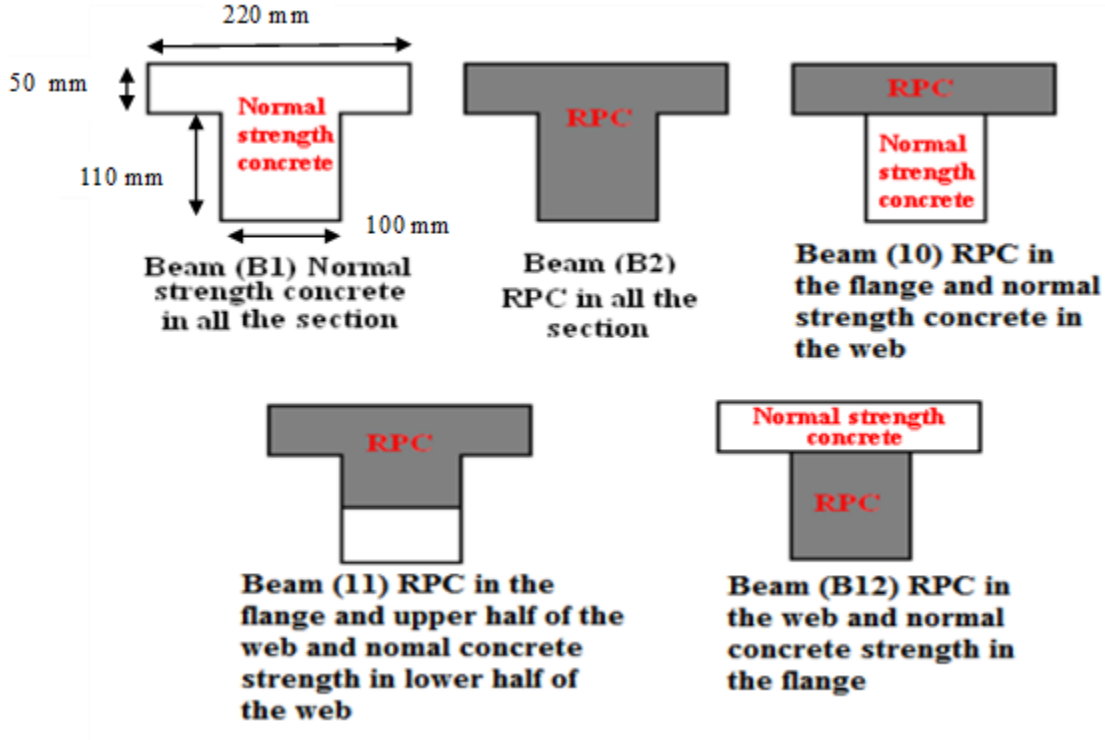

Figure 2.6 Cross-section of the tested specimens [26]

All beam specimens are simply supported with clear span of 1200 mm and tested under the effect of two-point static loads. The nominal dimensions of the tested

beams were 1300 mm in overall length and 160 mm in depth. The flange width and thickness were 220 mm and 50 mm respectively. The web of the beam had height and width were 110 mm and 100mm respectively. Figure 2.6 shown the cross-sectional of the tested beams.

The experimental results showed that the use of RPC in the web and normal strength concrete in the flange effectively increased the performance of hybrid T-section beams compared to normal strength concrete T-beam. However, increases in the first crack load, ultimate deflection and ultimate flexural load were 86.67%, 29.19% and 60% respectively. In contrast, the increasing of RPC in the flange and normal concrete strength in the web had been 20%, 34.28% and 14.97 respectively, compared to the normal T-beam concrete strength.

Iskhakov et al. in 2017 [5] was conducted an experimental investigation of continuous two-layer of reinforced concrete beam. The study focused on testing a continuous two span, TLB with optimal steel fiber ratio of dimensions (4000×150×300) mm and using two points load each one act at the middle of each span. Figure 2.7 shown bending moment diagram and the corresponding layout of normal strength concrete NSC and steel fiber high strength concrete SFHSC layers. The aim of the study is to show how a continuous two-layer beam CTLB responds to positive and negative bending moments in the span and above the middle support, as well as the effect of bending moment redistribution on CTLB behavior.

Up to the ultimate limit state of the tested beam, no cracks between the SFHSC and NSC layers were observed, demonstrating proper layer interaction. The results of this study enable CTLB to be recommended for practical use as effective and economical continuous bending elements. Deflection increases after the plastic hinge forms at the middle support until the beam reaches its ultimate state, at which two more plastic hinges form at the load application points in spans AB and BC.

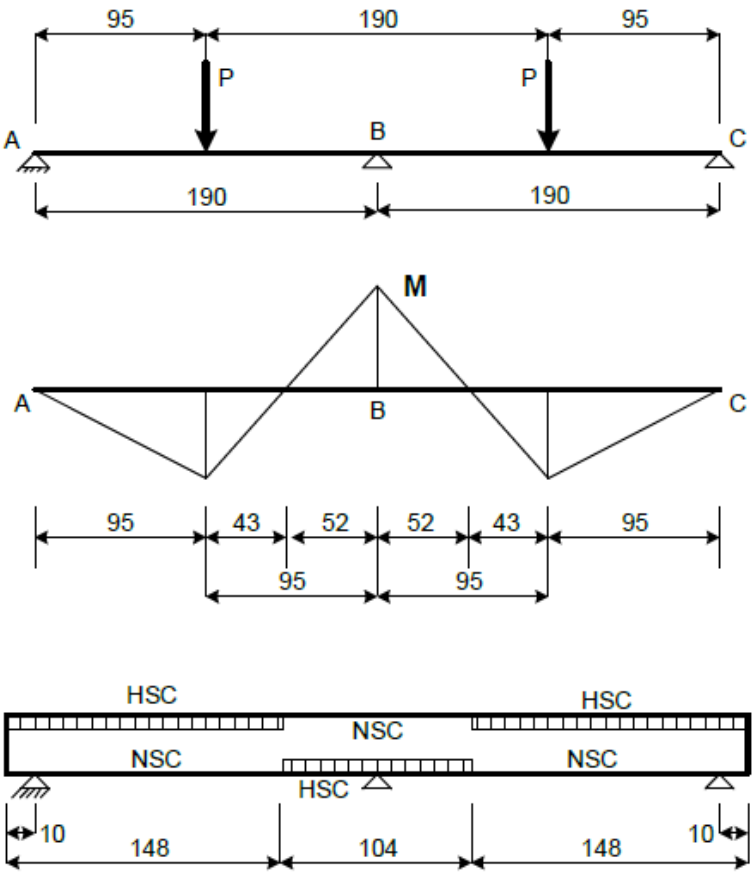

all dimensions in cm

Figure 2.7 Continuous two-layer beam static scheme, bending moment diagram and corresponding layout of NSC and SFHSC layers [5]

In other words, one of the main concerns for moment redistribution is the increase in applied load after the first plastic hinge up to the ultimate load value. And it has been shown experimentally that increasing the deflections of a two-layer continuous beam causes the formation of plastic hinges in the beam spans, such as it does in single layer beams.

Alawsh and Mehdi in 2018 [27] introduced the behavior of reinforced concrete hybrid trapezoidal box girders using ordinary and highly strength concrete.

The general behavior of reinforced concrete hybrid box girders was investigated by experimental and numerical investigations. Experimental work involves casting monolithically five specimens of trapezoidal cross-section box girders. All specimens had the same dimensions as shown in Figure 2.8, and tested as simply supported under two-point loading.

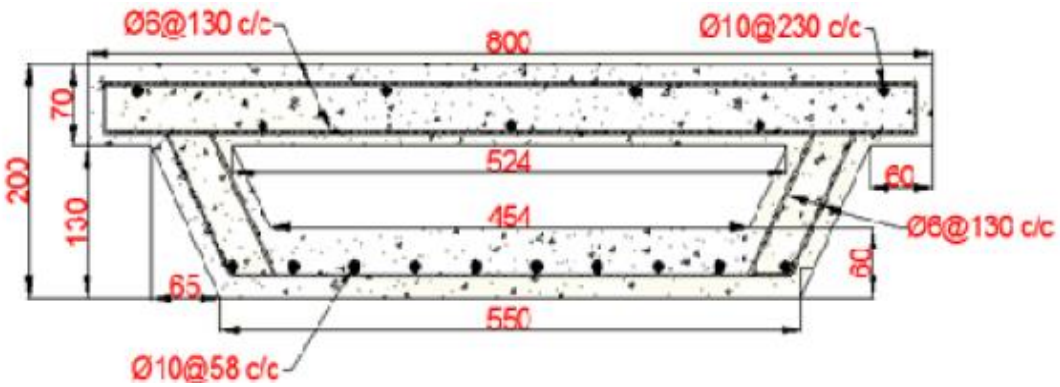

Figure 2.8 Transverse section (typical trapezoidal cross section) [27]

Two of them were cast as homogeneous box girders full normal and high strength with compressive strength of 35 and 55 MPa respectively. Three of the specimens were cast as hybrid box girders HSC in upper flange only, HSC in upper flange and half depth of webs, and HSC in bottom flange and total depth of webs. Experimental results showed significant effects of concrete hybridization on the structural behavior of the box girder samples, such as cracking loads, failure modes, cracking patterns and ultimate strengths. The ultimate strength of the hybrid box girders increased by 23% as average when compared to the homogenous box girder (full NSC) and decreased by 9 % as average when compared to the homogenous box girder of full HSC. The numerical investigation results by (ANSYS 50) program showed an acceptable agreement with the experimental work with a difference of about ranged between 3.12% and 9.588 % as the average for ultimate load and deflection respectively.

2.4 Concluding Remarks

It was possible to withdraw the following points from previous studies relating to moment redistribution in continuous RC beams or those relate to beams of hybrid compressive strength:

1. The moment-redistribution trend in statically indetermined structures, merged with many techniques to enhance the structural behavior.
2. The hybrid concept could be considered as smart technique to reduce the overall design cost.
3. There are no studies concerned with reinforced concrete moment-redistribution investigation of fully hybrid strength section.

CHAPTER THREE: EXPEREMENTAL WORK

3.1 General

The purpose of this experimental program is to investigate moment redistribution assessment in continuous reinforced concrete beams of hybrid compressive strength. In addition, an experimental work presented: mix design, preparation of materials and the specimens as well as experimental set-up.

3.2 Details of Developed Specimens

A total of twelve reinforced continuous concrete beams were prepare for the test. All of them to study the flexural behavior of the reinforced concrete hybrid beams with a rectangular cross-section. All the twelve beams were similar in their dimensions but the difference in steel reinforcement details, the overall length of the specimens was 3000 mm and the cross-section were (120×200) mm width and depth respectively. The main variables in this study were concrete compressive strength (20 and 60) MPa, hybrid section of strength, the enhancement ratios (00%, 15% and 30%).

The beams were divided into three groups depending on its enhancement ratio and each beam of those groups having compressive strength differ than the other, there were normal strength of lower and upper limit strength (20 and 60) MPa or hybrid beam in deferent forms (50% 20 MPa and 50% 60 MPa). The flexural reinforcement and transvers reinforcement rebar were the same ∅ 6 mm, the stirrups had closed spaces about 50 mm interval. The first group of zero % enhancement consist of four beams (U 20 00, U 60 00, H 20/60 00 and H60/20 00) have 7∅6 mm in negative region and 4∅6 mm in positive region, the second one of 15% enhancement consist

of four beams (U 20 15, U 60 15, H 20/60 15 and H 60/20 15) have 6∅6 mm in negative region and 5∅6 mm in positive region and the last group of 30% enhancement also have four beams (U 20 30, U 60 30, H 20/60 30 and H 60/20 30) have 5∅6 mm in negative region and 6∅6 mm in positive region, the beams reinforcement are the same for all beams in each group. Table 3.1 and Figure 3.1 shows the details of the specimens. The quantities of reinforcing steel whether longitudinal or for shear, were selected in accordance with the requirements of the design and according to ACI code, and to achieve the required ductility as a condition to achieve moments redistribution.

Table 3.1 The details of specimens

Group No.	* I.D beams description	Compressive strength F_{cu} (MPa)		Longitudinal steel reinforcement bars F_y =380MPa			
		top	bottom	Mid span		Mid support	
				bottom	top	top	bottom
G1	U 20 00	20	20	4Ø6	4Ø6	7Ø6	4Ø6
	U 20 15	20	20	5Ø6	4Ø6	6Ø6	5Ø6
	U 20 30	20	20	6Ø6	3Ø6	5Ø6	6Ø6
G2	U 60 00	60	60	4Ø6	4Ø6	7Ø6	4Ø6
	U 60 15	60	60	5Ø6	4Ø6	6Ø6	5Ø6
	U 60 30	60	60	6Ø6	3Ø6	5Ø6	6Ø6
G3	H 20/60 00	20	60	4Ø6	4Ø6	7Ø6	4Ø6
	H 20/60 15	20	60	5Ø6	4Ø6	6Ø6	5Ø6
	H 20/60 30	20	60	6Ø6	3Ø6	5Ø6	6Ø6
G4	H 60/20 00	60	20	4Ø6	4Ø6	7Ø6	4Ø6
	H 60/20 15	60	20	5Ø6	4Ø6	6Ø6	5Ø6
	H 60/20 30	60	20	6Ø6	3Ø6	5Ø6	6Ø6

*The considered dimensions of all beams are (3000×120×200) mm

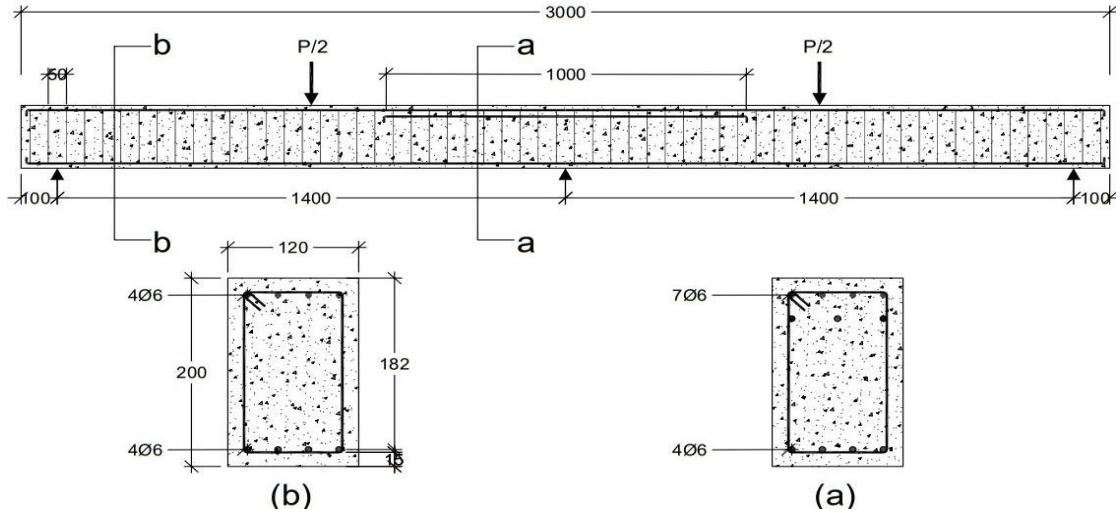

a. lower limit strength of 0 % R

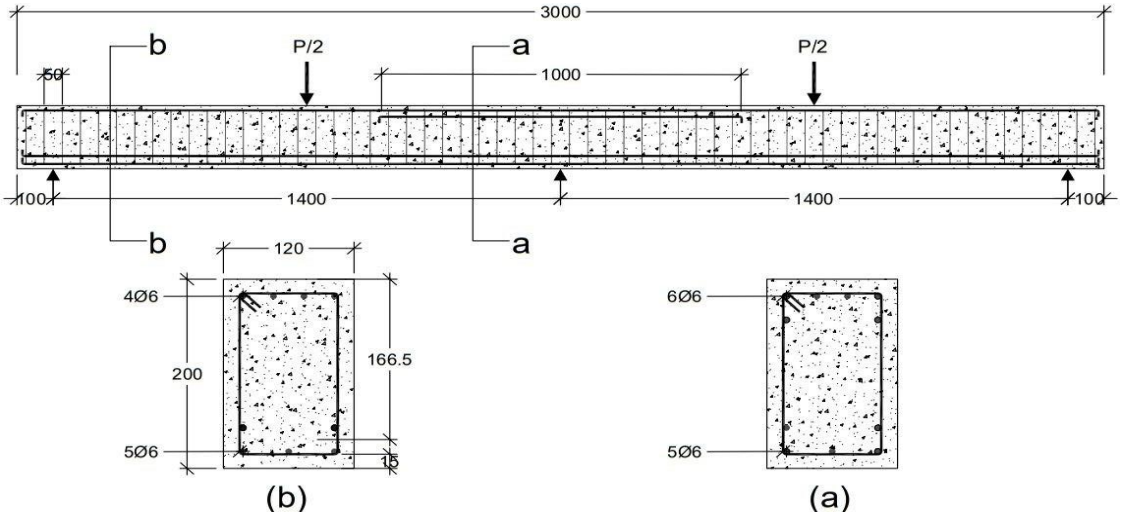

b. lower limit strength of 15% R

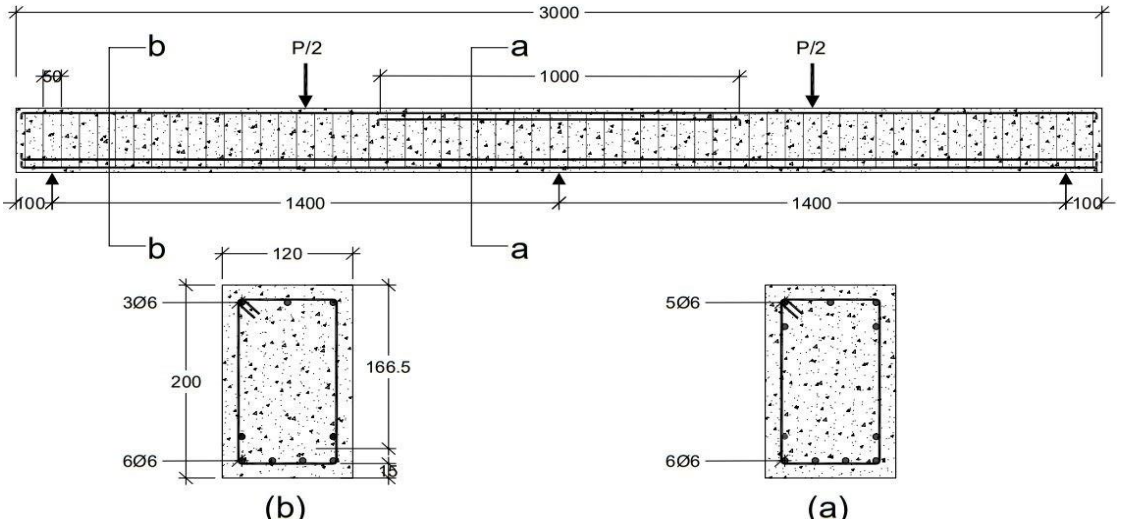

c. lower limit strength of 30% R

Figure 3.1 The details of reinforcement of the specimens

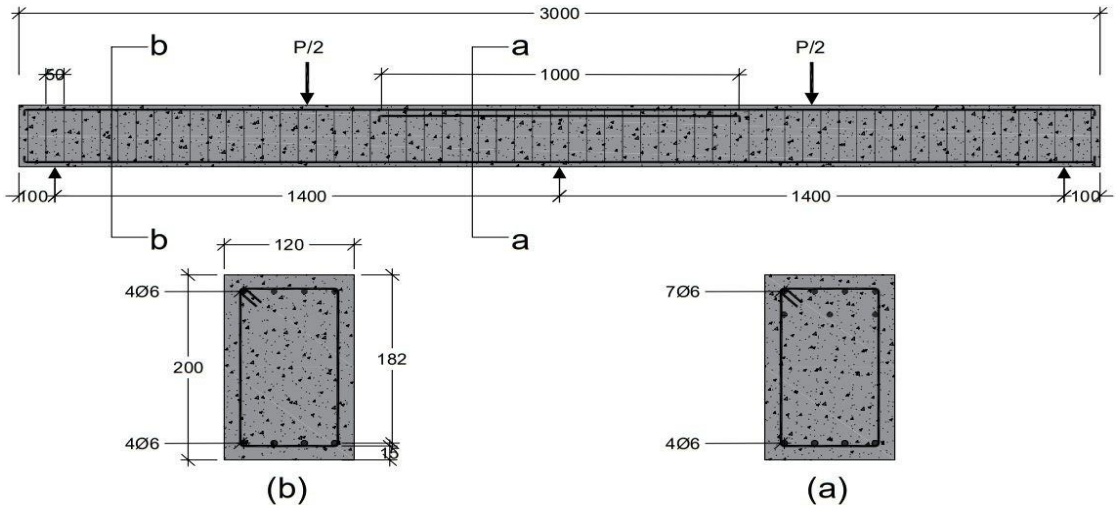

d. upper limit strength of 0 % R

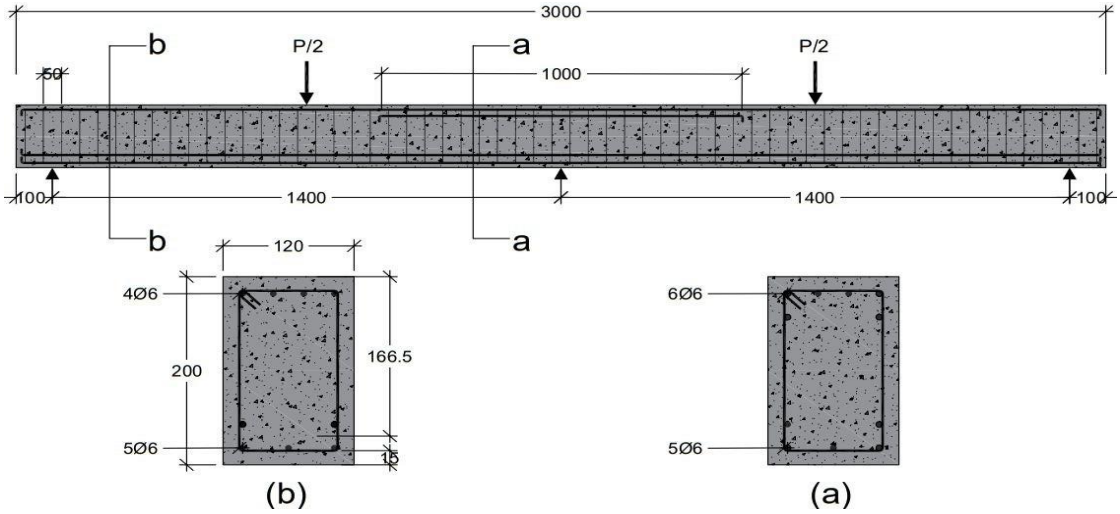

e. upper limit strength of 15% R

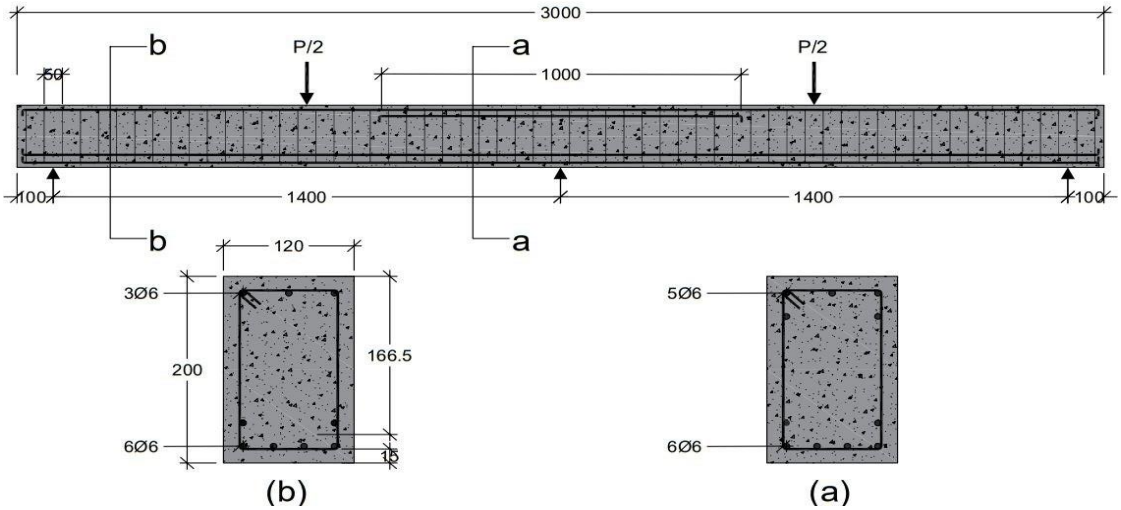

f. upper limit strength of 30% R

Figure 3.1 continue

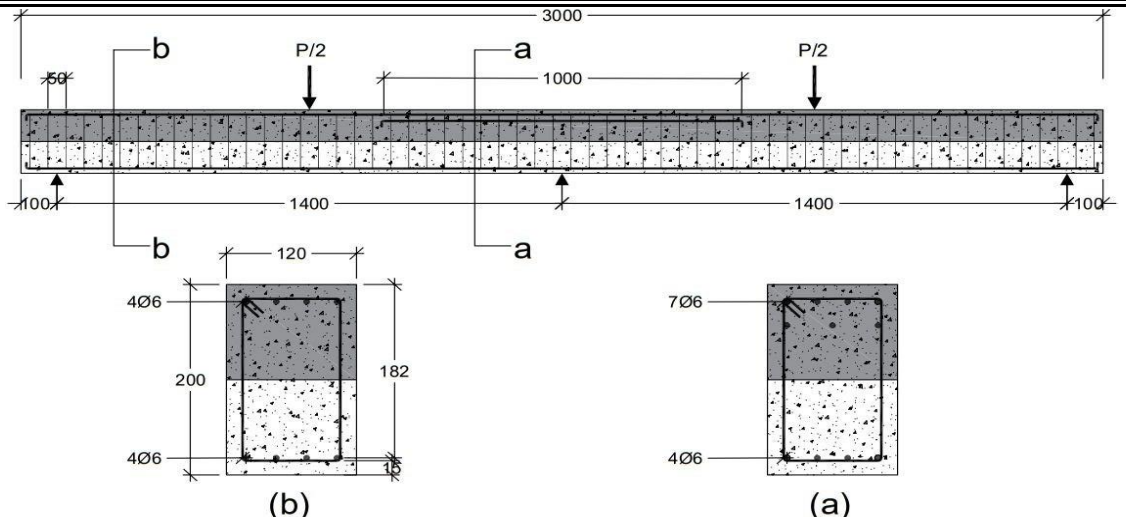

g. hybrid section mode I (upper: lower) limit strength of 0% R

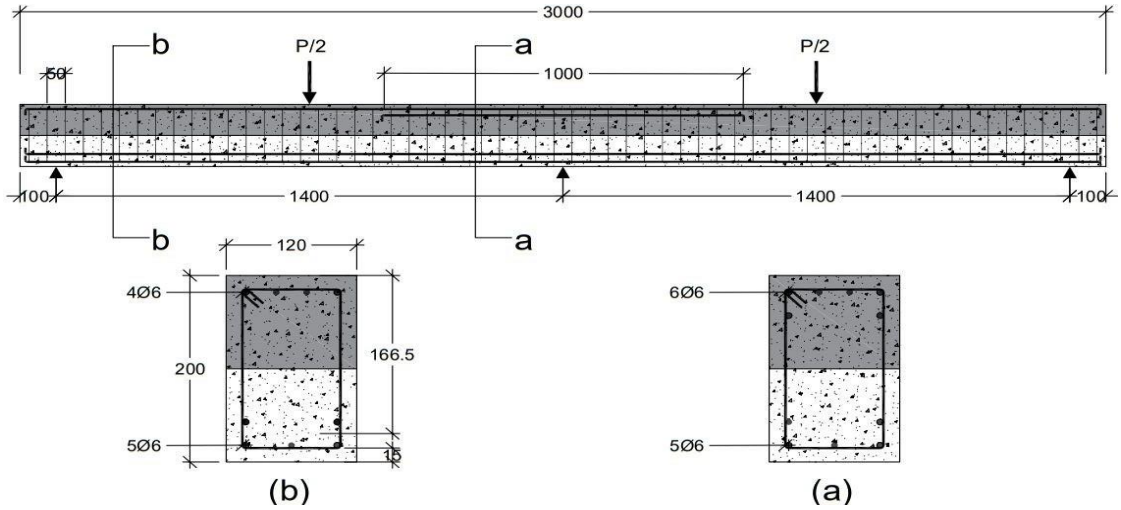

h. hybrid section mode I (upper: lower) limit strength of 15% R

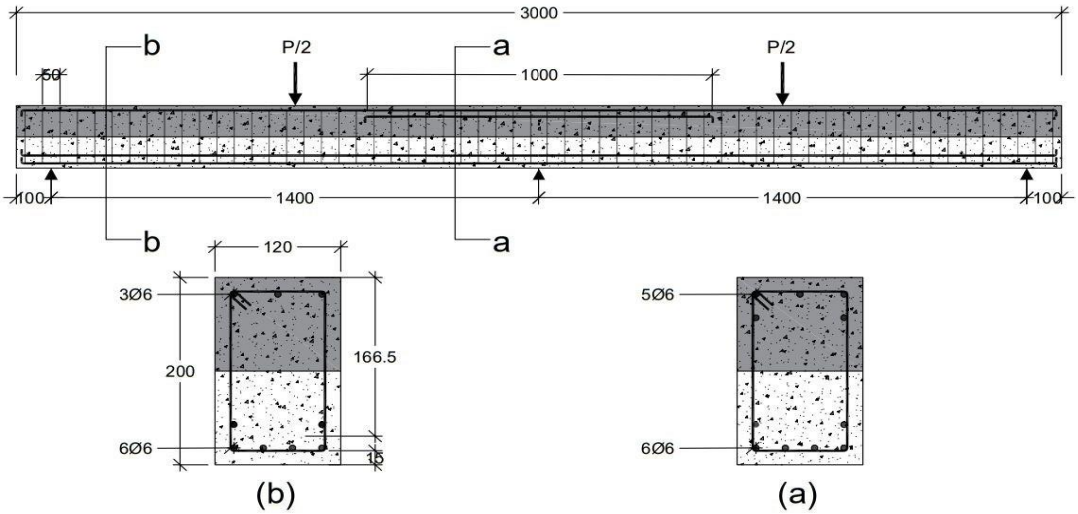

i. hybrid section mode I (upper: lower) limit strength of 30% R

Figure 3.1 continue

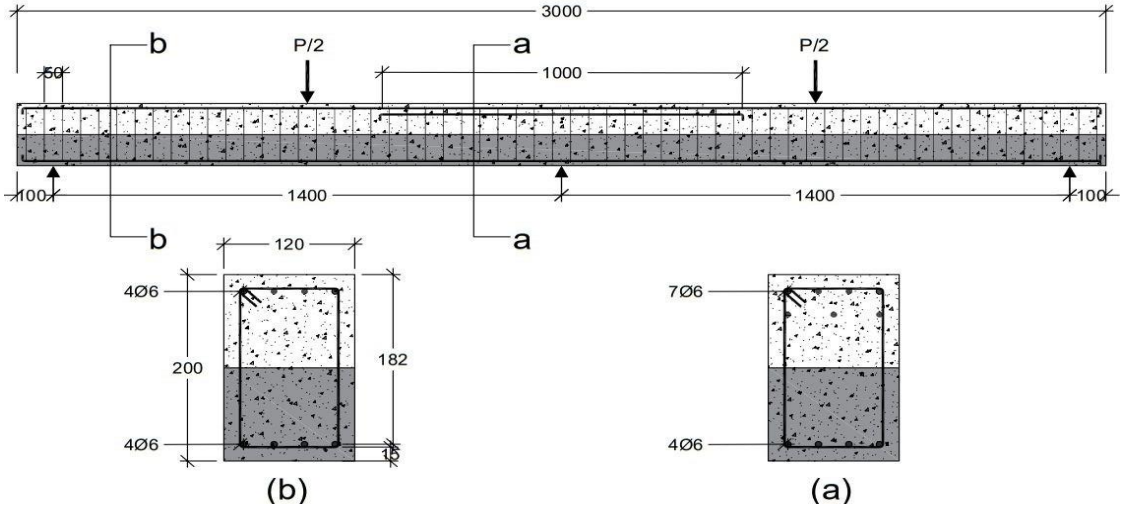

j. hybrid section mode II (lower: upper) limit strength of 0 % R

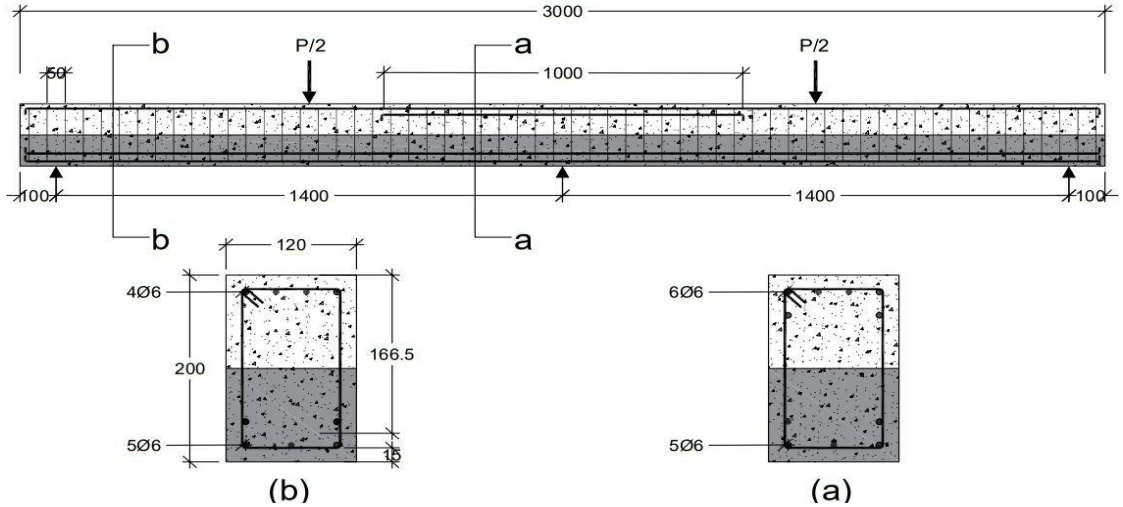

k. hybrid section mode II (lower: upper) limit strength of 15% R

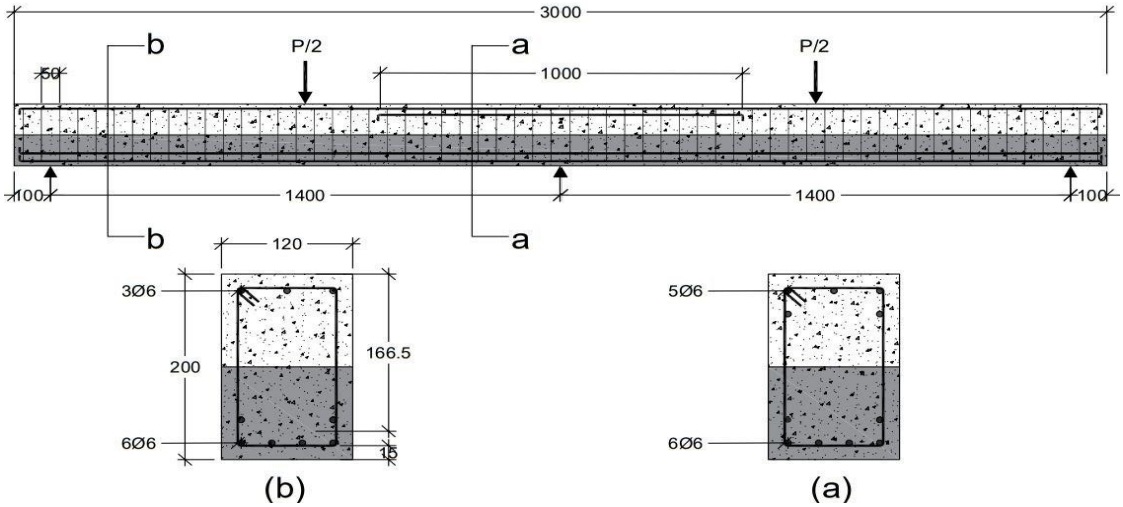

l. hybrid section mode II (lower: upper) limit strength of 30 % R

Figure 3.1 continue

3.3 Materials

The materials used in the research program general definition and requirements which are cement, sand, gravel, reinforcing steel and superplasticizer, and those material with its properties are listed below.

3.3.1 Cement

The cement locally called Cresta and it's an ordinary Portland cement was used for all concrete mixture that used in the casting of the specimens, to avoid exposure to unfavorable weather conditions, they were stored it in a dry place. The chemical and physical properties of the used cement are according to Iraqi standard NO. 5/1984 (specification, 1984b) [28] and they are given in Table 3.2 and Table 3.3 respectively.

3.3.2 Fine Aggregate

Natural sand was using in all type of concrete mixture. The maximum grain size is 4.75 mm. Sand laboratory tests were carried out in accordance with Iraqi specifications No. 45/1984 (Specification, 1984a) [29]. The tests results have been listed in Table 3.4.

Table 3.2 Chemical composition of the cement

Chemical analysis	Percentage by weight	Limits of IQS No.5/1984
Lime (CaO)	62.00	_
Silica (SiO_2)	22	_
Alumina (Al_2O_3)	3.8	_
Iron Oxide (Fe_2O_3)	3.2	_
Magnesia (MgO)	2.3	<5
Sulfate (SO_3)	2.1	<2.8
Loss on Ignition (L.O.I)	3	<4
Lime saturation factor (L.S.F)	0.84	0.66-1.02
Insoluble residue (I.R)	0.8	<1.5

Table 3.3 Physical properties of cement

Physical properties	Test result	Limits of IQS No. 5/1984
Fineness Using Blaine Air Permeability Apparatus (m2/kg)	296	≥230
Setting time Using Vicat's Instruments Initial (hrs: min.) Final (hrs: min	 1:20 4:15	 ≥45min ≤10hr
Soundness Using Autoclave Method	0.44	<0.8
Compressive Strength 3 days (MPa) 7 days (MPa)	 20.6 29	 ≥15 ≥23

Table 3.4 Grading of fine aggregate

No.	Sieve size (mm)	% Passing by weight	
		Fine aggregate	Limits according to IQS 45/1984 Zone2
1	10	100	100
2	4.75	100	90-100
3	2.36	96	75-100
4	1.18	84	55-90
5	0.6	56	35-59
6	0.3	20	8-30
7	0.15	9	0-10

3.3.3 Coarse Aggregate

In this study, gravel was using in all concrete mixtures having maximum size 10 mm rounded coarse aggregate. Table 3.5 shown sieve analysis test for coarse aggregate. The results of the laboratory tests indicate that it complies with the Iraqi Standard's

limits of Iraqi standard No.45/1984 (Specification, 1984a) [29] for graded gravel with a maximum size of 10 mm.

Table 3.5 Grading for coarse aggregate

No.	Sieve size	% Passing by weight	
		Coarse aggregate	Limits according to IQS 45/1984 Zone2
1	12.5	100	100
2	10	97.3	90-100
3	4.75	21.6	0-25
4	2.36	2.4	0-5

3.3.4 Water

Reverse osmosis (R.O.) water used for all concrete mixtures, washing aggregate before casting and for curing of specimens.

3.3.5 Superplasticizer

One of the important things to produce a high strength concrete mixture is reducing water content which it became difficult to mix, then it's necessary to add plasticizer to improve workability of the mixture. A superplasticizer, type HyperPlast PC260 was used. This plasticizer complies with ASTM C494-99 A and G. (ASTM, 1999) [30]. This plasticizer is chloride-free and is built on a poly carboxyl polymer with a long chain specifically designed to enable water to improve efficiency, directly affecting the improved operability of concrete and providing adequate flow through confused joints. Table 3.6 describes the technical specifications for this type of plasticizer.

Table 3.6 Technical description of PC 260 [30]

Chemical base	Modified poly carboxylates-based polymer
Freezing point	-7°C approximately
Appearance /colors	Light yellow liquid
Specific gravity @25°C	1.1±0.02
Dosage	0.5 to 4 liter per 100 kg of binder
Air entrainment	Typically, less than 2% additional air is entrained above control mix at usual dosage
Storage condition /shelf life	12 months if stored at temperatures between 2°C and 50°C

3.4 Steel Reinforcement

A deformed bars of 6 mm diameter was used in this study for both of longitudinal reinforcement and stirrups were tested at the laboratory of constructer material at the Department of Civil Engineering. The properties of steel reinforcing bars showed in Table 3.7. The rebar was tested in (Iraq limits 2091/1999) [31]. Figure 3.2 shows stress-strain curve of steel bar and Figure 3.3 showed tensile strength for reinforcing test bars.

Table 3.7 Properties of steel bar reinforcement

Bars size (mm)	Bar No.	Test results		
		Yield strength (N/mm2)	Ultimate Strength (N/mm2)	Elongation (%)
6	1	370	425	12.54
	2	375	415	11.93
	3	400	450	12.68

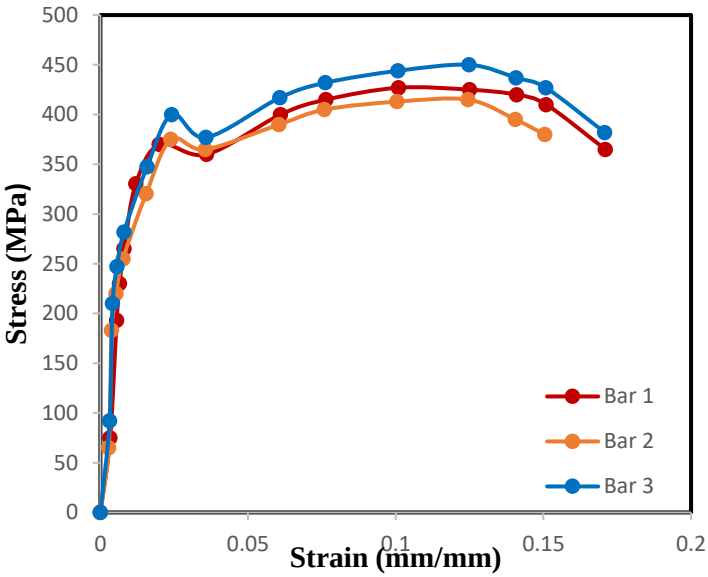

Figure 3.2 stress-strain curves of steel bar Ø 6 mm

Figure 3.3 Tensile strength of reinforcement test bars

3.5 Preparation of Test Specimens

3.5.1 Mix Design

Two concrete mixes were selected to use to investigate the influence of concrete strength on the behavior of continuous hybrid strength reinforced concrete beams of rectangular section after tests several experimental mixtures of 20, 40 and 60 MPa.

One of them was normal lower limit concrete 20 MPa compressive strength and another one was normal of upper limit strength 60 MPa. The mix proportions of the ingredients of lower limit strength mixture [1 cement: 2 sand: 4 gravel], and the w/c ratio were 70% which is the maximum limit of water content according to ACI code limitation, to get cube compressive strength of about 20 MPa at age of 28 days. For the second mix, the proportions of the ingredients of upper limit strength mixture [1 cement: 1 sand: 2 gravel], and the w/c ratio were 34%, and 0.6% superplasticizer by weight of cement to get a cube compressive strength of about 60 N/mm^2 at age of 28 days.

The contents considered in the preparing of the two types of concrete are listed in Table 3.8

Table 3.8 Weights of materials included in concrete mixtures

Mixture I. D	Symbol of concrete	Cement (kg/m^3)	Sand (kg/m^3)	Gravel (kg/m3)	W/C	Super plasticizer (kg/m^3)	F_{cu}(MPa) in 28 days
1	Normal lower limit strength concrete	308.9	617.8	1235.6	0.7	-	20
2	Normal upper limit strength concrete	540.85	540.85	1081.7	0.34	3.25	60

3.6 Mixing Procedure

3.6.1 Normal Strength Concrete

The process of preparing the concrete mixture and casting process was carried out using the central mixing in company, where the preparation of quantities was supervised (weighed and packed in clean and dry container before mixing). Putting clean and dry gravel, sand and cement in a rotary mixer for 5 minutes approximately.

And then water was added to the dry ingredients and remixed for 10 to 12 minutes to obtain a homogenous mixture that's for normal lower strength concrete. While for upper strength concrete of 60 MPa also putting the dry ingredients in the container after weighed and mixed for few minutes, then the superplasticizer was dissolved in water and the solution of water with superplasticizer was added to the rotary mixer gradually. Then the concrete was pouring into two big pans and mix well and then pouring to the molds gradually in two layers and compacting each layer by using electrical pencil vibrator to ensure the proper placement of concrete in and around the reinforcement cage.

3.7 Mechanical Properties of Concrete

During casting, six (150×150×150) mm cubes, six prisms (100×100×500) mm, and six (150×300) mm cylinders for each type of concrete mixture, as shown in Figure 3.4. All molds were prepared, cleaned, and lubricated before casting.

Figure 3.4 Specimens of hard concrete tests (cubes, cylinders and prism)

3.7.1 Compressive Strength

The test was conducting using 2000 kN compression testing machine at the laboratory of constructer material at the Department of Civil Engineering. The cube

compressive strength of concrete was obtained according to BS1881: Part 16: 1983 (BS 1881, 1989) [32]. The average compressive strength obtained of normal lower and upper strength concrete are 24 MPa and 61.3 MPa, respectively. The test results are presented in Table 3.9, as shown in Figure 3.5

Table 3.9 Compressive strength results of normal and high strength concrete

Compressive strength (MPa)		
Age	Lower limit strength concrete	Upper limit strength concrete
7 days	17.2	42.6
	18.0	44.2
	17.8	42.4
Average of 7 days	17.7	43.1
28 days	24.3	61.2
	23.5	62.3
	24.1	60.5
Average of 28 days	24.0	61.3

3.7.2 Split Tensile Strength

ASTM- C496 (C496, 2006) [34] has been used to test the split tensile strength of cylindrical concrete (150×300) mm. This test was carried out at the University of Misan's College of Engineering, using a compression testing machine with a capacity of 2000 kN. The test results are presented in Table 3.10, as shown in Figure 3.6

The following Equation 3.1 was used to compute the split tensile strength of concrete

$$f_t = \frac{2F}{\pi DL} \quad 3.1$$

Where; f_t: tensile strength (MPa)

F: maximum force (N)

D: diameter of cylinder specimen (mm)

L: length of specimen (mm)

Table 3.10 Results of splitting tensile strength

Split tensile strength (MPa)		
Age	Lower limit strength concrete	Upper limit strength concrete
7 days	1.40	2.20
	1.40	2.30
	1.30	2.30
Average of 7 days	1.37	2.27
28 days	2.00	3.60
	2.10	3.60
	2.00	3.50
Average of 28 days	2.03	3.60

Figure 3.5 Compressive strength test

Figure 3.6 Split tensile strength test

3.7.3 Flexural Strength Test

The ASTM- C78 (C78, 2002) [35] specification was used to test the flexural strength of the concrete used in this study. The prism samples dimensions (100×100×500) mm were examined using the testing machine of flexure with a capacity of (5000 kN) in college of engineering, as shown in Figure 3.7. The results of the test show in Table 3.11. The following Equation 3.2 is used to calculate the bending strength:

$$F_r = \frac{3PL}{2BD^2} \quad 3.2$$

where: F_r= modulus of rupture (MPa)

P= maximum applied load (N)

L= span length (mm)

B= average width of the specimen (mm)

D= average depth of specimen (mm)

Table 3.11 Flexural strength result

Flexural strength (MPa)		
Age	Lower limit strength concrete	Upper limit strength concrete
7 days	1.80	3.51
	1.83	3.72
	1.81	3.40
Average of 7 days	1.81	3.54
28 days	2.60	4.62
	2.45	4.30
	2.50	4.55
Average of 28 days	2.50	4.50

Figure 3.7 Flexural strength test

3.8 Casting Procedure

Wooden formwork was using to cast all concrete beams. All molds were consisted of a wooden base and four movable sides connected to base with screws and nails. The length of mold was 3000 mm for all beams. The beam cross-section was (120×200) m. The molds were coating from the interior face with oil prior to casting and before the reinforcement cage was placed in position, after that the reinforcement cage (after distributed the longitudinal and stirrups where horizontal and vertical bars were assembled by steel wires and adhesion the strength gauge on the bars in its suitable place) placed inside the molds and used plastic spacers to maintain the cover of concrete and to keep the right position of reinforcement during the casting of concrete. The mixing of concrete takes a range between 10 to 12 minutes to obtained a homogenous mix, and to ensure proper placement and consolidation of the concrete in and around the reinforcement cage, the mixture was poured into the molds (for the homogeneous beams poured at three layers with compaction between each layer, while for hybrid section beams poured the first layer and then after 15 minutes poured the second one also with compaction for each one)

and the mechanically compacted with a standard rod vibrator. Finally leveling and smoothing the top surface of concrete, and then the curing of the specimen. Figure 3.8 shows preparing the molds, fabrication and casting procedure of the specimens.

Figure 3.8 Preparing and casting procedure of the specimens

3.9 Instrumentation and Equipment of the Test

3.9.1 Test Machine

It's an automatic compression machine in laboratory in College of Engineering at Misan University of 600 kN was used to test all beams, as shown in Figure 3.9.

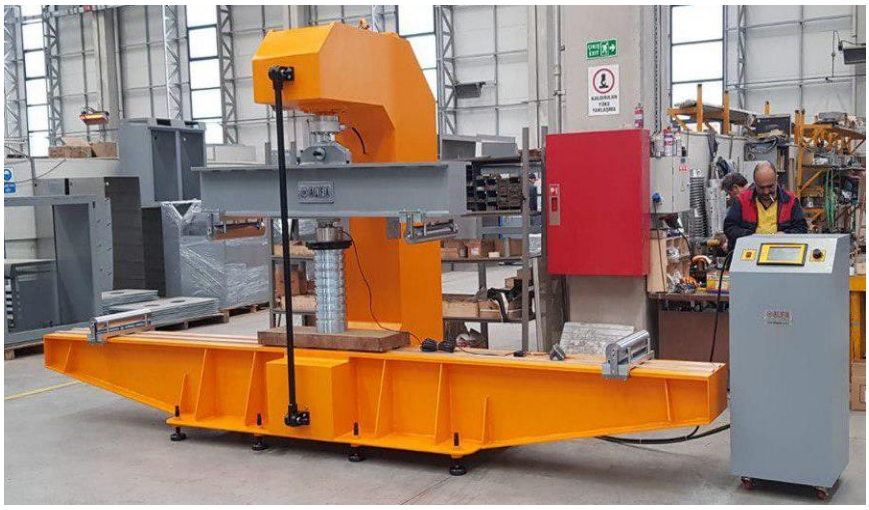

Figure 3.9 Flexural testing machine

3.9.2 Data Obtaining System

The data obtaining system contains a personal computer, a strain indicator called the data logger and its function is receiving data from a collection of strain gauges that adhere on the beam, the name of data logger is GEODATALOG 30-WF6016 and its properties are 16 channels data acquisition unit. 110-240 V, 50-60 Hz, 1ph supplied complete with DATACOMM software for PC data acquisition, as shown in Figure 3.10

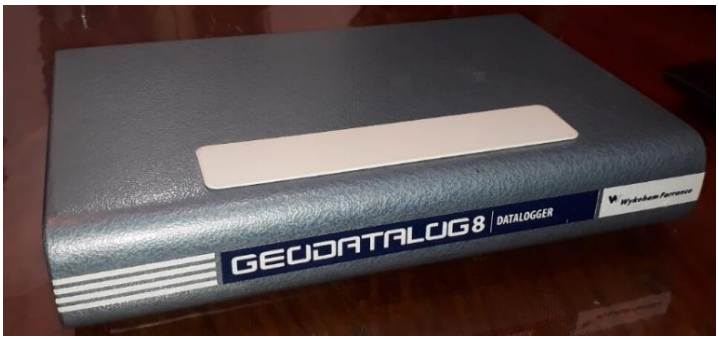

Figure 3.10 Data logger

3.9.3 Strain Gauges

Two strain gages 30 mm were adhesive on the surface of concrete beam of the beams in its compression zone one at the lower of the middle support and another one at the upper of the mid span of each beam, and two strain gages (6 mm) were attached to the reinforcement in its tension zone were placed one at the upper of the middle support and the other one at the lower of the mid span. It was connected to data acquisition device to obtain strain reading at each load increment as shown in Figure 3.11. The strain gauge was attaching to the previously treated surface of the beam with CN-E cyanoacrylate adhesive and wrapping with Sb tape to prevent possible damage that effects on it. The located of the strain gauges are shows at Figure 3.13.

a. strain gauge of concrete

b. strain gauge of steel

c. adhesive strain gauge of steel on reinforcement

Figure 3.11 Strain gauge

3.9.4 Deflection Measurement

The mid-span and the inner quarter deflection of each beam was measured by using LVDT with automatically recording of reading as shown in Figure 3.12.

Figure 3.12 LVDT position on the beam

3.10 Test Procedure

The beams were tested by universal testing machine in College of Engineering in Misan University as shown in Figure 3.13 and 3.14. All specimens were cleaned and colored with white and gray color to organized the compressive strength, were white color for normal lower limit strength 20 MPa and gray color for normal of upper limit strength 60 MPa and to demonstrate the propagation of cracks. The machine applied to concentrated load on the beam through steel loading roll over a thin rubber strip which it used to achieve a uniform contact between the specimen and the load. In all testing, the load applied in small increments, deflection, strain, and load values were recorded at each increment. The load was gradually increasing until it collapsed.

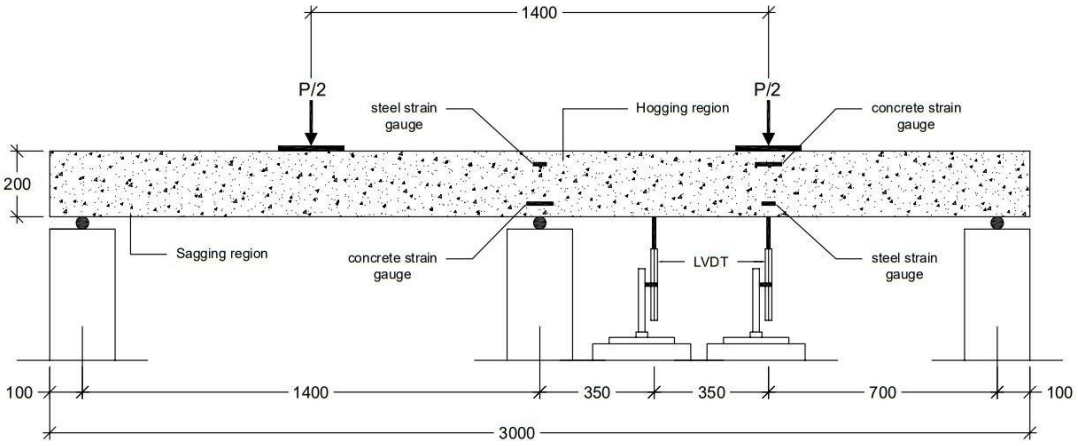

Figure 3.13 Details of typical test specimens

Figure 3.14 Flexural test of specimens

CHAPTER FOUR: RESULTS AND DISCUSSIONS

4.1 General

Strength capacity and moment redistribution regards continues RC beams of developed hybrid section strength are investigated. Normal of lower and upper limit compressive concrete strength are utilized within various hybrid section fashions which are companied by mid span section strength enhancement besides section strength reduction in middle support region so as to investigate the moment redistribution.

The suggested hybrid mode concept is introduced as concrete strength redistribution to get smart material utilization. The hybrid mode based on reducing the strength in some regions and increasing it in other regions.

Two hybrid mode are adopted and classified according to concrete compressive strength ranking within section

1. Hybrid Mode I, upper limit strength concrete utilized above section center line while lower limit concrete strength below section center line.
2. Hybrid Mode II, upper limit strength concrete strength that utilized under section center line and lower limit concrete strength above section center line.

Two reference groups of homogeneous strength specimens are considered:

The first without any strength reduction and it is of 60 MPa and denoted as Upper limit while the second group is considered as reference for the adopted lower strength reduction which is of 20 MPa.

Figure 4.1 shows the adopted hybrid modes besides the control sections of normal of upper and lower limit strength. Throughout this chapter, the structural behavior

and the moment redistribution of suggested modes are considered in addition to comparative analysis between them.

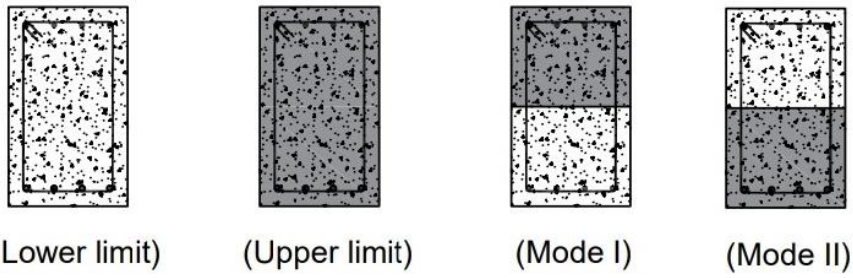

Figure 4.1 Adopted control section beside hybrid strength section of mode I and II

4.2 Moment Redistribution Analysis

Beam Moment redistribution refers to the behavior of statically indeterminate structures that are not completely elastic, but have some reserve plastic capacity [9]. Figure 4.2(a) shows adopted continuous beam of two spans under the effect of mid span concentrated loads Q;

According to the structural theory, the elastic bending moment diagram is determined and shown in Figure 4.2(b).

For further loading, as Q is increased the moments at B and D will eventually reach the value M_p Figure 4.2(c), where the beam is no longer a structure but a mechanism; the collapse mode is often referred to as the collapse mechanism.in Figure 4.2(d),

Let Q_u be the value of Q at collapse. From Figure 4.2(c), Equation 4.1

$$M_B = \frac{Q_u l}{4} - \frac{M_c}{2} \qquad 4.1$$

Where now both M_B and M_C equal M_p, the bending moment at point B is at Equation 4.2 or Equation 4.3

$$M_p = \frac{Q_u l}{4} - \frac{M_p}{2} \qquad 4.2$$

or

$$Q_u = 6\left(\frac{M_p}{l}\right) \qquad 4.3$$

Therefore, at collapse as shown in Equation 4.4, the moment at section C is

$$M_c = M_p = \frac{1}{6} Q_u l \tag{4.4}$$

If the beam had remained elastic, the elastic moment at support as shown in Equation 4.5 and Equation 4.6;

$$M_{um} = \left(\frac{5}{32}\right) Q_u L \tag{4.5}$$

$$M_{us} = \left(\frac{3}{16}\right) Q_u L \tag{4.6}$$

The moment redistribution ratio q defines as the ratio of the bending moment at a section after redistribution to that before redistribution, Equation 4.7

$$q = \frac{moment\ after\ redistribution}{moment\ before\ redistribution} \tag{4.7}$$

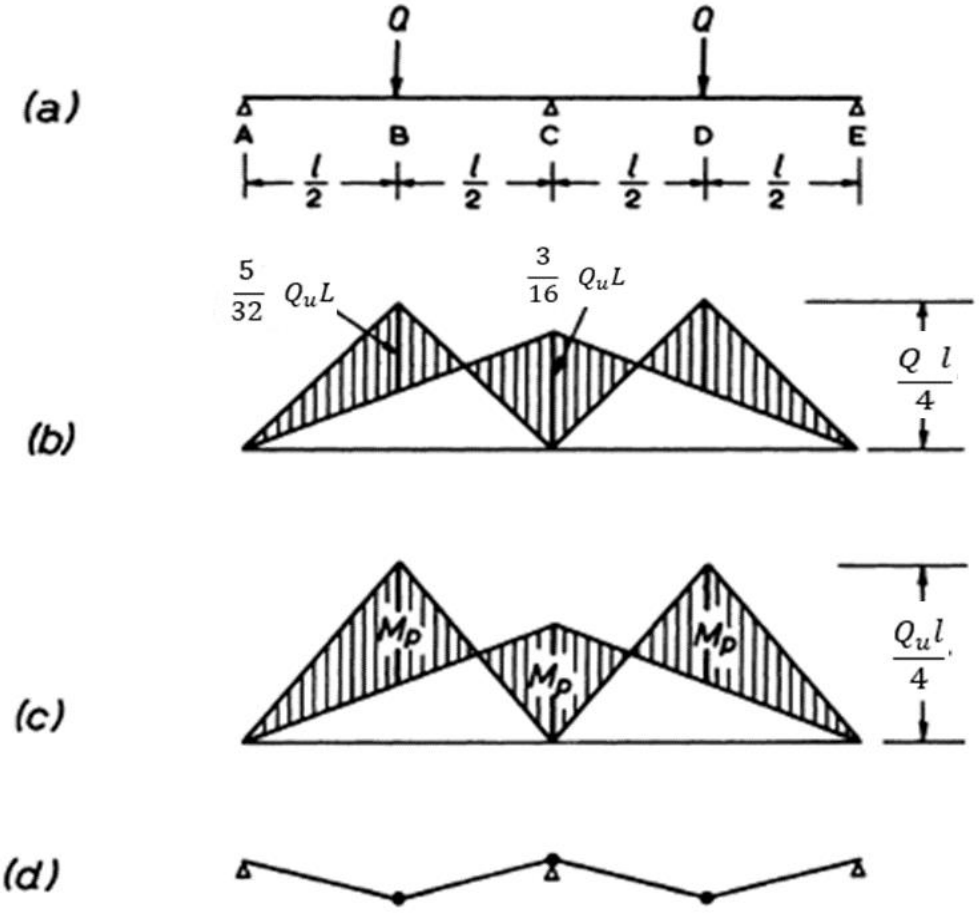

Figure 4.2 Typical moment redistribution and mechanism [9]

And due to moment redistribution, q value would change between reducing (q_s) and improving (q_m) impact, which led to plastic hinge construction sequencens and thus collapase mechanisum.

If the design of section strength capacity changed according to moment redistribution concept, reduction or enhancement section moment resistance ratio (R) is introduced, which is a function of the provided steel reinforcement.

In current research methodology, by design, the beam in Fig. 4.2(a) has;

M_{pm}= (1-R) M_p is a reduced section moment resistance at mid span.

M_{ps}= (1+R) M_p is an enhanced section moment resistance at middle support

So, the moment redistribution ratios at mid span and middle support are shown in Equation 4.8 and Equation 4.9 respectively;

$$q_m = \frac{M_{Pm}}{M_{um}} \quad 4.8$$

$$q_s = \frac{M_{Ps}}{M_{us}} \quad 4.9$$

For control section (R=0), the determined moment redistribution ratios at mid span and middle support are (1.067 and 0.899) respectively. These ratios improved with the increasing of enhanceent strength factor (R) at mid span which is corresponding to the same value of section strength reduction at middle support, the correspnding redistribution ratios are (1.227, 0.75) and (1.38,0.625) for enhancement ratios 15 and 30, respectively, as shown in Figure 4.3. Figure 4.4

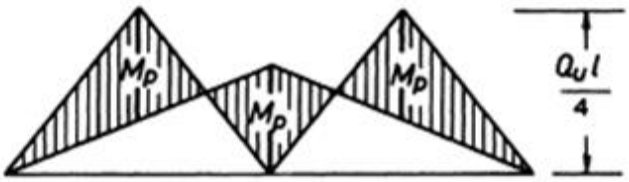

a. (R= 0% q_m=1.067 q_s= **0.899**)

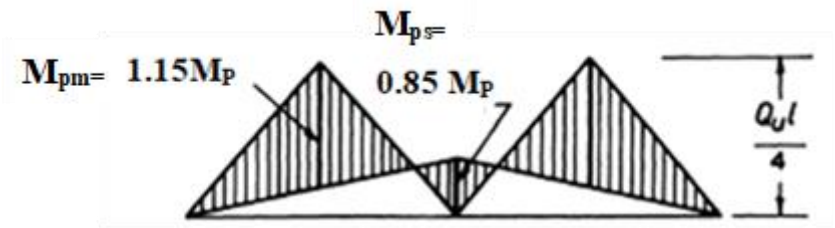

b. (R= 15% q_m=1.227 q_s=0.75)

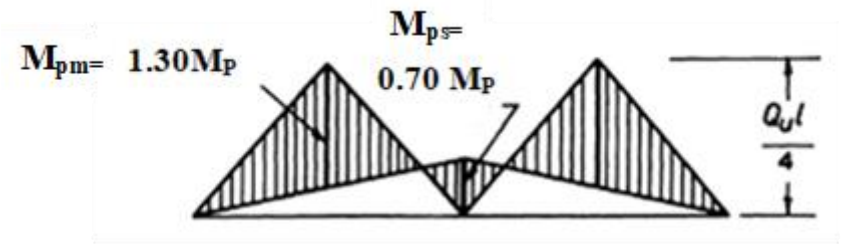

c. (R= 30% q_m=1.38 q_s= 0.625)

Figure 4.3 Moment capacity redistribution

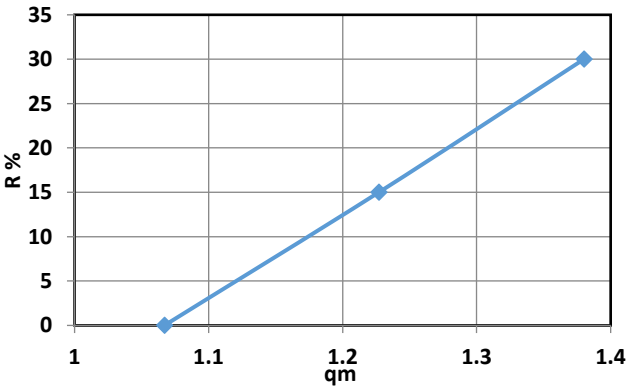

a. at mid span

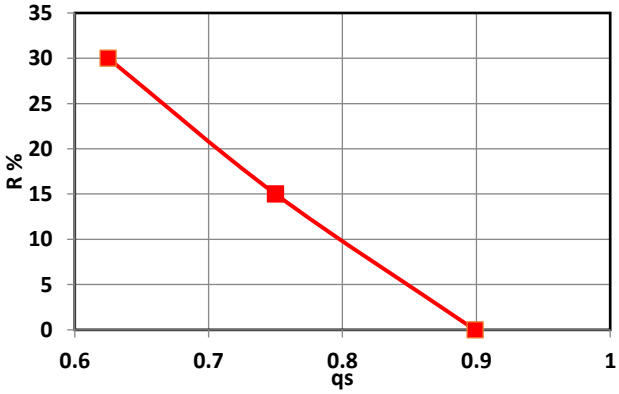

b. at middle support

Figure 4.4 Moment redistribution ratios in scope of adopted enhancement ratios

4.3 Hybrid Section Strength, Mode I

4.3.1 Moment Capacity

The experimenta results of homogeneous and hybrid strength section of mode I (60:20) MPa are shown in Table 4.1. For homogeneous beams section of R= 0 were plastic moment at mid span and middle support (10.967, 10.967) for (20 and 60) MPa respectivily. With the increasing of enhancement ratio its clear to notice that the increase of the results at mid span and decrease at the middle support at R=15 the ratios were (12.88, 13.685) at mid span for 20 and 60 MPa respectivily, and (9.520, 10.115) at middle support, for R=30 the ratios were (15.470,17.593) at mid span and (8.330,9.473) at middle support. While for hybrid section beams showd that the results clearly depicts slightly strengths reduction at mid span and middle support regions in comparing to section of homogenious strength of lower and upper state (20 and 60) MPa, the moment capacity rating are (0.979 and 0.968) respectively, these ratios improved when mid span section strength enhanced by an enhancement strength factor (R) which is corresponding to the same value of section strength reduction at middle support, the correspnding ratios are (1.146, 1.078) and (1.275,1.121) for enhancement ratios 15 and 30, respectively. Figure 4.5 clearly illustrates the assigned strength loads of varios specimens.

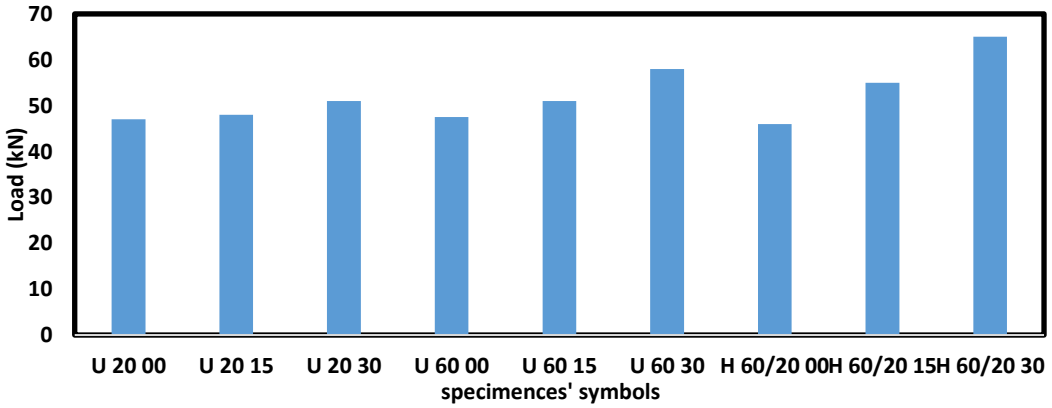

Figure 4.5 The assigned loads of various specimens

Table 4.1 Test result of specimens in Mode I

Group. No	No.	*Specimens	R, %	Q_u, kN	$M_{um}=5Q_uL/32$	$M_{us}=3Q_uL/16$	$M_{Pm}=(1+R)(Q_uL/6)$	$M_{Ps}=(1-R)(Q_uL/6)$	M_{Pm}/M_{Pmi}		M_{Ps}/M_{Psi}	
									Lower limit	Upper limit	Lower limit	Upper limit
Specimens of full lower limit strength												
G1	1	U 20 00	0	47	10.281	12.338	10.967	10.967				
	2	U20 15	15	48	10.500	12.600	12.880	9.520				
	3	U 20 30	30	51	11.156	13.388	15.470	8.330				
Specimens of full upper limit strength												
G2	4	U 60 00	0	47.5	10.391	12.469	11.083	11.083				
	5	U 60 15	15	51	11.156	13.388	13.685	10.115				
	6	U 60 30	30	58	12.688	15.225	17.593	9.473				
Specimens of hybrid strengths (Mode I)												
G4	7	H 60/20 00	0	46	10.063	12.075	10.733	10.733	0.979	0.968	0.979	0.968
	8	H 60/20 15	15	55	12.031	14.438	14.758	10.908	1.146	1.078	1.146	1.078
	9	H 60/20 30	30	65	14.219	17.063	19.717	10.617	1.275	1.121	1.275	1.121

*L= 1400 mm

4.3.2 Load - Deflection Response

The load – deflection responses related to the beams of homogeneous section of lower and upper strength limits, 20 and 60 MPa at the mid of span and at the middle support; are depicted in Figures 4.6 and 4.7, respectively. The same findings were indicated in specimens of hybrid section, Mode I (60:20) as shown in Figure 4.8. while, Figures 4.9 to 4.11; illustrate comparative views related to load deflection responses of hybrid section in respect to those of homogeneous section of lower and upper strength limits for various enhancement strength ratios, R=0%, 15%, and 30% respectively. For beams of lower limit strength Figure 4.6 observed that the behavior of beam at R=15 and 30 were partially matched, while for the upper limit strength Figure 4.7 were there decreasing in stiffness at specimen of R= 30. In case of hybrid strength section Figure 4.8 notice that there were approximately maintain similar proportions with the increasing of enhancement rations. At the comparative between the cases of homogeneous upper and lower with hybrid mode, depict that with R=0 the curve of hybrid beam nearly close to that of lower limit, at R=15 its approaching to upper limit strength, while at R=30 which is differ than the other two cases were its deviated from the two paths.

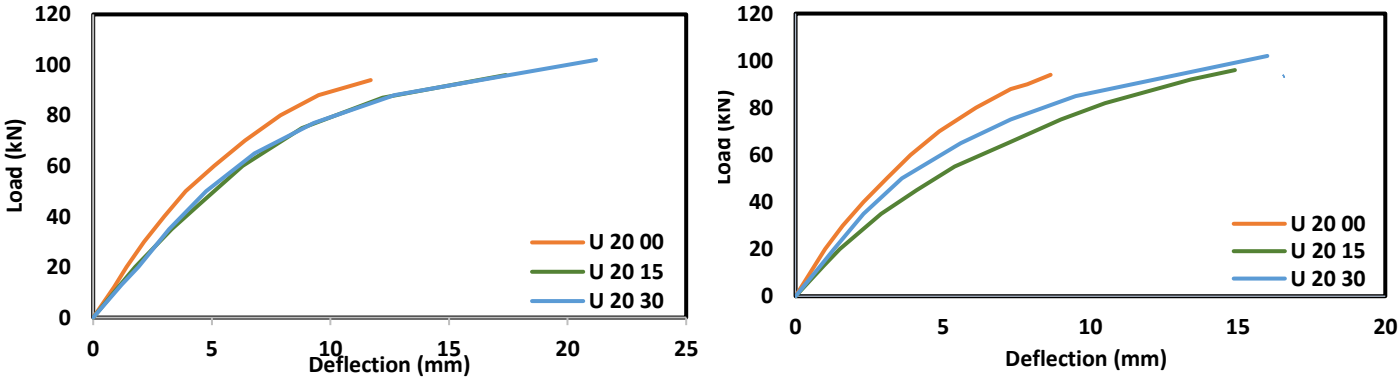

a. at mid span length b. at inner quarter length

Figure 4.6 Load – deflection behavior of homogeneous section specimens with lower strength limit

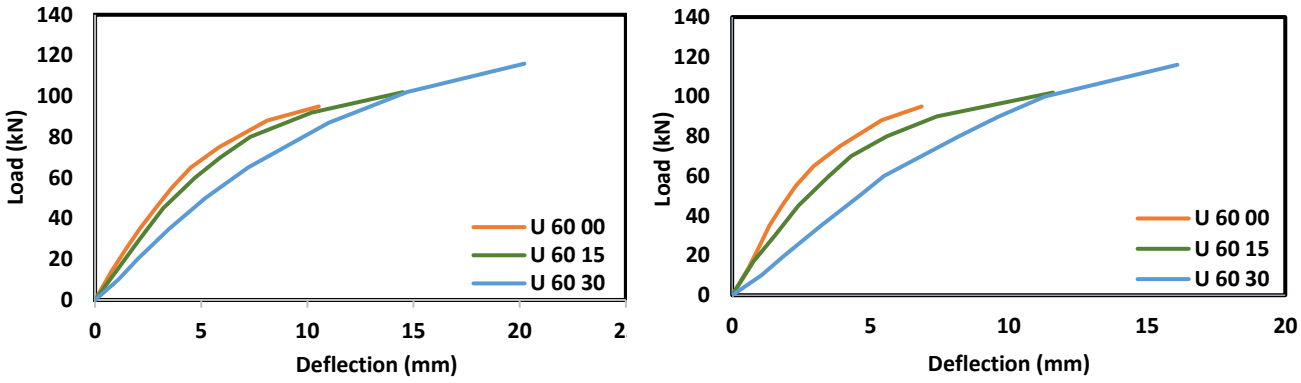

a. at mid span length b. at inner quarter length

Figure 4.7 Load – deflection behavior of homogeneous section specimens with upper strength limit

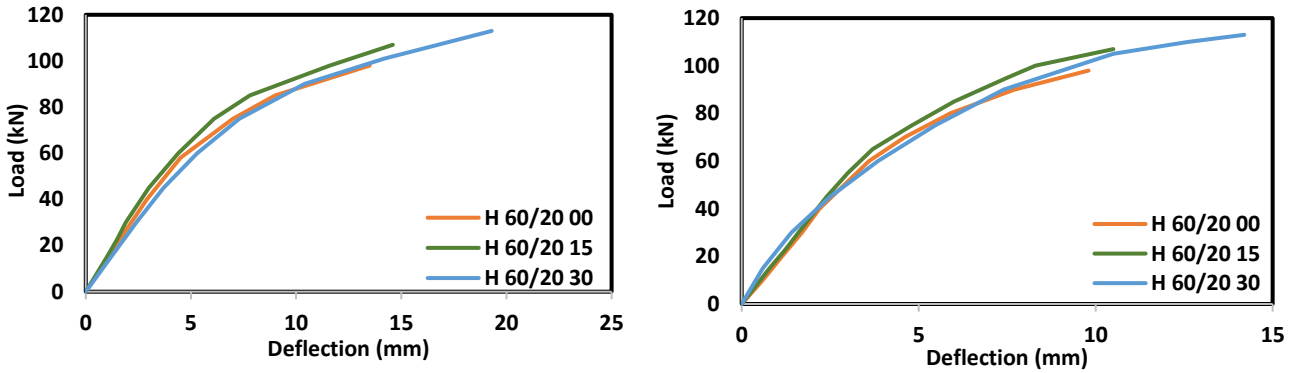

a. at mid span length b. at inner quarter length

Figure 4.8 Load – deflection behavior of hybrid section specimens (mode I)

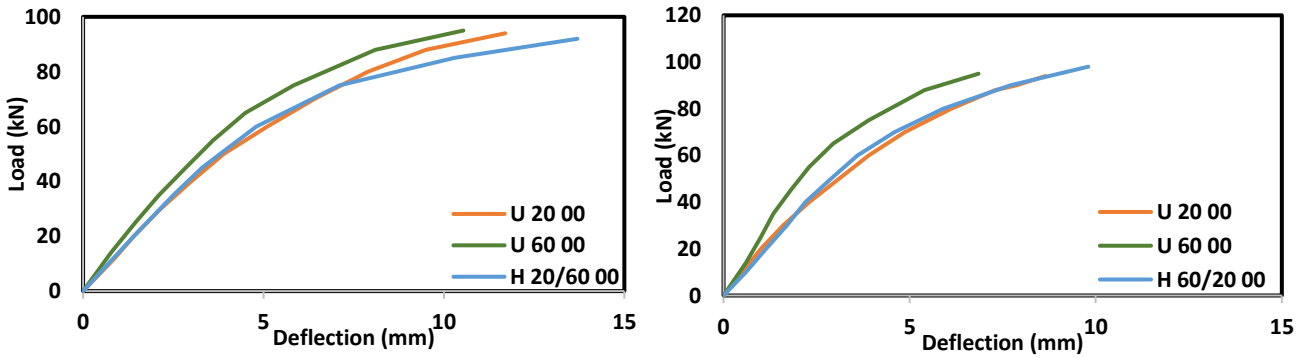

a. at mid span length b. at inner quarter length

Figure 4.9 Load – deflection of specimens with zero% reduction moment resistance ratio

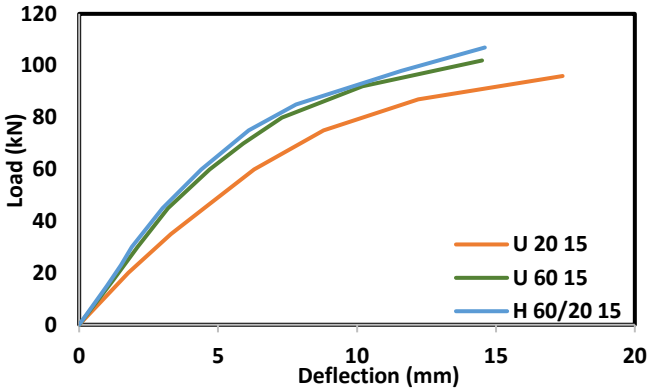

a. at mid span length

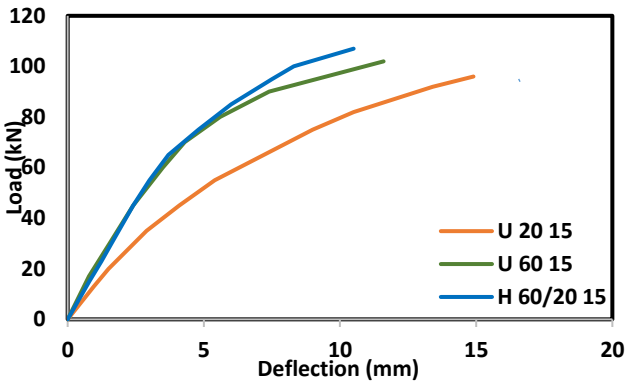

b. at inner quarter length

Figure 4.10 Load – deflection of specimens with 15% reduction moment resistance ratio

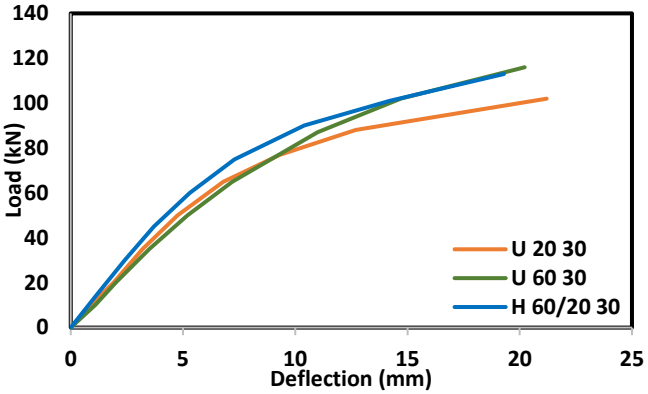

a. at mid span length

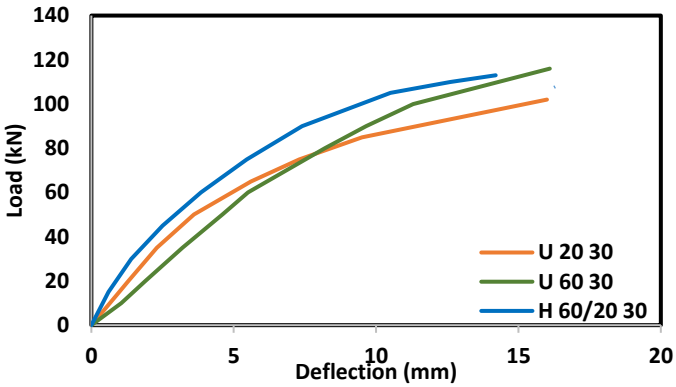

b. at inner quarter length

Figure 4.11 Load – deflection of specimens with 30% reduction moment resistance ratio

4.3.3 Flexural Stiffness

The initial stiffness is considered which is define as the slope of linear part for load-deflection curve and could be determine using Equation 4.10 [35]

$$Stiffness = \frac{Py}{\Delta y} \qquad 4.10$$

The Flexural stiffness analysis is shown in Table 4.2, and illustrated graphically in Figure 4.12. The results showed that, a reduction in stiffness is indicated, for hybrid mode I of R=0%; the reduction rating is 0.85 and 0.78 in respect to those of lower

and upper strength homogenous sections, and this result gives slightly improving or it maintain close proportions of stiffness when comparing with lower limit (1.08, 1.02) and with upper limit strength (1.12, 1.17) for R=15 and 30 respectively. The presence of upper limit strength in hybrid specimens lead to increase the flexural stiffness than that of homogeneous lower limit strength.

Table 4.2 Flexural stiffness

	No.	Specimens	Py, kN	Py /Pyi		Δ_y,mm	Δy /Δyi		Flexural Stiffness (λ), kN/m	λ /λi	
				lower limit	upper limit		lower limit	Upper limit		lower limit	Upper limit
Specimens of full lower limit strength											
G1	1	U 20 00	74			4.80			15.42		
	2	U20 15	78			6.50			12.00		
	3	U 20 30	80			7.20			11.11		
Specimens of full upper limit strength											
G2	4	U 60 00	77			4.60			16.74		
	5	U 60 15	79			6.20			12.74		
	6	U 60 30	87			8.20			10.61		
Specimens of Hybrid strengths (Mode I)											
G4	7	H 60/20 00	76	1.03	0.99	5.80	1.21	1.26	13.10	0.85	0.78
	8	H 60/20 15	78	1.00	0.99	6.00	0.92	0.97	13.00	1.08	1.02
	9	H 60/20 30	87	1.09	1.00	7.00	0.97	0.85	12.43	1.12	1.17

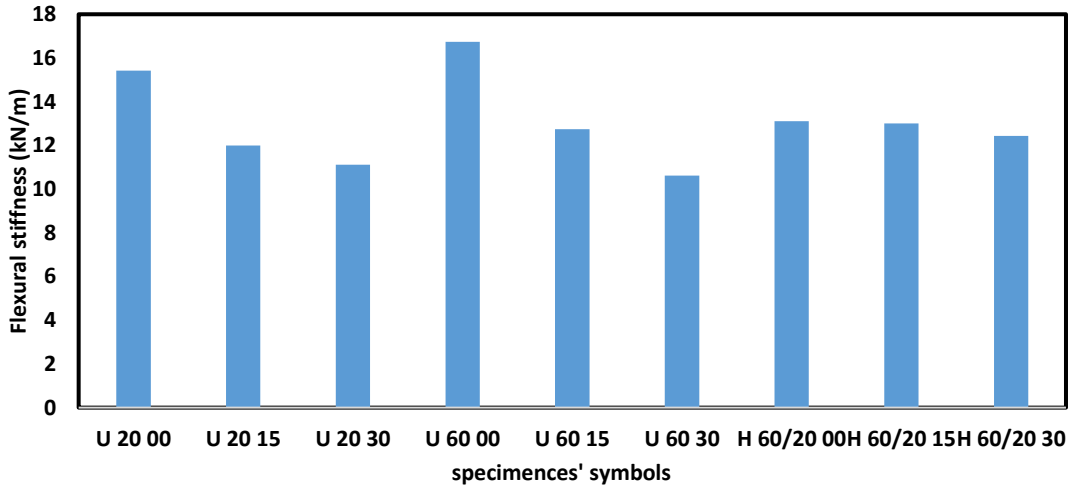

Figure 4.12 Flexural stiffness of specimens

4.3.4 Flexural Ductility

Ductility defined as the ability of members to endure significant deformations before the failure. The ductility index (D) may be calculated from the load-deflection curve by dividing the maximum, deflection (Δu) by the yield deflection (Δy) [35]. The Equation 4.11 is considered;

$$Ductility\ index = \frac{\Delta u}{\Delta y} \qquad 4.11$$

Table 4.3 lists the flexural ductility index related to the effect of current hybrid section of Mode I. The results showed that there are slightly ductility dropping in comparing with specimens of lower strength homogeneous section, the drop rating were 0.96, 0.91 and 0.94 for specimens of R= (0, 15 and 30) % receptively. On the other side, there are slightly upgrading in flexural ductility in comparing with specimens of upper limit strength of homogeneous section, the upgrading rating are 1.02, 1.04 and 1.12 for specimens of R= (0, 15 and 30) % respectively, these rating improved when the enhancement strength ratio increasing (R). Figure 4.13 clearly shows the flexural ductility for related specimens.

Table 4.3 Flexural ductility index

Group No.	No.	Specimens	Δ_y,mm	Δ_u,mm	Flexural ductility index, DI	D_I /D_{Ii}	
						lower limit	upper limit
Specimens of full lower limit strength							
G1	1	U 20 00	4.80	11.70	2.438		
	2	U20 15	6.50	17.40	2.677		
	3	U 20 30	7.20	21.20	2.944		
Specimens of full upper limit strength							
G2	4	U 60 00	4.60	10.54	2.291		
	5	U 60 15	6.20	14.50	2.340		
	6	U 60 30	8.20	20.22	2.466		
Specimens of Hybrid strengths (Mode I)							
G4	7	H 60/20 00	5.80	13.50	2.328	0.96	1.02
	8	H 60/20 15	6.00	14.60	2.433	0.91	1.04
	9	H 60/20 30	7.00	19.30	2.757	0.94	1.12

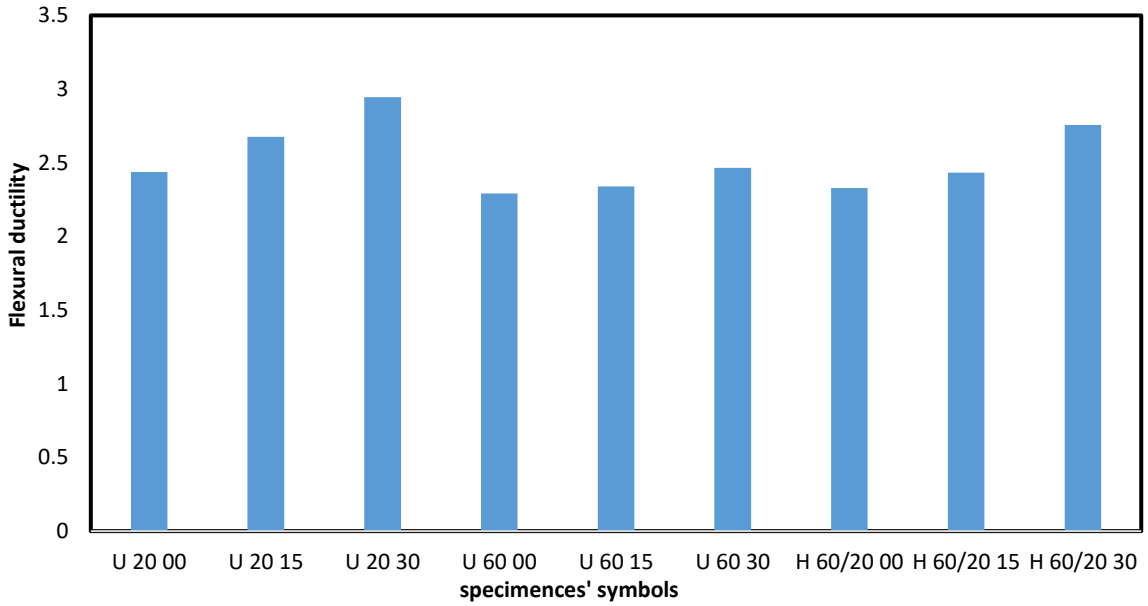

Figure 4.13 Ductility index of specimens

4.3.5 Strain Distribution

The steel tensile strain and concrete compressive strains are measured at mid span and middle support zone, for all tested specimens. Figures 4.14 to 4.16 clearly depict those strains in scope of comparative views in respect to lower and upper homogeneous strength sections for R= 0 %, 15%, and 30%, respectively; for mid span and middle support zones. For hybrid section Mode I of R=0%, the tensile steel strains are compatible with those of upper strength limit section while the compressive concrete strains are compatible with those of lower strength limits. With changing the enhancement ratio, the same observation is noted regards tensile steel strain while the compressive concrete strain tends to get more ductility in comparing with corresponding response of R=0%. The best enhancement assigned for specimens of R=30% where it can be observed that the behavior of concrete approximately matched to that of homogeneous upper limit strength. These observations are the same for mid span and middle support zones.

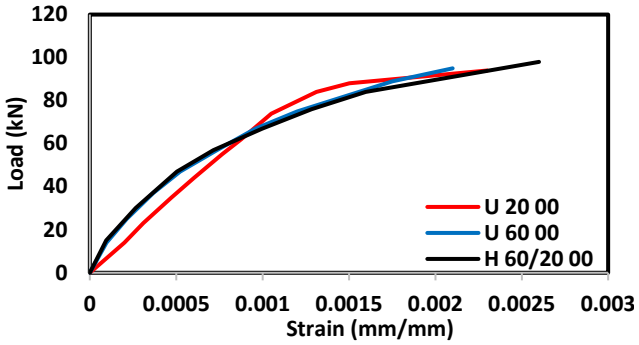

a. Steel mid span

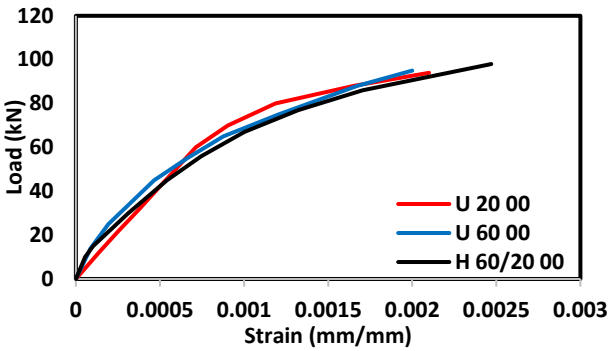

b. Steel middle support

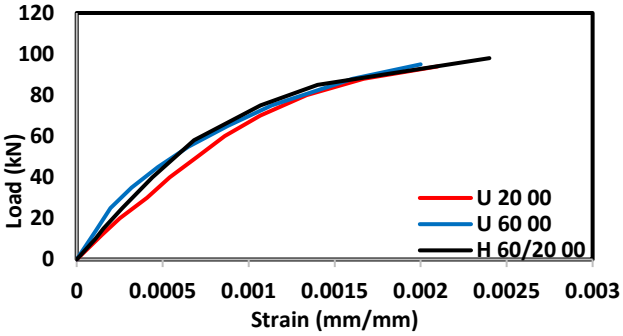

c. Concrete mid span

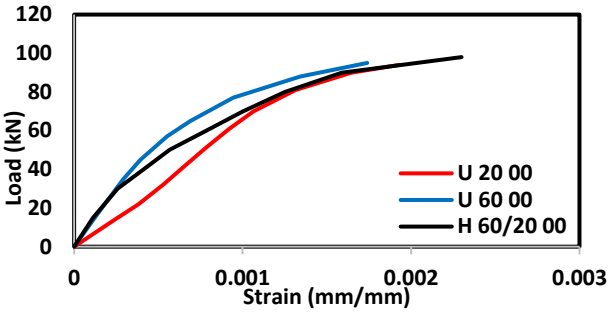

d. Concrete middle support

Figure 4.14 Strain distribution for specimens of R=0%

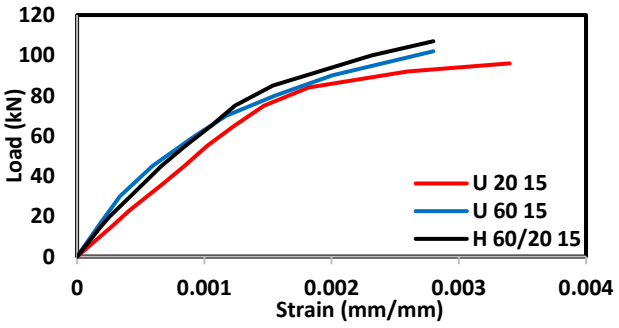

a. Steel mid span

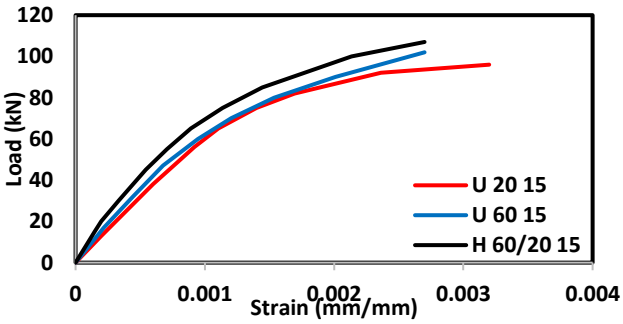

b. Steel middle support

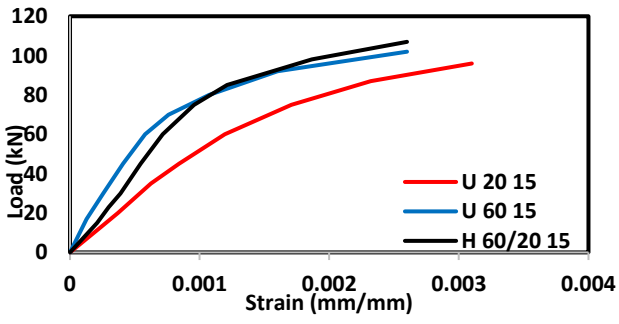

c. Concrete mid span

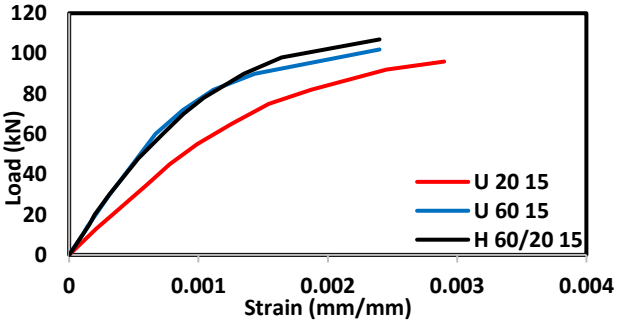

d. Concrete middle support

Figure 4.15 Strain distribution for specimens of R=15%

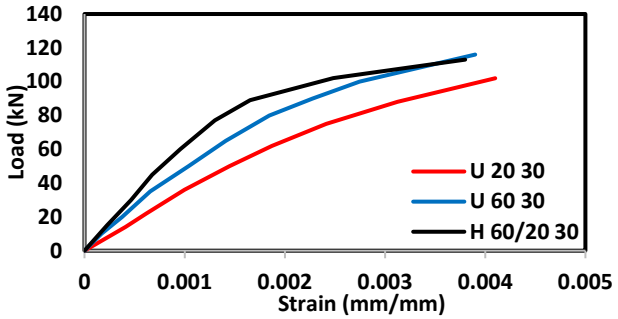

a. Steel mid span

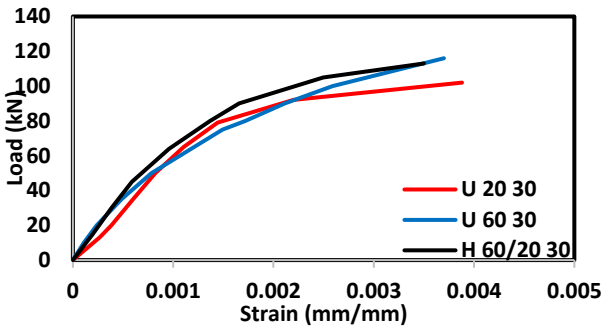

b. Steel middle support

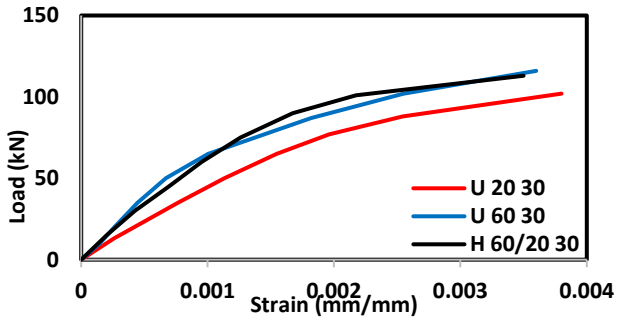

c. Concrete mid span

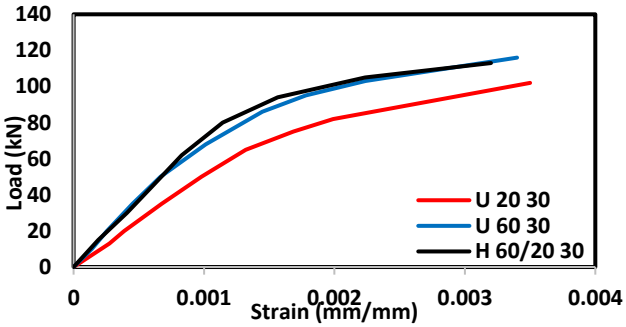

d. Concrete middle support

Figure 4.16 Strain distribution for specimens of R=30%

4.3.6 Plastic Rotation Capacity

The rotation capacity depends mainly on the ultimate strain capacity of concrete, the plastic hinge length, L_p, which can be taken approximately equal to the effective depth (L_p=d) and the depth of the compressive stress block, C [17], as shown in Figure 4.17.

The angle of rotation, θ, of a tensile plastic hinge could be estimated as the following Equation 4.12:

$$\theta = \frac{\varepsilon_p L_p}{c} \qquad 4.12$$

where ε_p is the increase in the strain in the concrete measured from the initial yielding of steel reinforcement in the section [17].

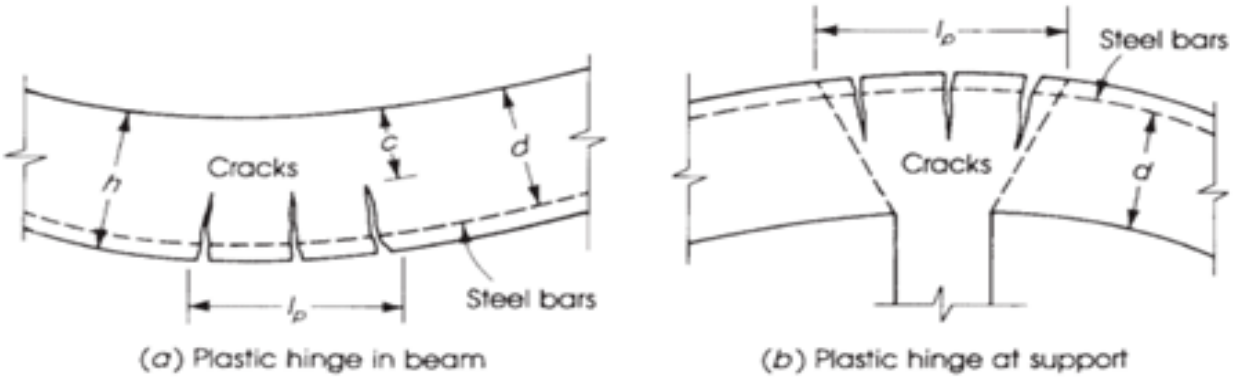

Figure 4.17 Failure mode [17]

The results related to plastic rotation capacity depicts in Table 4.4, generally, the hybrid fashion affects positively on plastic rotation capacity, the improving rates variable between (1.14- 0.88) in respect to homogeneous lower limit strength specimens, and (1.25- 0.95) in respect to homogeneous upper limit strength specimens for various R. While these improving rates decreased as the enhancement ratio increased.

Table 4.4 Plastic rotation capacity

Group No.	No.	Specimens	At Mid Span					
			ϵ_c	ϵ_p	L_p, mm	Θ, rad.	Θ/Θ_i	
							lower limit	Upper limit
Specimens of full lower limit strength								
G1	1	U 20 00	0.0021	0.00196	364	0.01321		
	2	U20 15	0.0031	0.00293	333	0.01807		
	3	U 20 30	0.0038	0.00362	333	0.0223**0**		
Specimens of full upper limit strength								
G2	4	U 60 00	0.0020	0.00179	364	0.01207		
	5	U 60 15	0.0026	0.00237	333	0.01460		
	6	U 60 30	0.0036	0.00335	333	0.02066		
Specimens of Hybrid strengths (Mode I)								
G4	7	H 60/20 00	0.0024	0.00224	364	0.01510	1.1429	1.2514
	8	H 60/20 15	0.0026	0.00234	333	0.01443	0.7986	0.9873
	9	H 60/20 30	0.0035	0.00319	333	0.01967	0.8824	0.9522

4.3.7 The Mechanism of the Beams

where the beam is no longer a structure but a mechanism; the collapse mode is often referred to as the collapse mechanism. [9] mechanism refers to the sequence of plastic hinge formation that caused the failure.

The first crack is appeared in middle supports and growth until the formation of plastic hinge. Throughout the time, mid span region and the next hinges are formed. The sequences of formation are the same for all specimens.

Figure 4.18 is clearly illustrating the getting mechanism, full matching is depicted with specimens of homogeneous high strength section for R= (15 and 30) %. The illustrated mechanism of various enhancement ratios differently shows that, with increasing R% which related to reduce provided steel reinforcement are affected the failure mode and get early collapse. Also, the mechanisms depict that, for no enhancement mid span section (R=0%), the mechanism confirm that the hybrid section tends to get more rotation capacity as segments of failed specimens tend to get more rotations. Figure 4.19 illustrates failed specimens related to hybrid mode I investigation.

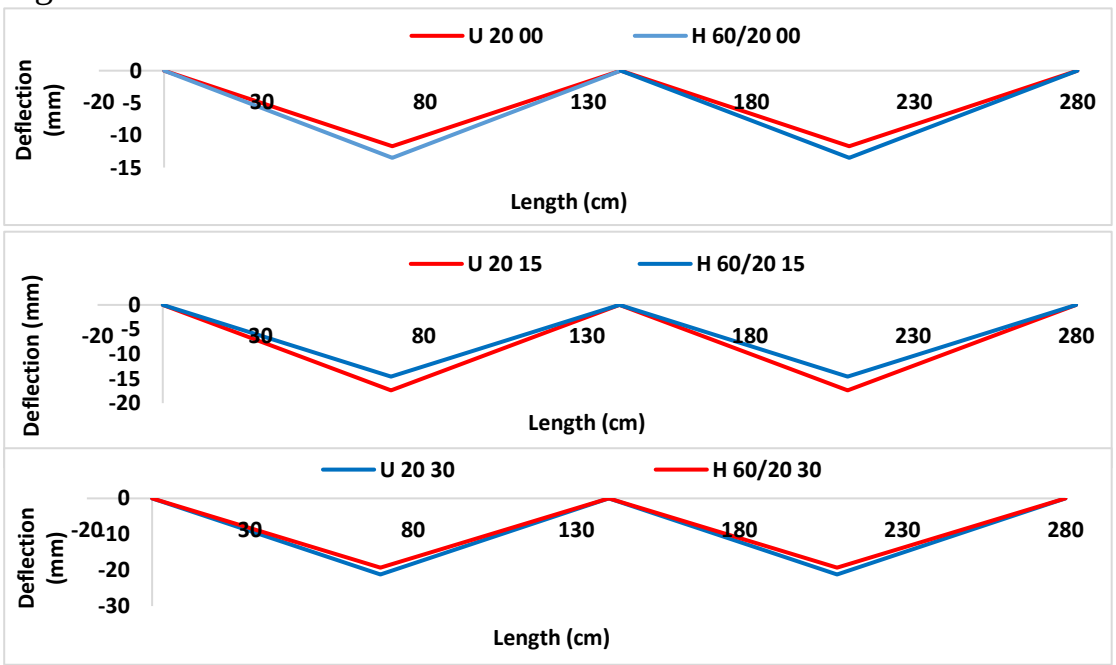

a. lower limit strength compared with hybrid section strength

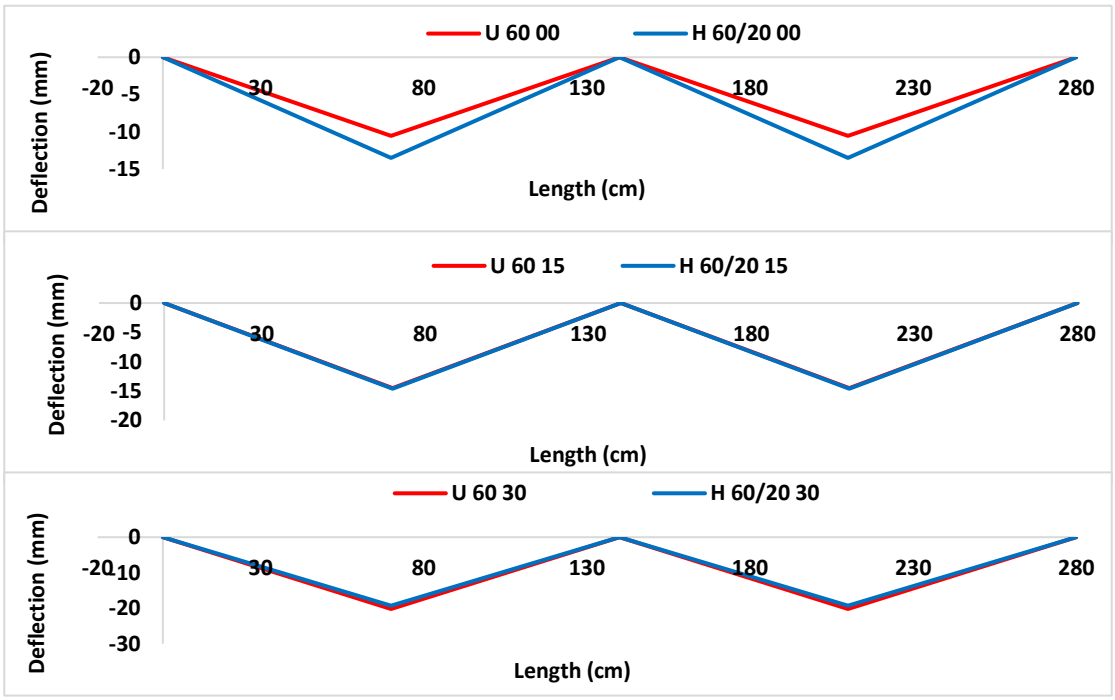

b. upper limit strength compared with hybrid section strength

Figure 4.18 (a) and (b) The mechanism of the beams for lower and upper limits compared with hybrid strength section

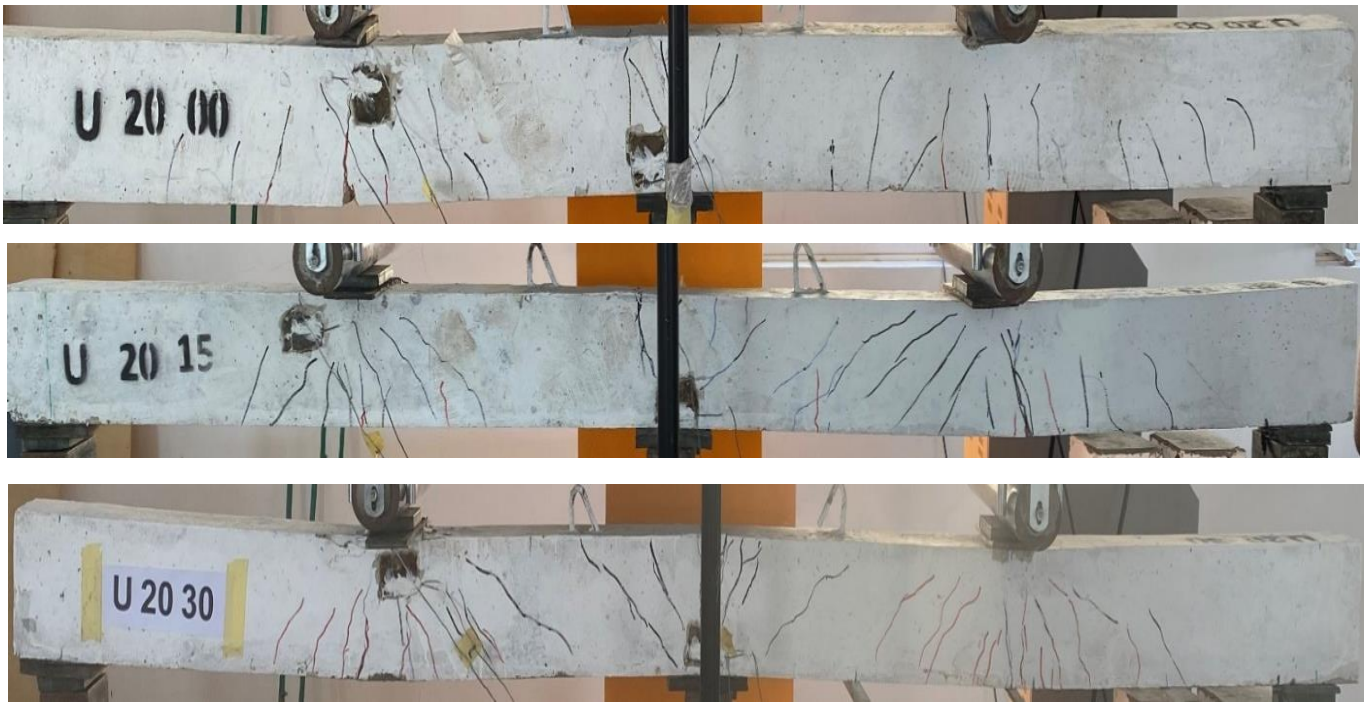

a. lower limit strength

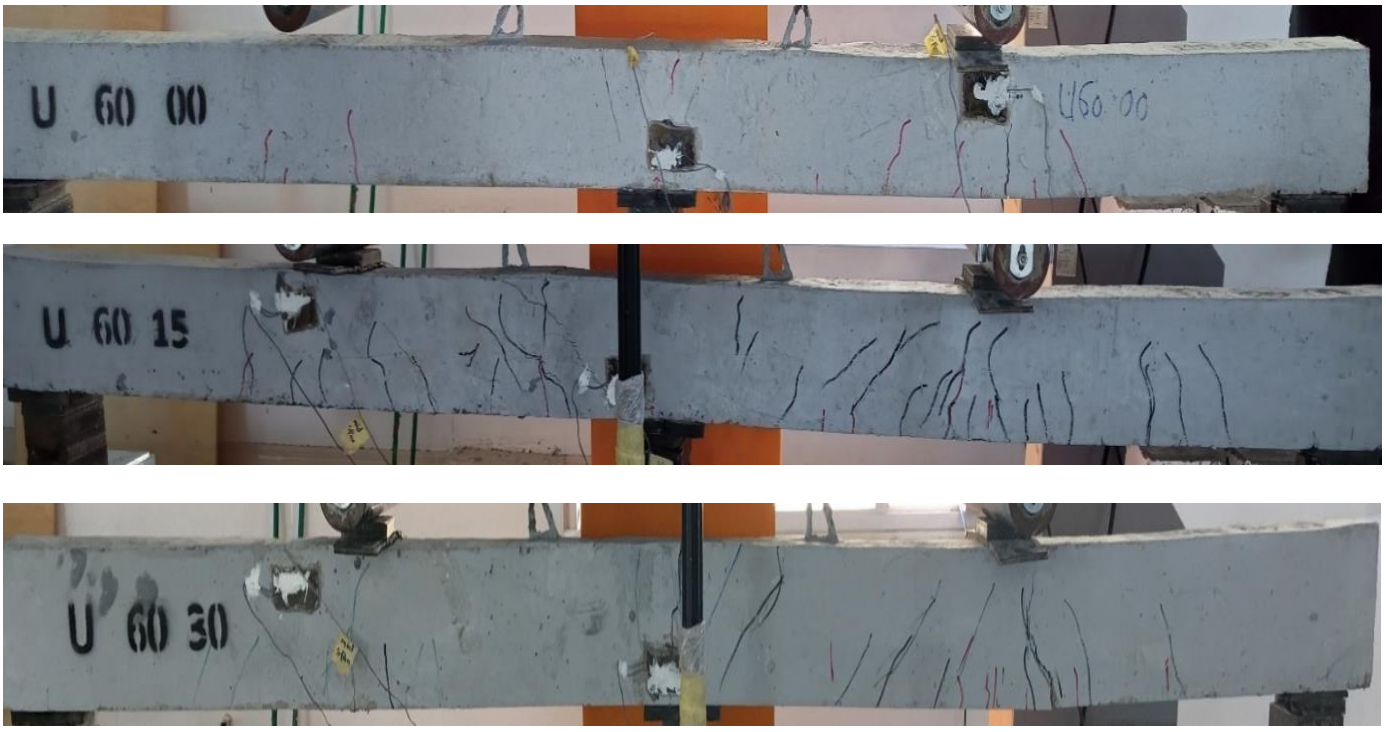

b. upper limit strength

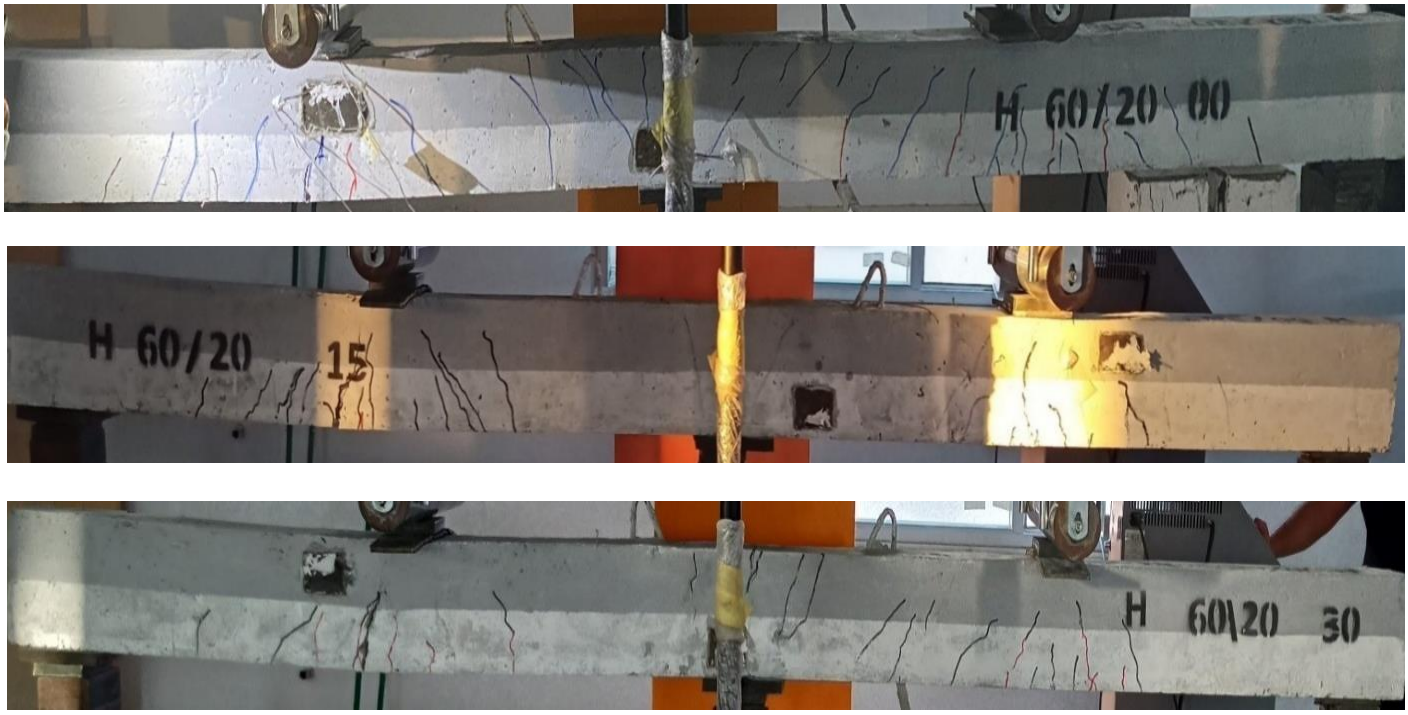

c. hybrid strength section (Mode I)

Figure 4.19 Cracking patterns of beams

4.3.8 The Dissipation of Energy

The virtual work method is considered in calculation of energy dissipation as clear in Equation 4.13:

$$Internal\ work = External\ work = P_u \times \Delta \qquad 4.13$$

Table 4.5 and Figure 4.20 shows the energy dissipation for the specimens, it could be observed the increase of energy dissipation linearly with the increase of enhancement ratio (R) for each homogenous and hybrid strength section specimen. The results were (1.2, 0.94, 1.01) for R= (0, 15, 30) respectively in comparing with homogeneous lower strength of 20 MPa, and equal to (1.32, 1.06 and 0.93) for the same rates of R in comparing with homogeneous upper strength of 60 MPa.

Table 4.5 The dissipation of energy

Group No.	No.	Specimens	Energy (kN.mm), T	T /Ti	
				lower limit	Upper limit
Specimens of full lower limit strength					
G1	1	U 20 00	1099.8		
	2	U20 15	1670.4		
	3	U 20 30	2162.4		
Specimens of full upper limit strength					
G2	4	U 60 00	1001.3		
	5	U 60 15	1479.0		
	6	U 60 30	2345.5		
Specimens of Hybrid strengths (Mode I)					
G4	7	H 60/20 00	1323.0	1.20	1.32
	8	H 60/20 15	1562.2	0.94	1.06
	9	H 60/20 30	2181.0	1.01	0.93

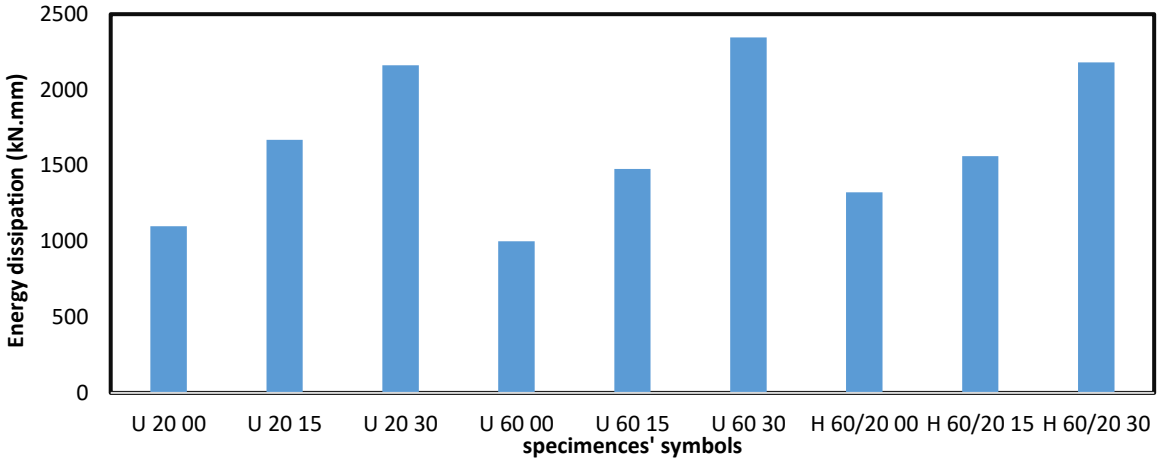

Figure 4.20 The dissipation of energy

4.4 Hybrid Section of Mode II

4.4.1 Moment Capacity

Table 4.6 shows the results related to specimens of hybrid section of Mode II (20: 60 MPa). For specimens of R=0, the results depict that moment capacity upgrading rates is (1.032 and 1.043) in comparing with homogeneous section strength of (20 and 60) MPa respectively, the upgrading rates are significantly improved as the enhancement ratio increased, where the corresponding upgrading rates are (1.115 and 1.049) and (1.108 and 0.974) for R=15 % and 30%, respectively. Figure 4.21 clearly depicts the variation in the obtained strength loads of various specimens.

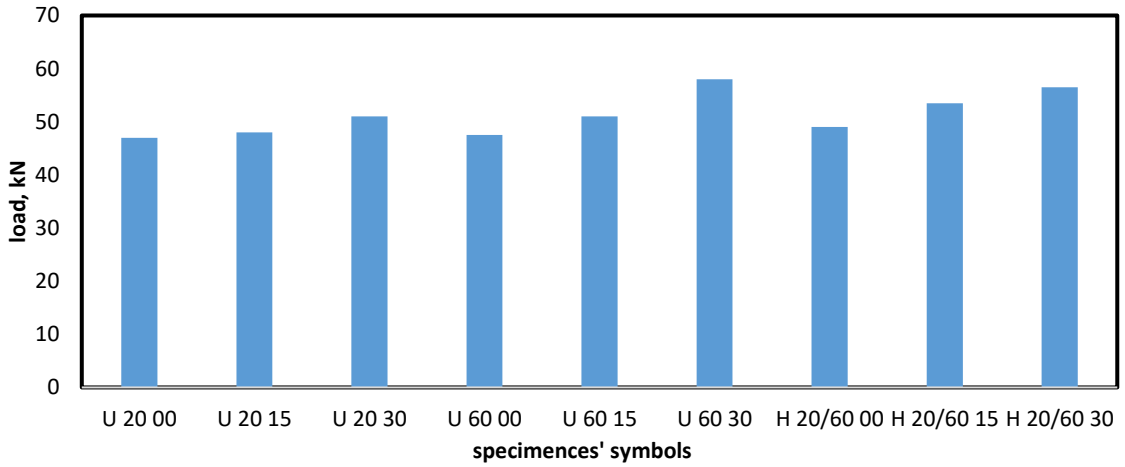

Figure 4.21 The assigned loads of various specimens

Table 4.6 Test results for Mode II specimens

Group No.	No.	Specimens	R, %	Q_u, kN	$M_{um}=5Q_uL/32$	$M_{us}=3Q_uL/16$	$M_{Pm}=(1+R)(Q_uL/6)$	$M_{Ps}=(1-R)(Q_uL/6)$	M_{Pm}/M_{Pmi}		M_{Ps}/M_{Psi}	
									Lower limit	Upper limit	Lower limit	Upper limit
Specimens of full lower limit strength												
G1	1	U 20 00	0	47.0	10.28	12.34	10.97	10.97				
	2	U20 15	15	48.0	10.50	12.60	12.88	9.52				
	3	U 20 30	30	51.0	11.16	13.39	15.47	8.33				
Specimens of full upper limit strength												
G2	4	U 60 00	0	47.5	10.39	12.47	11.08	11.08				
	5	U 60 15	15	51.0	11.16	13.39	13.69	10.12				
	6	U 60 30	30	58.0	12.69	15.23	17.59	9.47				
Specimens of Hybrid strengths (Mode II)												
G3	7	H 20/60 00	0	49.0	10.72	12.86	11.43	11.43	1.043	1.032	1.043	1.032
	8	H 20/60 15	15	53.5	11.70	14.04	14.36	10.61	1.114	1.049	1.114	1.049
	9	H 20/60 30	30	56.5	12.36	14.83	17.14	9.23	1.108	0.974	1.108	0.974

4.4.2 Load- Deflection Response

The load – deflection responses that related to the beams of homogeneous section of lower and upper strength limits, 20 MPa, and 60 MPa; are depicted in Figures 4.22 and 4.23, respectively. The same finding is indicated in specimens of hybrid section, Mode II (20:60) as shown in Figure 4.24. while, Figures 4.25, 4.26, and 4.27; illustrated comparative views related to load deflection responses of hybrid section in respect to those of homogeneous section of lower and upper strength limits for various enhancement strength ratios, R=0%, 15%, and 30% respectively. For R=0, the response of specimens of homogeneous exhibits more stiffness and strength than specimens of hybrid mode II, will with the increasing of enhancement rates, the stiffness and strength are significantly improved. This observation doesn't indicate in specimens of Mode I, as the response was the same for all adopted R. This could be contributed to the effect of present of 60 MPa as dominated concrete strength in middle region which serve from early deformation.

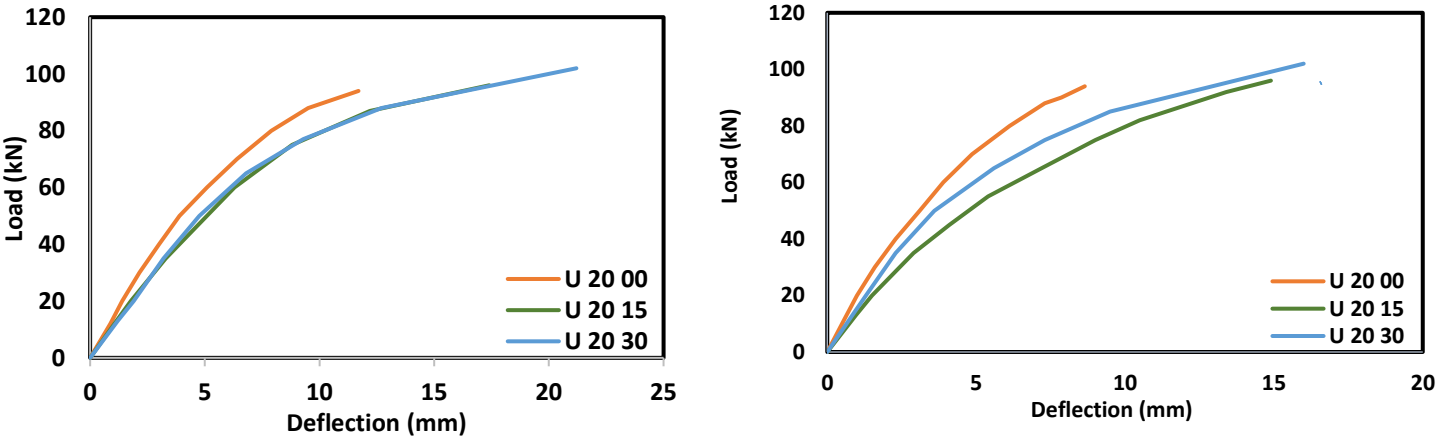

a. at mid span length b. at inner quarter length

b. Figure 4.22 Load – deflection of specimens with homogeneous strength of lower limit

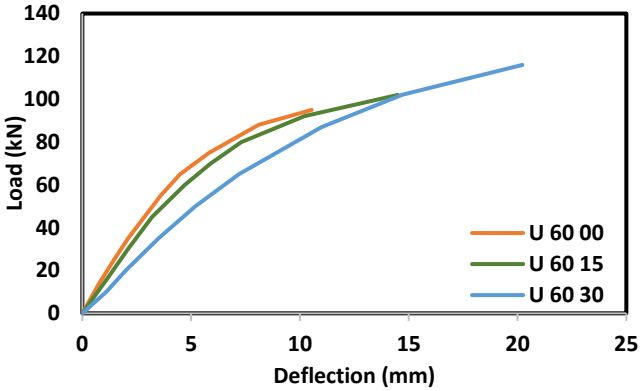

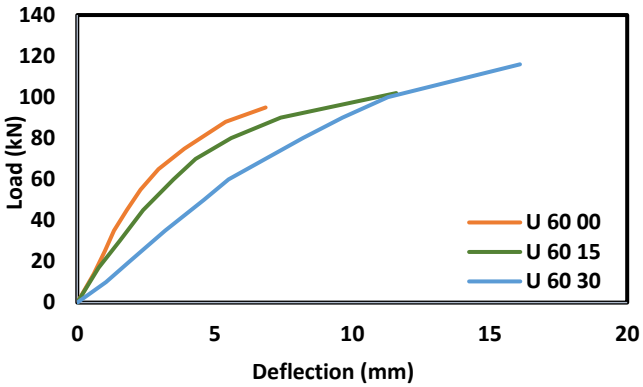

a. at mid span length b. at inner quarter length

Figure 4.23 Load – deflection of specimens with homogeneous strength of upper limit

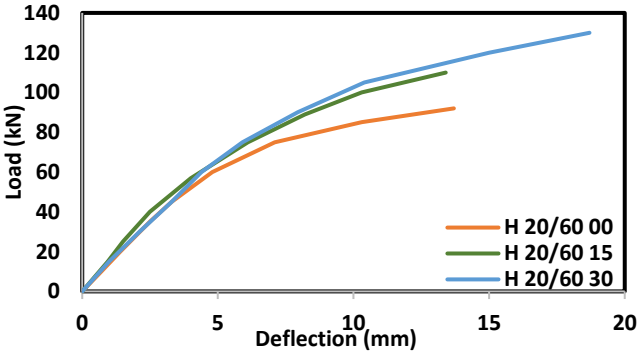

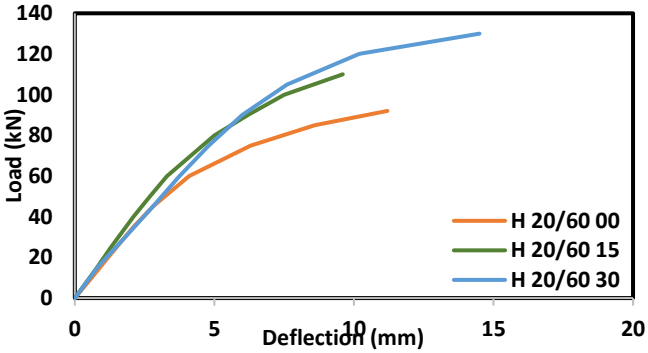

a. at mid span length b. at inner quarter length

Figure 4.24 Load – deflection of specimens with hybrid strength

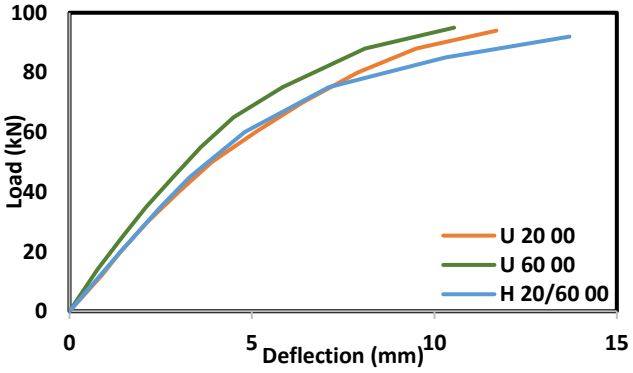

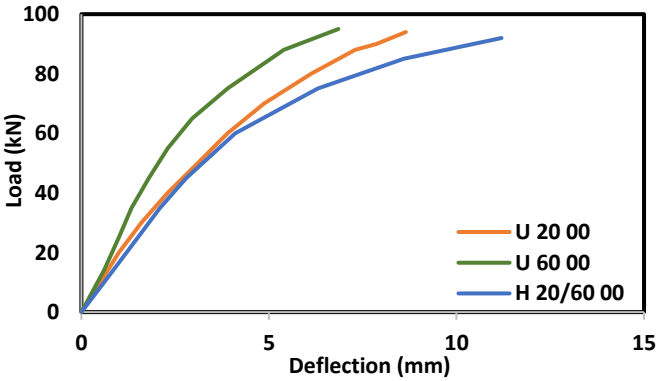

a. at mid span length b. at inner quarter length

Figure 4.25 Load – deflection of specimens with zero% reduction moment resistance ratio

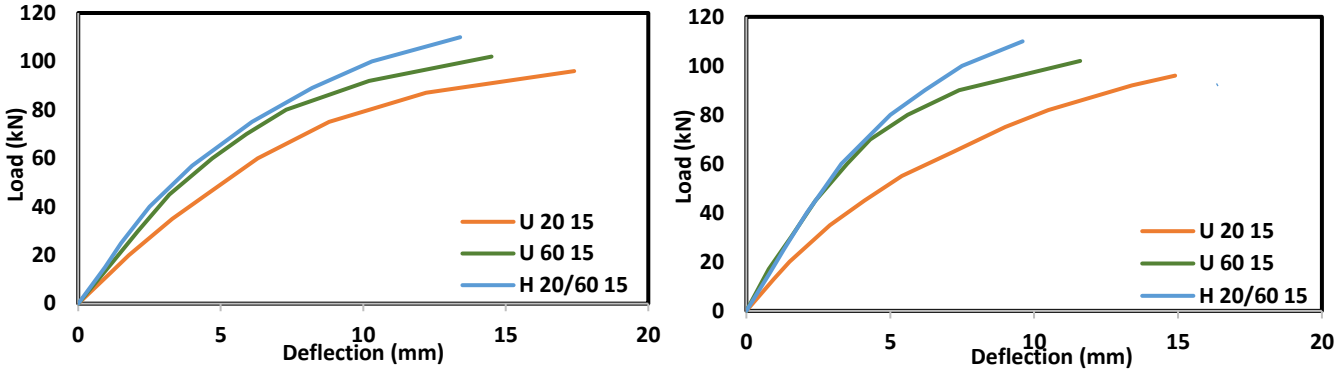

a. at mid span length b. at inner quarter length

Figure 4.26 Load – deflection of specimens with 15% reduction moment resistance ratio

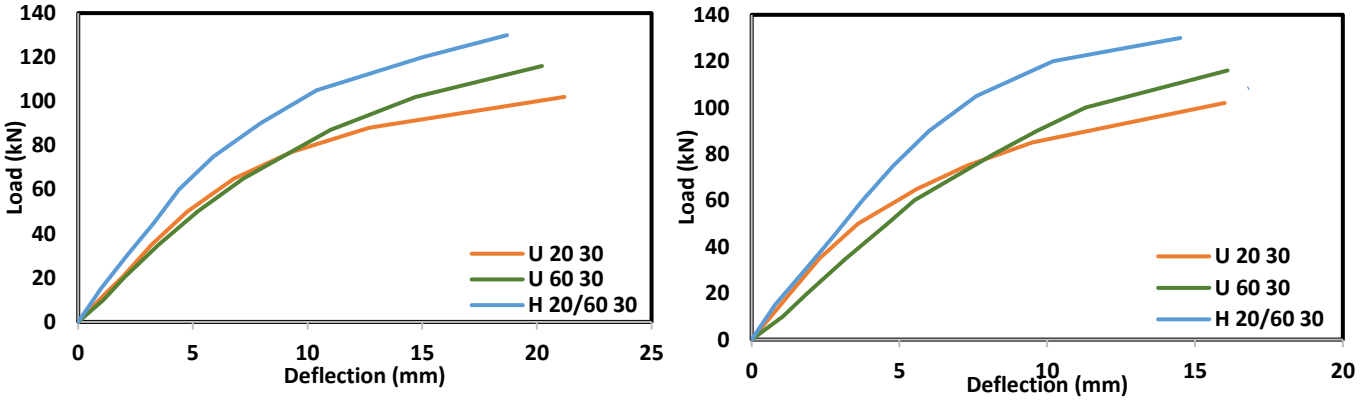

a. at mid span length b. at inner quarter length

Figure 4.27 Load – deflection of specimens with 30% reduction moment resistance ratio

4.4.3 Flexural Stiffness

Table 4.7 and Figure 4.28 shown the measured and related analysis of flexural stiffness of beams of hybrid strength section in comparing with those of homogeneous strength section of lower and upper limit. A reduction in flexural stiffness is attainted in hybrid specimen of R=0, while; with the increasing of R, the reduction turns to upgrading. For R= 15%, the upgrading rates are 1.37 and 1.22 in

comparing with lower strength limit and 1.29 and 1.28 in comparing with specimens of upper strength limit.

Table 4.7 Flexural stiffness

Group No.	No.	Specimens	Py, kN	Py /Pyi of lower limit	Py /Pyi of upper limit	Δ_y mm	Δy /Δyi of lower limit	Δy /Δyi of Upper limit	Flexural Stiffness (λ), kN/m	λ /λi of lower limit	λ /λi of Upper limit
Specimens of full lower limit strength											
G1	1	U 20 00	74			4.8			15.42		
	2	U20 15	78			6.5			12.00		
	3	U 20 30	80			7.2			11.11		
Specimens of full upper limit strength											
G2	4	U 60 00	77			4.6			16.74		
	5	U 60 15	79			6.2			12.74		
	6	U 60 30	87			8.2			10.61		
Specimens of Hybrid strengths (Mode II)											
G3	7	H 20/60 00	75	1.014	0.97	5.1	1.06	1.11	14.71	0.95	0.88
	8	H 20/60 15	82	1.050	1.04	5.0	0.77	0.81	16.4	1.37	1.29
	9	H 20/60 30	92	1.150	1.06	6.8	0.94	0.83	13.53	1.22	1.28

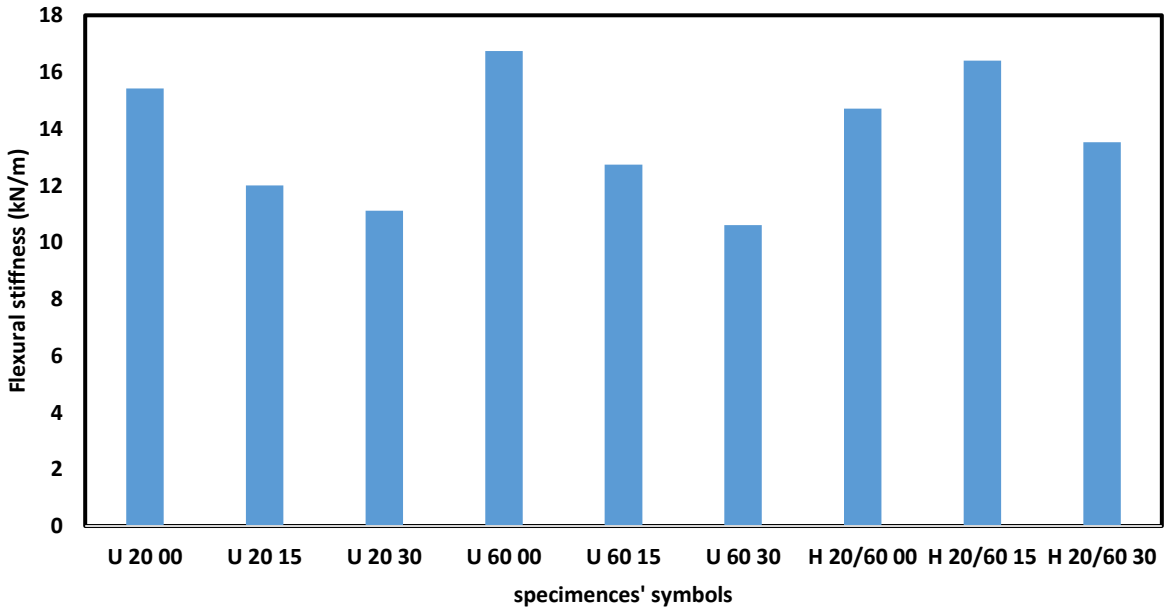

Figure 4.28 Flexural stiffness of specimens

4.4.4 Flexural Ductility

Table 4.8 and Figure 4.29 exhibit the result and related analysis regards flexural ductility of specimens of hybrid strength section (mode II). The results depict that, the specimens of hybrid mode II exhibit better flexural ductility that those of homogeneous high strength section and relatively compatible with those of homogeneous normal strength section. The comparing with homogeneous section of lower and upper limit strength exhibit that, for homogeneous strength section of high strength, the ductility increased as R increased, the rating are 1.17, 1.15 and 1.12 for R = (0, 15 and 30%) respectively; while for homogeneous strength section of normal strength section the increase in ductility is slightly improving. Generally, the flexural ductility improving is dropped as enhancement rate increase which is against the observation in specimens of Mode I with exhibit improving in ductility with R increasing. The relatively best ductility confirms that, the flexural ductility dominated by the concrete properties of lower layer of mid span region.

Table 4.8 Flexural ductility index

Group No.	No.	Specimens	Δ_y, mm	Δ_u, mm	Flexural ductility index, D_I	D_I / D_{Ii}	
						lower limit	upper limit
Specimens of full lower limit strength							
G1	1	U 20 00	4.8	11.70	2.438		
	2	U20 15	6.5	17.40	2.677		
	3	U 20 30	7.2	21.20	2.940		
Specimens of full upper limit strength							
G2	4	U 60 00	4.6	10.54	2.291		
	5	U 60 15	6.2	14.50	2.340		
	6	U 60 30	8.2	20.22	2.466		
Specimens of Hybrid strengths (Mode II)							
G3	7	H 20/60 00	5.1	13.70	2.686	1.10	1.17
	8	H 20/60 15	5.0	13.40	2.680	1.00	1.15
	9	H 20/60 30	6.8	18.70	2.750	0.93	1.12

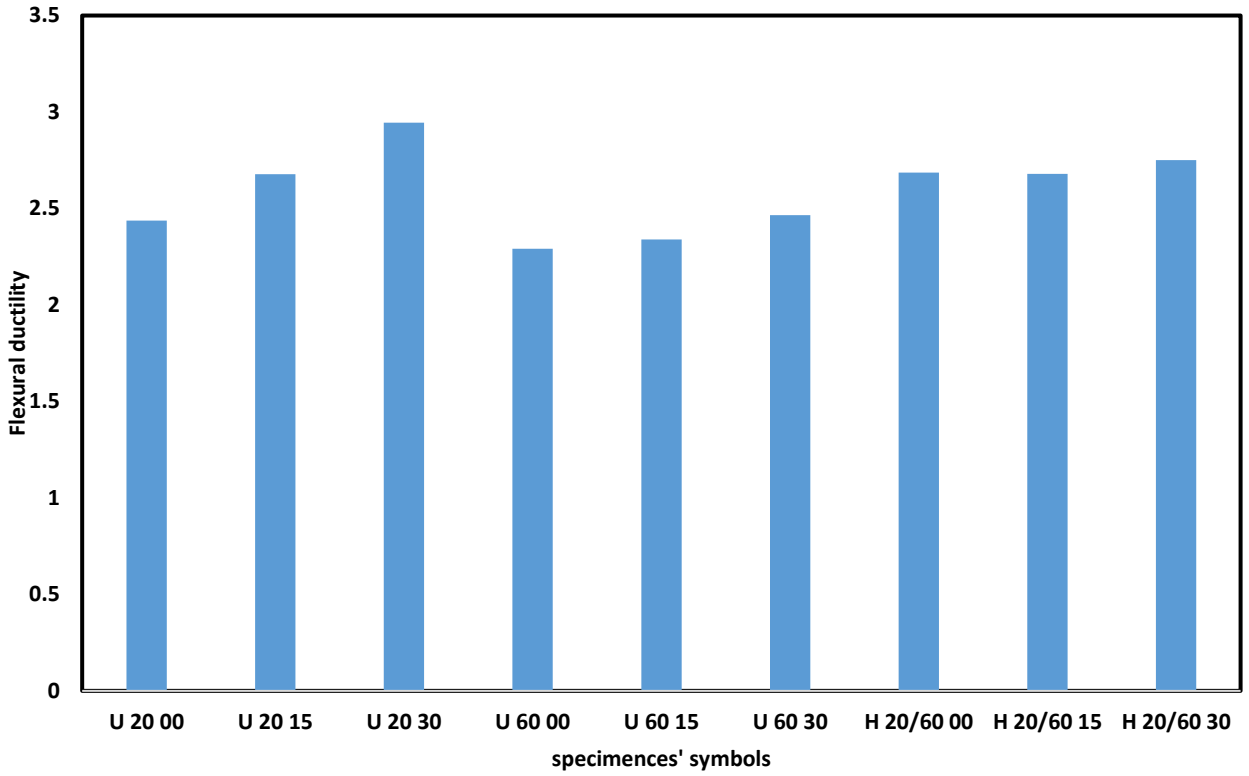

Figure 4.29 Ductility index of specimens

4.4.5 Strain Distribution

The steel tensile strain and concrete compressive strains are measured at mid span and middle support zone, for all adopted moment redistribution ratios. Figures 4.30, to 4.32 clearly depict those strains in scope of comparative views in respect to lower and upper homogeneous strength sections for R= 0 %, 15%, and 30%, respectively; for mid span and middle support zones. Which are clearly depict that, the compressive concrete strain and steel tensile strain are compatible and the variation in response could be distinguished with enhancement ratio increasing, the hybrid specimens exhibit higher stiffness and strength and the got improving with R increasing.

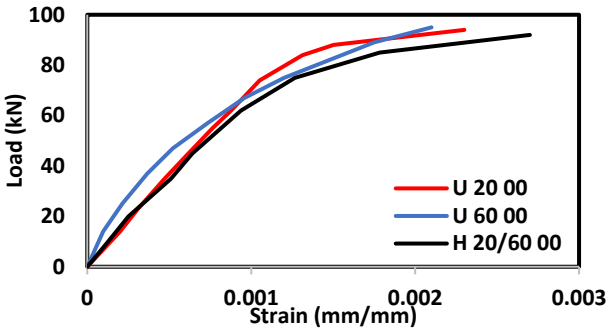

a. Steel mid span

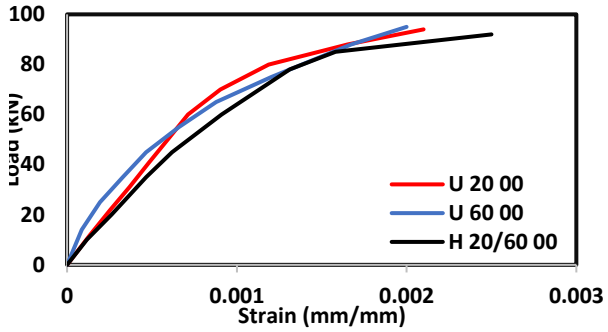

b. Steel middle support

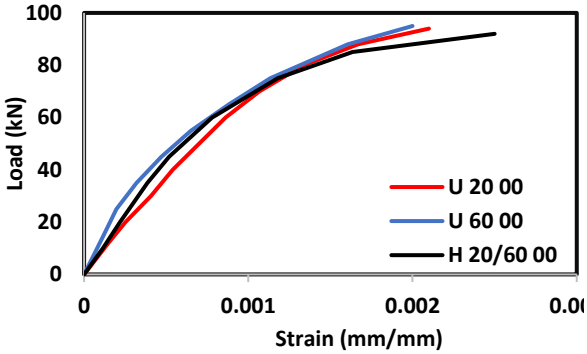

c. Concrete mid span

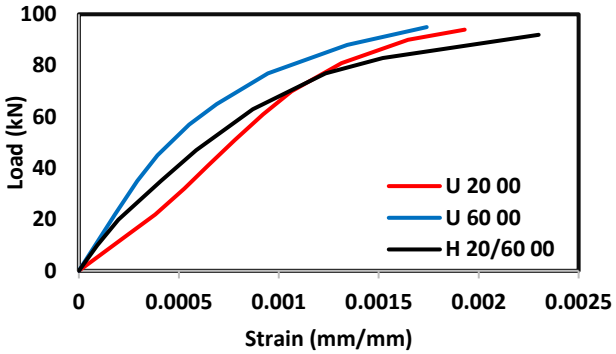

d. Concrete middle support

Figure 4.30 Strain distribution for specimens of R=0%

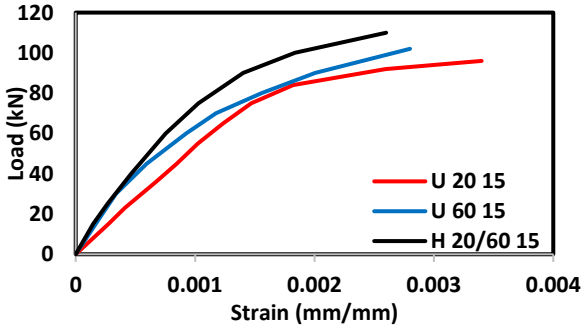

a. Steel mid span

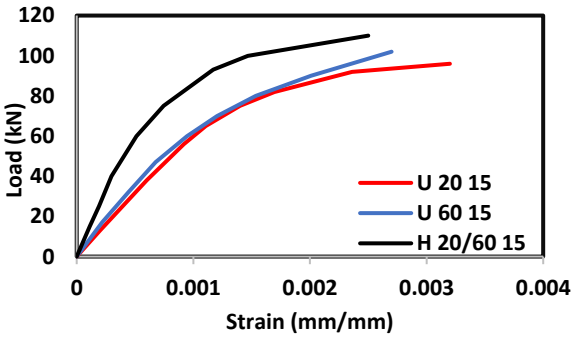

b. Steel middle support

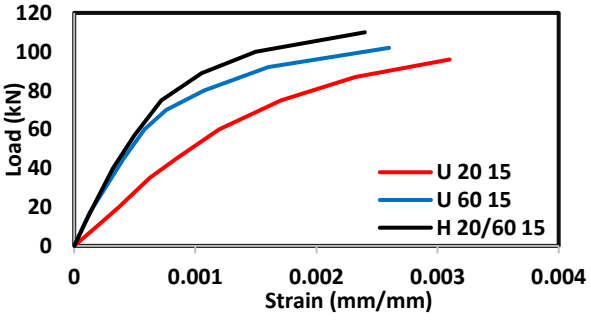

c. Concrete mid span

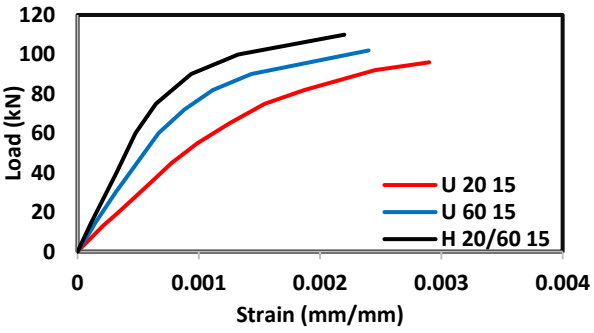

d. Concrete middle support

Figure 4.31 Strain distribution for specimens of R=15%

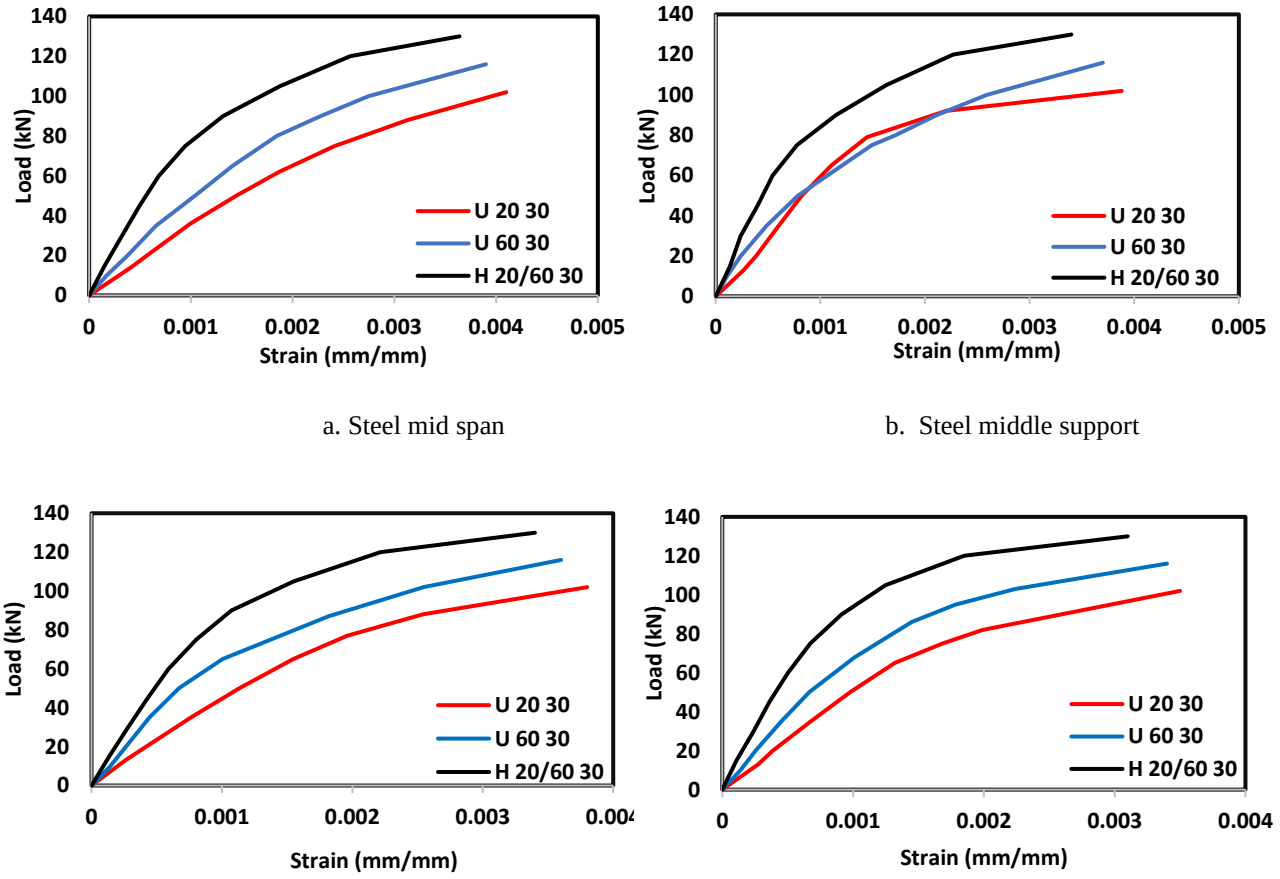

a. Steel mid span

b. Steel middle support

c. Concrete mid span

d. Concrete middle support

Figure 4.32 Strain distribution for specimens of R=30%

4.4.6 Plastic Rotation Capacity

Table 4.9 depict plastic rotation capacity of tested hybrid specimens of mode II and related analysis with those of homogeneous strength.

The indicated plastic rotation capacities are approximately the same as that of specimens of homogeneous high strength and get relatively decreasing in comparing with those of lower strength.

Table 4.9 Plastic rotation capacity

Group No.	No.	Specimens	At Mid Span					
			ϵ_c	ϵ_p	L_p, mm	Θ, rad.	Θ/Θ_i	
							lower limit	Upper limit
Specimens of full lower limit strength								
G1	1	U 20 00	0.0021	0.00196	364	0.0132		
	2	U20 15	0.0031	0.00293	333	0.0181		
	3	U 20 30	0.0038	0.00362	333	0.0223		
Specimens of full upper limit strength								
G2	4	U 60 00	0.002	0.00179	364	0.0121		
	5	U 60 15	0.0026	0.00237	333	0.0146		
	6	U 60 30	0.0036	0.00335	333	0.0207		
Specimens of Hybrid strengths (Mode II)								
G3	7	H 20/60 00	0.0025	0.00237	364	0.0160	1.2092	1.3240
	8	H 20/60 15	0.0024	0.00226	333	0.0139	0.7713	0.9536
	9	H 20/60 30	0.0034	0.00323	333	0.0199	0.8935	0.9642

4.4.7 The Mechanism of the Beams

Likewise, mode I, the first crack is appeared in middle supports and growth until the formation of plastic hinge. Throughout the time, mid span region and the next hinges are formed. The sequences of formation are the same for all specimens. Figure 4.33 clearly illustrates the getting mechanism, full matching is depicted with specimens of homogeneous high strength section for R= (15 and 30) %. The illustrated mechanism of various enhancement ratios differently shows that, with increasing R% which related to reduce provided steel reinforcement are affected the failure mode and get early collapse. Figure 4.34 illustrates failed specimens related to hybrid mode II.

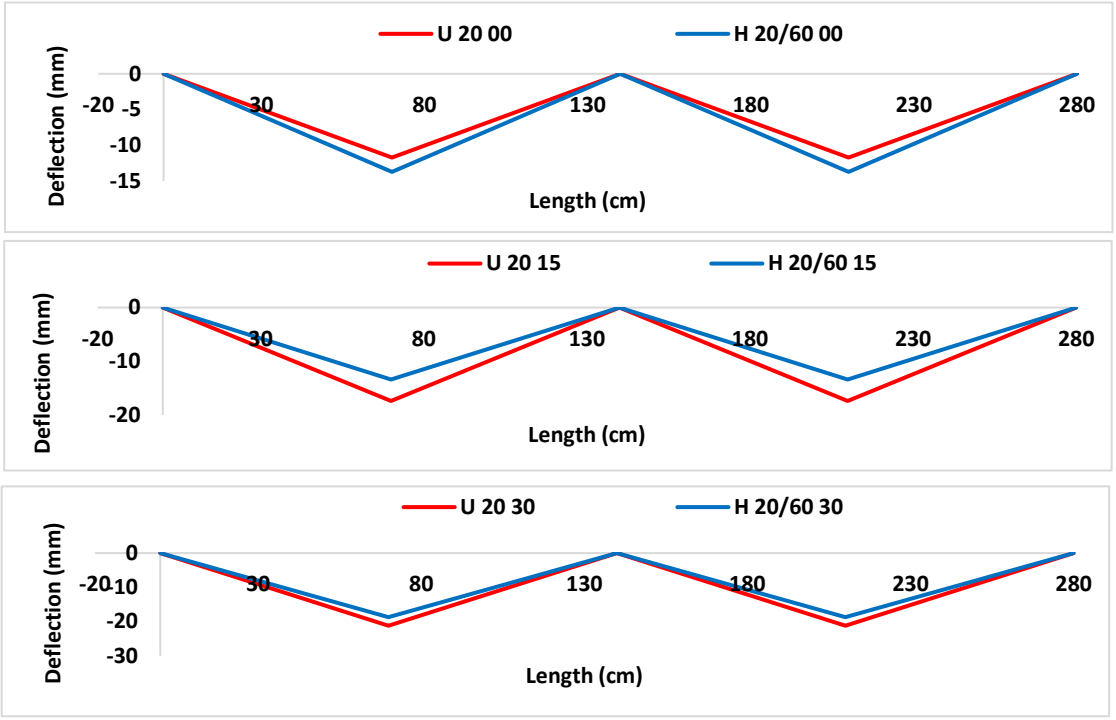

a. lower limit strength compared with hybrid section strength

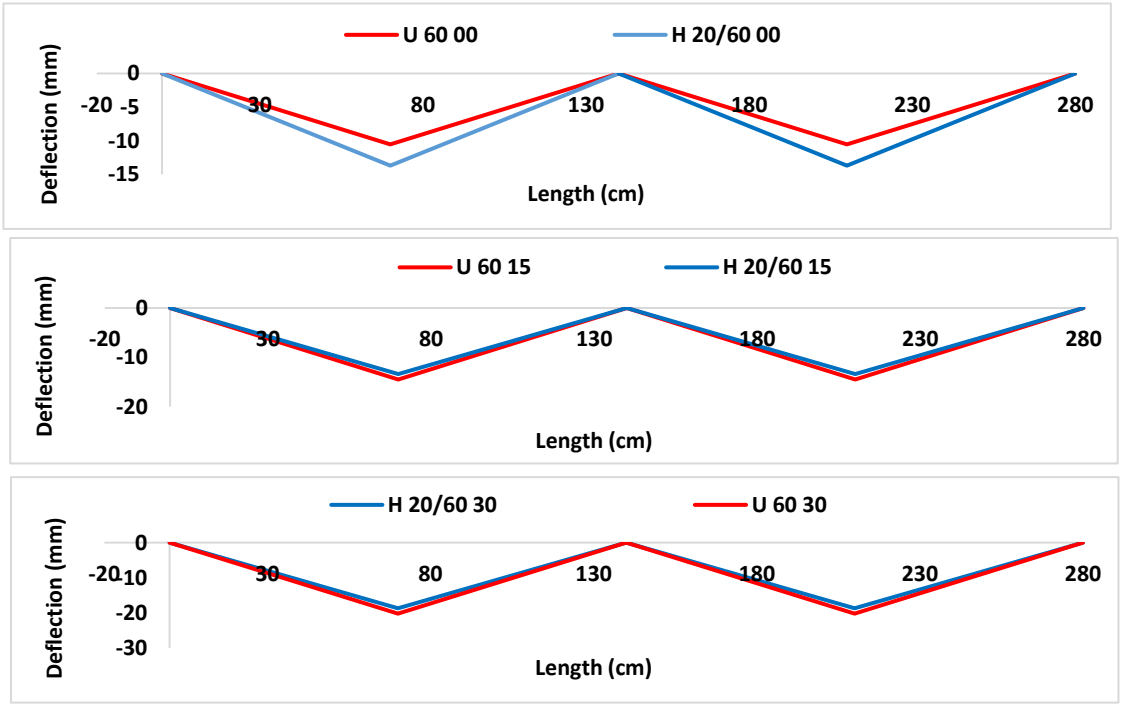

c. upper limit strength compared with hybrid section strength

Figure 4.33 (a) and (b) Mechanism; comparative views of hybrid sections related to normal and high strength sections respectively (mode II)

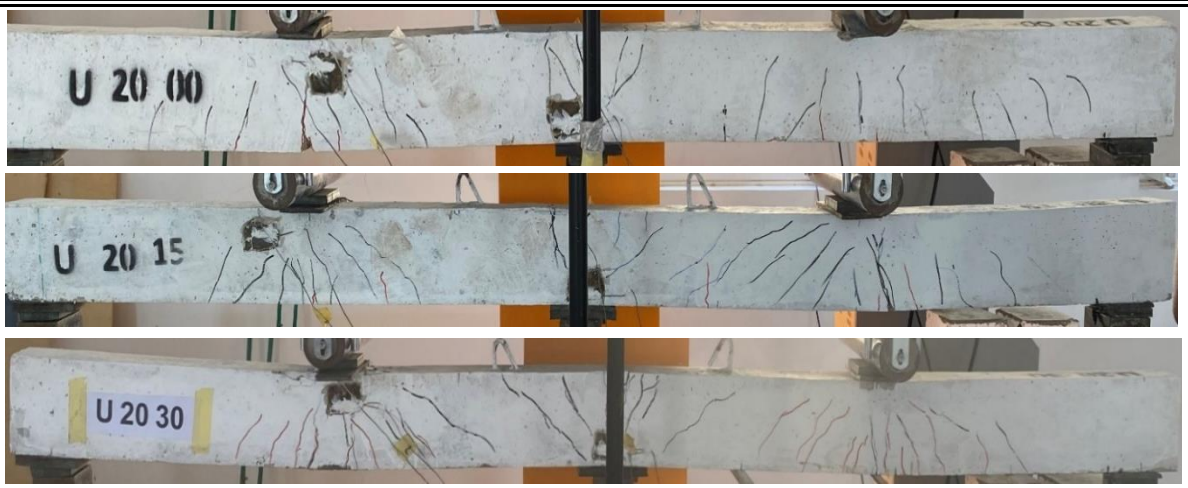

a. lower limit strength

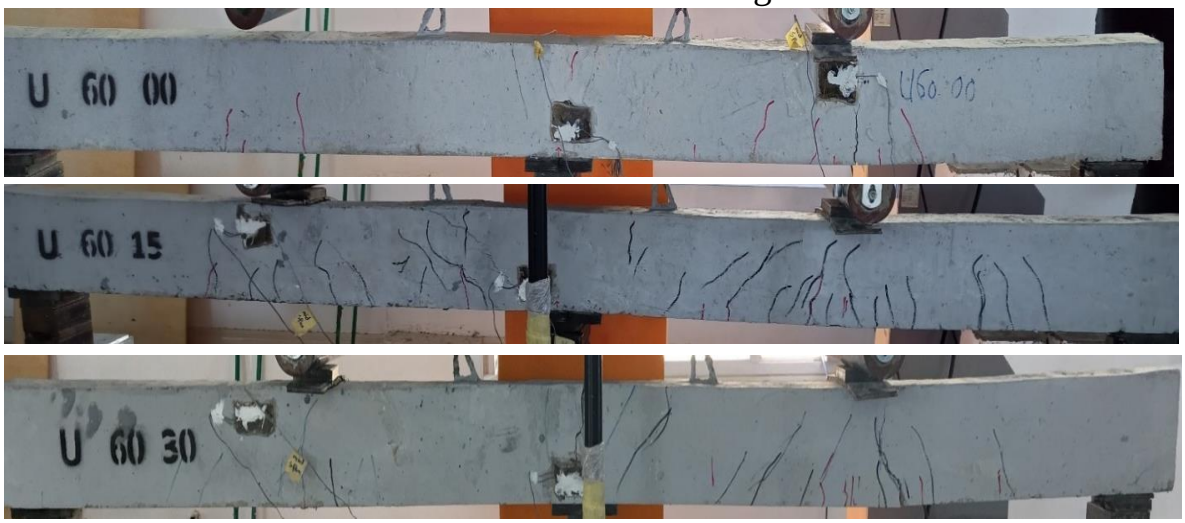

b. upper limit strength

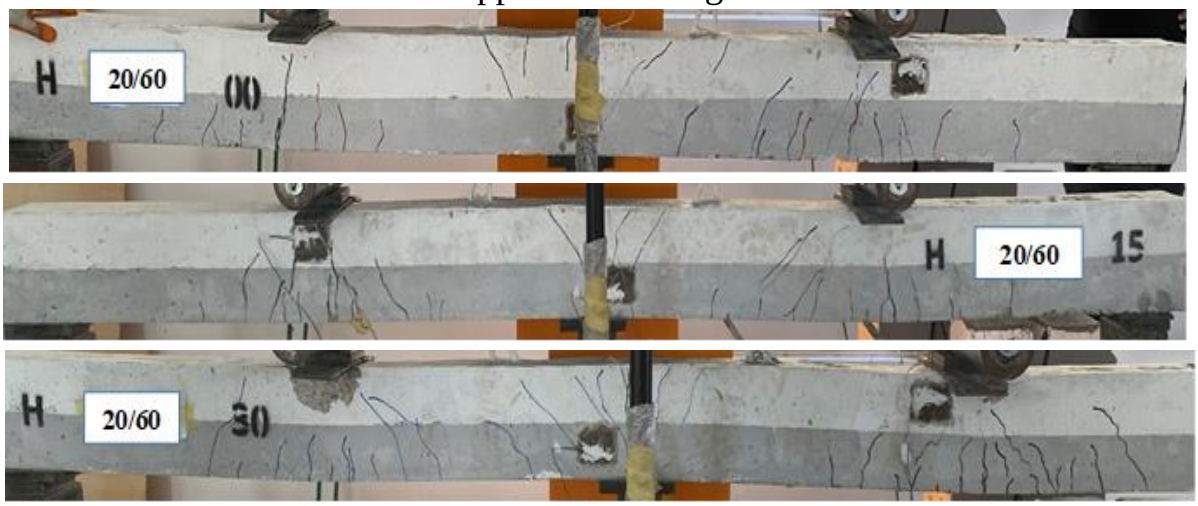

c. hybrid section strength

Figure 4.34 Cracking patterns of beams

4.4.8 The Dissipation of Energy

Table 4.10 and Figure 4.35 shown energy dissipation of tested specimens of homogeneous strength section of lower and upper limit strength in comparing with hybrid strength section of mode II.

The results exhabites that the specimens of uniform strength (normal or high) have lower energy dissipation. The enhancing of section strength by 15%, 30 % correspond to get energy improving for different modes,

For specimens of hybrid mode of various enhancement rates, R (0, 15, 30), the energy dissipation improving rate are 1.15, 0.88 and 1.12 in repect to those of homogenious normal strength concrete gives, the get improving rates are 1.26, 1 and 1.04 in repect to those of homogenious high strength.

The enhancement of 15% leads to relative reduction of energy distribution which is correspond to ductility relative reduction that compared with strength improving . while the energy of specimen of 30% exhabits the higher energy improving.

Table 4.10 The dissipation of energy

Group No.	No.	Specimens	Energy (kN.mm), T	T/T_i	
				lower limit	Upper limit
Specimens of full lower limit strength					
G1	1	U 20 00	1099.8		
	2	U20 15	1670.4		
	3	U 20 30	2162.4		
Specimens of full upper limit strength					
G2	4	U 60 00	1001.3		
	5	U 60 15	1479.0		
	6	U 60 30	2345.5		
Specimens of Hybrid strengths (Mode II)					
G3	7	H 20/60 00	1260.4	1.15	1.26
	8	H 20/60 15	1474.0	0.88	1.00
	9	H 20/60 30	2431.0	1.12	1.04

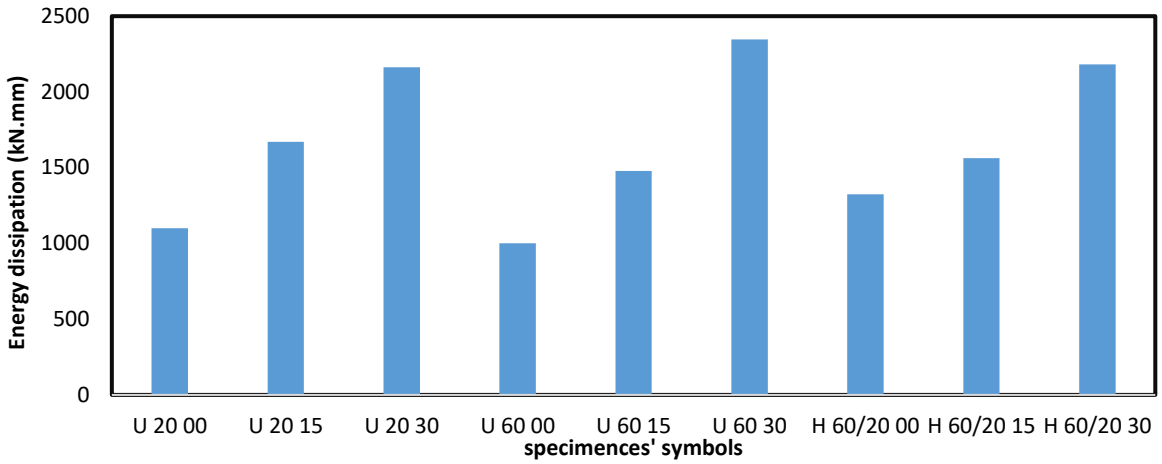

Figure 4.35 The dissipation of energy

4.5 Comparative Analyses Between Adopted Hybrid Modes

4.5.1 Moment Capacity

The comparative analysis between the adopted hybrid modes effect on the obtained moment capacity is exhibited in Table 4.11. For both modes, the moment capacity tends to increase with enhancement rating increasing and the best improving is corresponding to those of hybrid mode II as the comparing rated of Mode I in respect to Mode II are vary between 1.06 to 0.869 where the best improving corresponding R=30%.the variation of the obtained strength loads, indicated in Figure 4.36.

Table 4.11 Moment redistribution analysis; comparative analysis

Group No.	No.	Specimens	R, %	Q_u, kN	$M_{um}=5Q_uL/32$	$M_{us}=3Q_uL/16$	$M_{Pm}=(1+R)(Q_uL/6)$	MPs=(1-R) (QuL/6)	M_{Pm} (mode II)/ M_{Pm} (mode I)	M_{Ps} (mode II)/ M_{Ps} (mode I)
Specimens of Hybrid strengths (Mode I)										
G4	1	H 60/20 00	0	46.0	10.063	12.075	10.733	10.733		
	2	H 60/20 15	15	55.0	12.031	14.438	14.758	10.908		
	3	H 60/20 30	30	65.0	14.219	17.063	19.717	10.617		
Specimens of Hybrid strengths (Mode II)										
G3	4	H 20/60 00	0	49.0	10.719	12.863	11.433	11.433	1.065	1.065
	5	H 20/60 15	15	53.5	11.703	14.044	14.356	10.611	0.973	0.973
	6	H 20/60 30	30	56.5	12.359	14.831	17.138	9.228	0.869	0.869

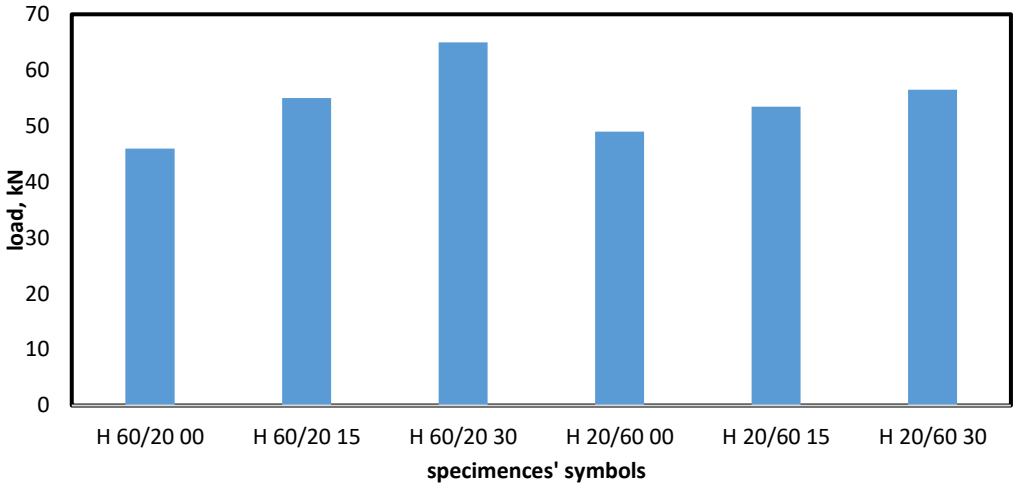

Figure 4.36 The assigned loads of various specimens

4.5.2 Load- Deflection Response

The load-deformation response relates to specimens of different modes with the same R, are illustrated in Figures 4.37, 4.38, and 4.39.

The comparison between their response indicated that, the enhancement ratio affects the response, while for R= 0 their response is the same and the significant divergence indicated for R=30 and may this due to the present of the same strength in current hybrid mode I which utilized lower strength in tension zone.

The same observation is clearly indicated for the mid of span and at the inner quarter of the span.

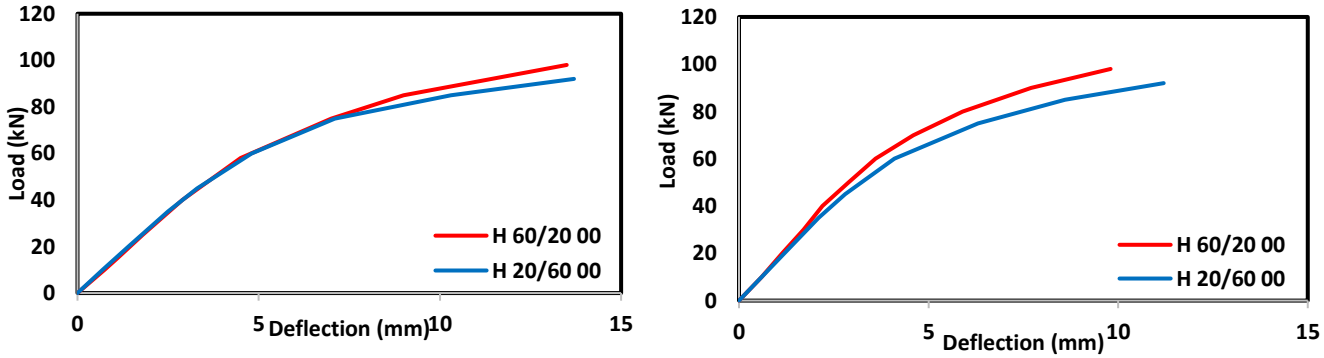

a. at mid span length b. at inner quarter length

Figure 4.37 Load – deflection of specimens with zero% R

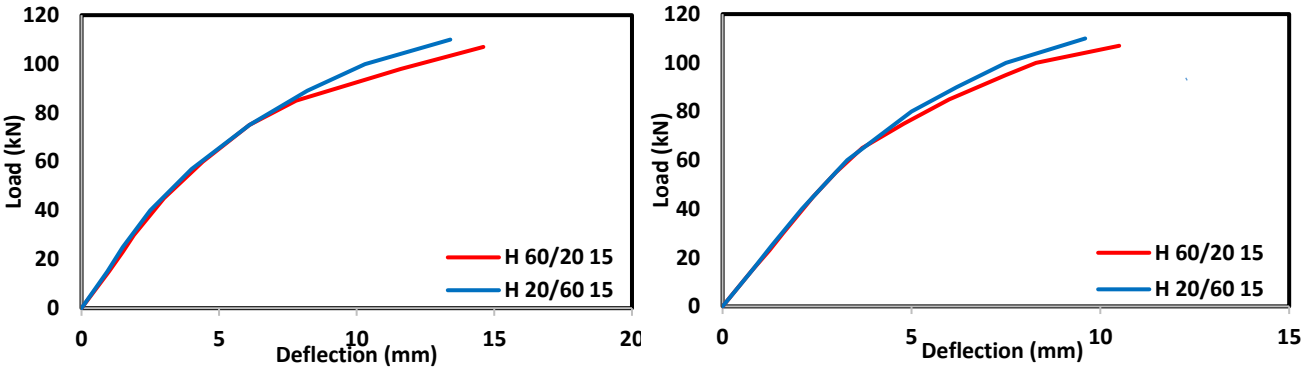

a. at mid span length b. at inner quarter length

Figure 4.38 Load – deflection of specimens with 15% R

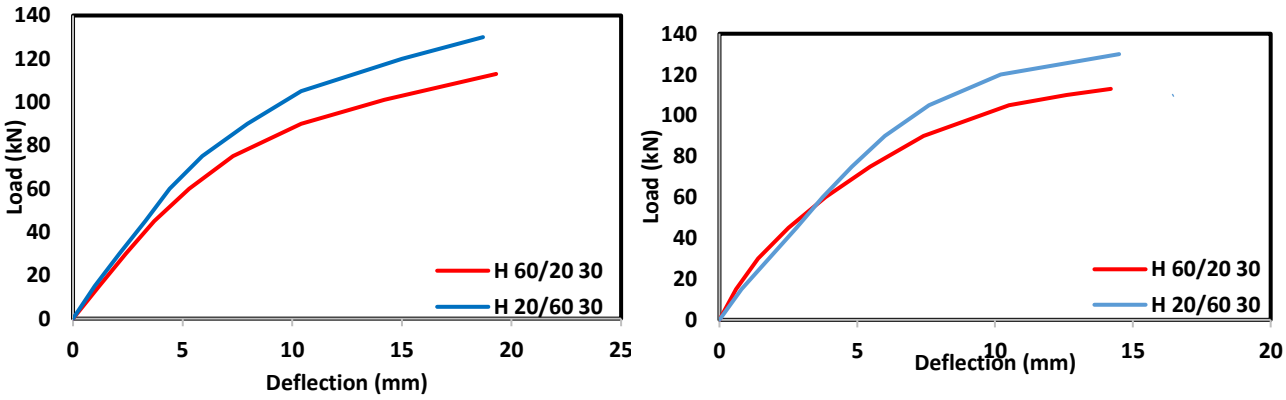

a. At mid span length b. at inner quarter length

Figure 4.39 Load – deflection of specimens with 30% R

4.5.3 Flexural Stiffness

Table 4.12 shows the results of flexural stiffness for hybrid strength section of mode I and II, the results depict that, the hybrid specimens of Mode II, better than the corresponding specimens of Mode I, in scope of flexural stiffness and this observation might be explained by the hybrid effect, in which the section stiffness is dominated by the high strength layer. From the Figure 4.40 slightly decrease in the results with changing of R ratio of mode I could be observed. Generally, the mode I gives regular results of flexural stiffness.

Table 4.12 Flexural stiffness

Group No.	No.	Specimens	Py, kN	Δ_y, mm	Flexural Stiffness (λ), kN/m	λ_{II}/λ_I
Specimens of Hybrid strengths (Mode I)						
G4	1	H 60/20 00	76	5.8	13.10	
	2	H 60/20 15	78	6.0	13.00	
	3	H 60/20 30	87	7.0	12.43	
Specimens of Hybrid strengths (Mode II)						
G3	4	H 20/60 00	75	5.1	14.71	1.122
	5	H 20/60 15	82	5.0	16.40	1.262
	6	H 20/60 30	92	6.8	13.53	1.089

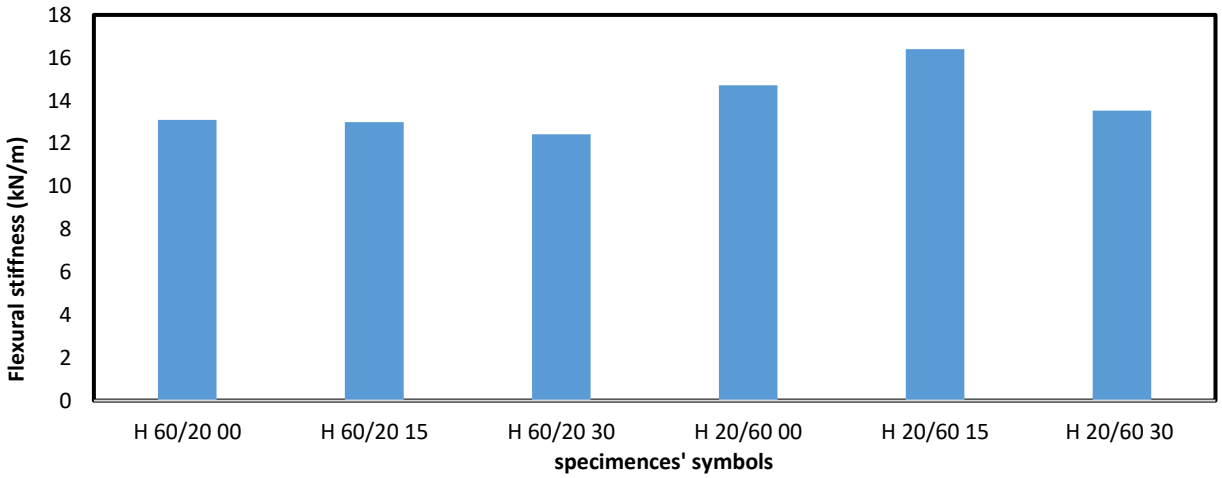

Figure 4.40 Flexural stiffness of specimens

4.5.4 Flexural Ductility

The getting results of ductility shows in Table 4.13 and Figure 4.41 for the different modes. For the adopted two modes, the flexural ductility is improved as enhancement rating is increased with relative more improving for specimens of mode II while the improving rating tends to be matched for higher enhancement rate (30%). The obvious for the two modes that the different in increment way where the increase for mode I was linear increasing and that relation to high strength concrete within a tension zone, while slightly increasing for the other mode.

Table 4.13 Flexural ductility index

Group No.	No.	Specimens	Δ_y, mm	Δ_u, mm	Flexural ductility index, DI	D_{II}/D_I
Specimens of Hybrid strengths (Mode I)						
G4	1	H 60/20 00	5.8	13.5	2.328	
	2	H 60/20 15	6.0	14.6	2.433	
	3	H 60/20 30	7.0	19.3	2.757	
Specimens of Hybrid strengths (Mode II)						
G3	4	H 20/60 00	5.1	13.7	2.686	1.15
	5	H 20/60 15	5.0	13.4	2.680	1.10
	6	H 20/60 30	6.8	18.7	2.750	1.00

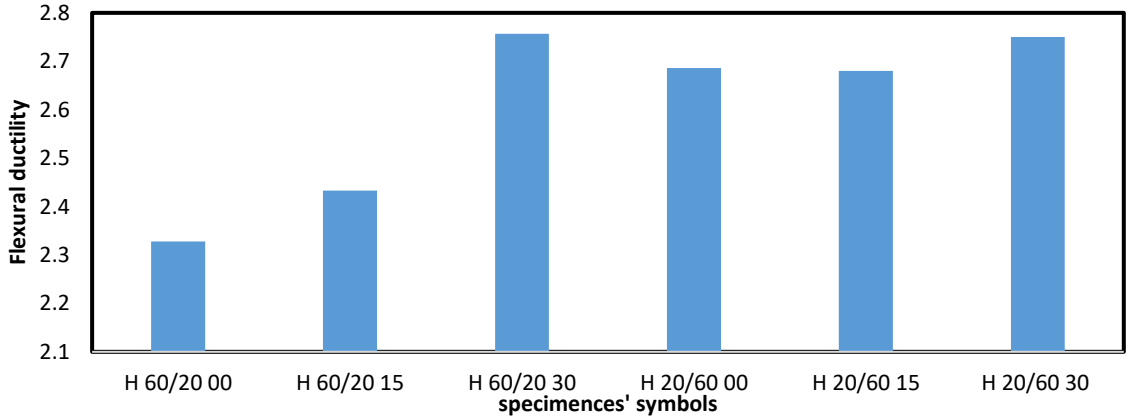

Figure 4.41 Ductility index of specimens

4.5.5 Strain Distribution

Figures 4.42, 4.43 and 4.44 illustrate load- strain trends that related to tensile strain of reinforcement steel and compressive strain in extreme fiber of compressive stress block; of specimens of hybrid Mode I in comparing with those of the correspond specimens of hybrid Mode I. The figures depict that, the load –strain responses that related to specimens of both hybrid modes, tend to diverge as enhancement rating increase and that due to the effect of lower limit strength of Mode I. Also, for both modes and in all enhancement ratios (0, 15, and 30%) the load – steel tensile strains are in compatibility state with the corresponding load –

concrete compressive strain and the same responses are recorded within middle supports for the same reason.

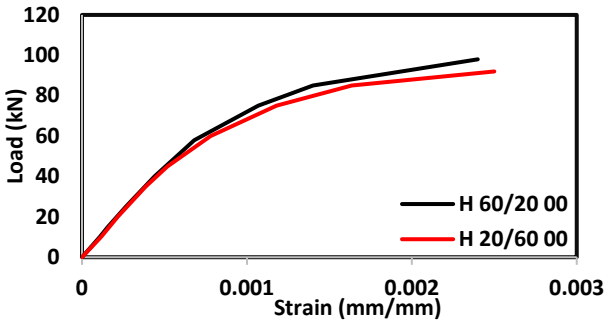

a. Steel mid span

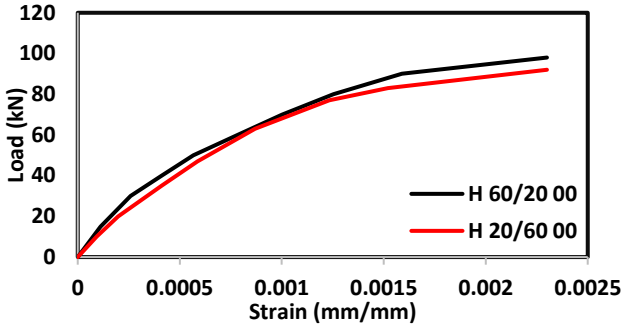

b. Steel middle support

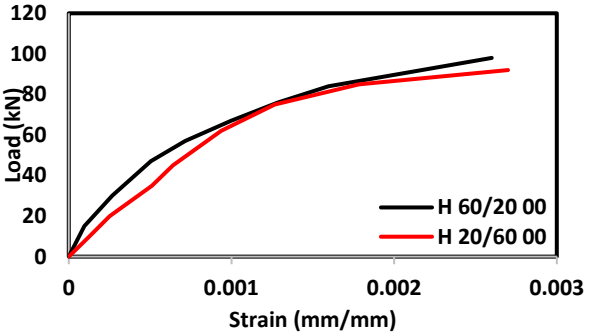

c. Concrete mid span

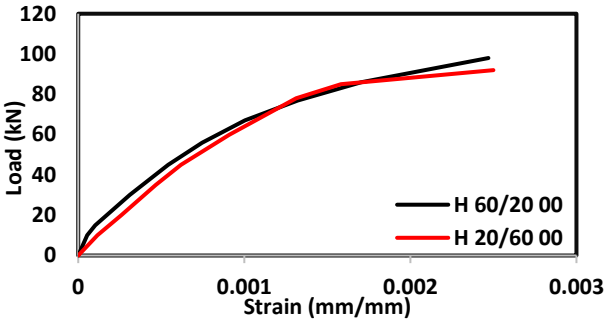

d. Concrete middle support

Figure 4.42 Load – strain responses, R=0 %

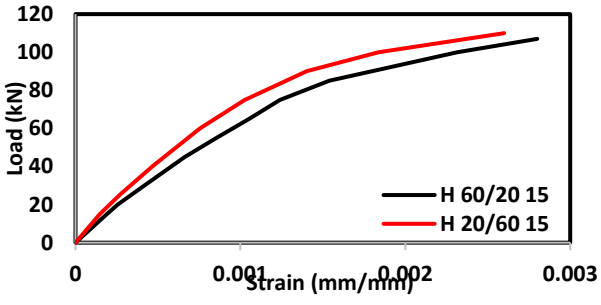

a. Steel mid span

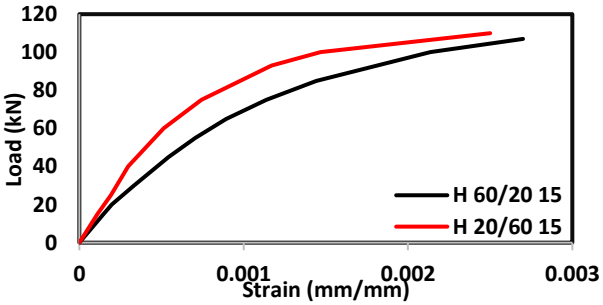

b. Steel middle support

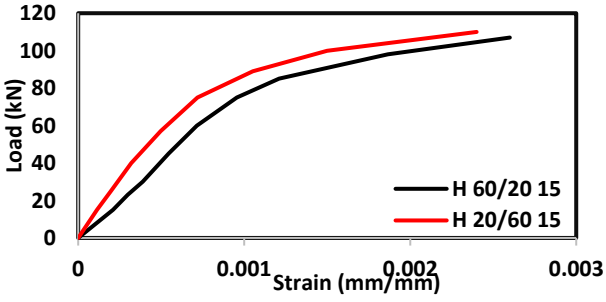

c. Concrete mid span

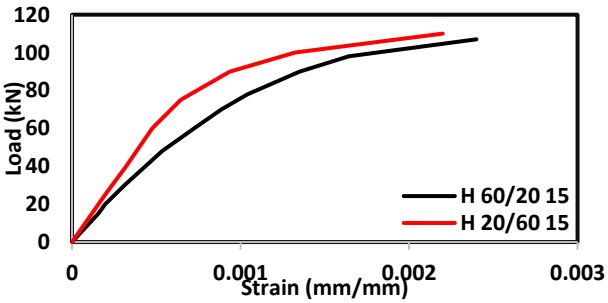

d. Concrete middle support

Figure 4.43 Load – strain responses, R=15 %

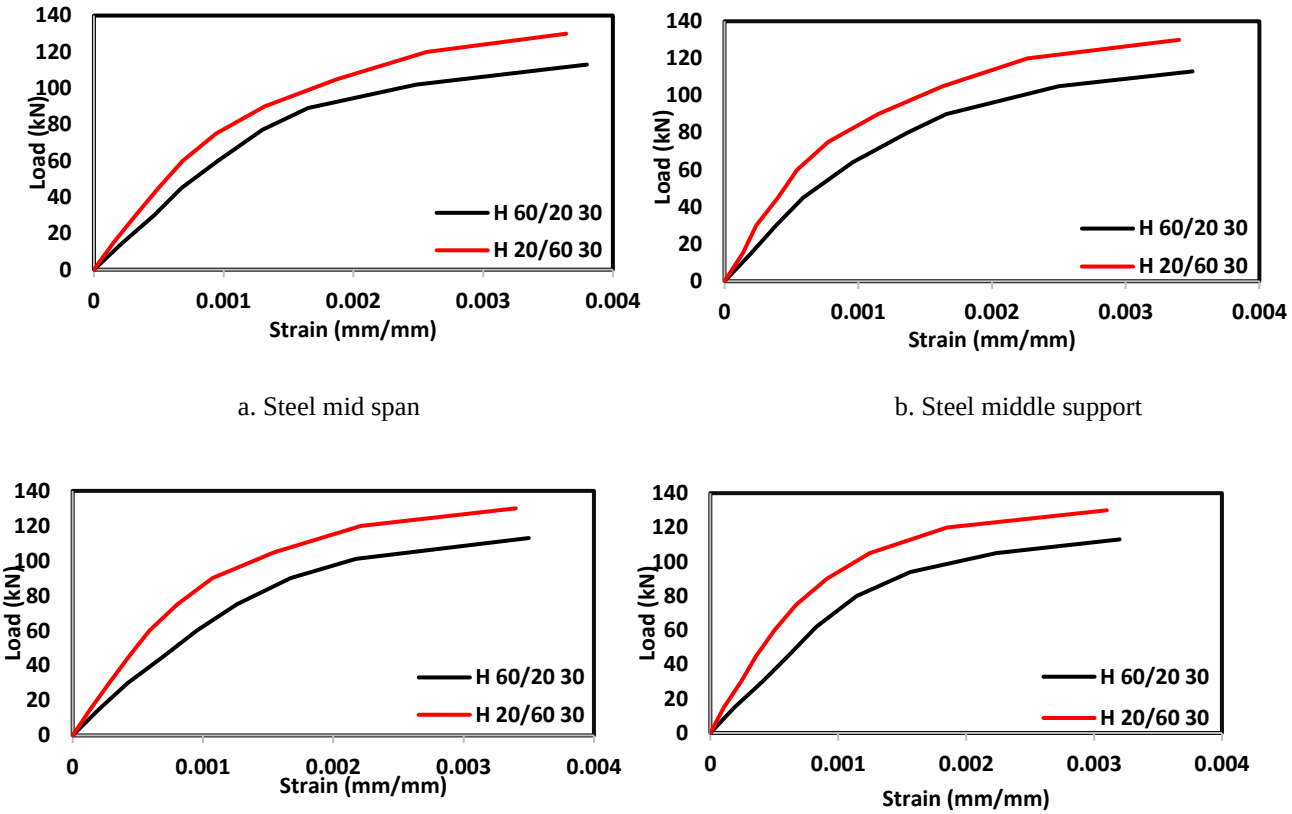

a. Steel mid span

b. Steel middle support

c. Concrete mid span

d. Concrete middle support

Figure 4.44 Load – strain responses, R=30%

4.5.6 Plastic Rotation Capacity

The top fiber mid span concrete compressive plastic strains of tested specimens are measured and utilized to compute the corresponding plastic rotation capacities. The results clearly show that, the increasing of enhancement ratio (R) companied with significant plastic rotation capacity improving. Table 4.14 lists the determined plastic rotation capacity and related comparative rates of mode II in respect to these of Mode I. The results depict that, the hybrid specimens of Mode II, extremely better than the corresponding specimens of Mode I, in scope of provided plastic rotation capacity, the comparing rates vary between 1.05 and 1.01.

Table 4.14 Plastic rotation capacity

Group No.	No.	Specimens	At Mid Span				
			ϵ_c	ϵ_p	L_p, mm	Θ, rad.	$\Theta_{II}/\Theta i_I$
Specimens of Hybrid strengths (Mode I)							
G4	1	H 60/20 00	0.0024	0.00224	364	0.0151	
	2	H 60/20 15	0.0026	0.00234	333	0.0144	
	3	H 60/20 30	0.0035	0.00319	333	0.0197	
Specimens of Hybrid strengths (Mode II)							
G3	4	H 20/60 00	0.0025	0.00237	364	0.01560	1.058
	5	H 20/60 15	0.0024	0.00226	333	0.0139	0.966
	6	H 20/60 30	0.0034	0.00323	333	0.0199	1.013

4.5.7 The Mechanism of the Beams

Figure 4.17 is clearly illustrating the getting mechanism, full matching is depicted with specimens of homogeneous high strength section for R= (15 and 30) %. The illustrated mechanism of various enhancement ratios differently shows that, with increasing R% which related to increase provided steel reinforcement, the plastic rotation capacities at mid span are increased. Also, the mechanisms depict that, for no enhancement mid span section (R=0%), the mechanism confirm that the hybrid section tends to get more rotation capacity as segments of failed specimens tend to get more rotations. Figure 4.18 illustrates failed specimens related to hybrid mode I investigation.

Figure 4.45 shows the comparative mechanisms of hybrid strength section of the two modes. The comparative views of the observed mechanism of various mode exhibit that, the specimens of the same R have the same mechanism.

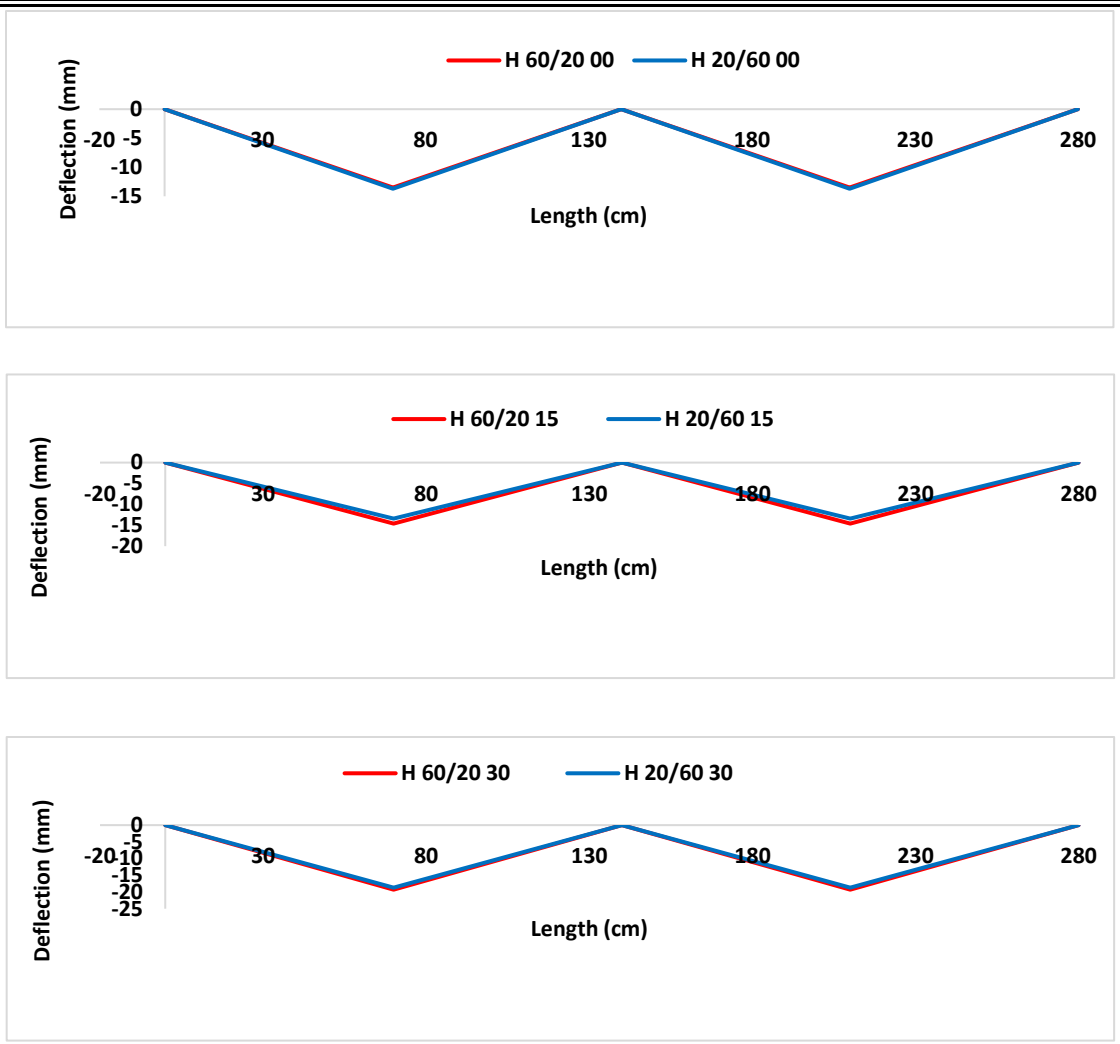

Figure 4.45 The mechanism of hybrid specimens of mode I and II

4.5.8 The Dissipation of Energy

Table 4.15 and Figure 4.46 exhibit result related to energy distribution of comparing analysis between mode I and II. The obtained result confirms the observation mechanisms which are clearly depicts that, the specimens of the same R have the same mechanism trend while the dissipation of energy comparing rates while the assigned energy dissipation of specimens of hybrids mode II in respect to those of mode I, have slightly variation for various R as the relative rates (0.953, 0.944 and

1.115) for R= 0, 15 and 30 percent, respectively; which are depict that Mode I provide more energy dissipation previous failure for smaller enhancement rating.

Table 4.15 The dissipation of energy

Group No.	No.	Specimens	Energy (kN.mm), T	T_{II}/T_I
Specimens of Hybrid strengths (Mode I)				
G4	1	H 60/20 00	1323.0	
	2	H 60/20 15	1562.2	
	3	H 60/20 30	2181.0	
Specimens of Hybrid strengths (Mode II)				
G3	4	H 20/60 00	1260.4	0.953
	5	H 20/60 15	1474.0	0.944
	6	H 20/60 30	2431.0	1.115

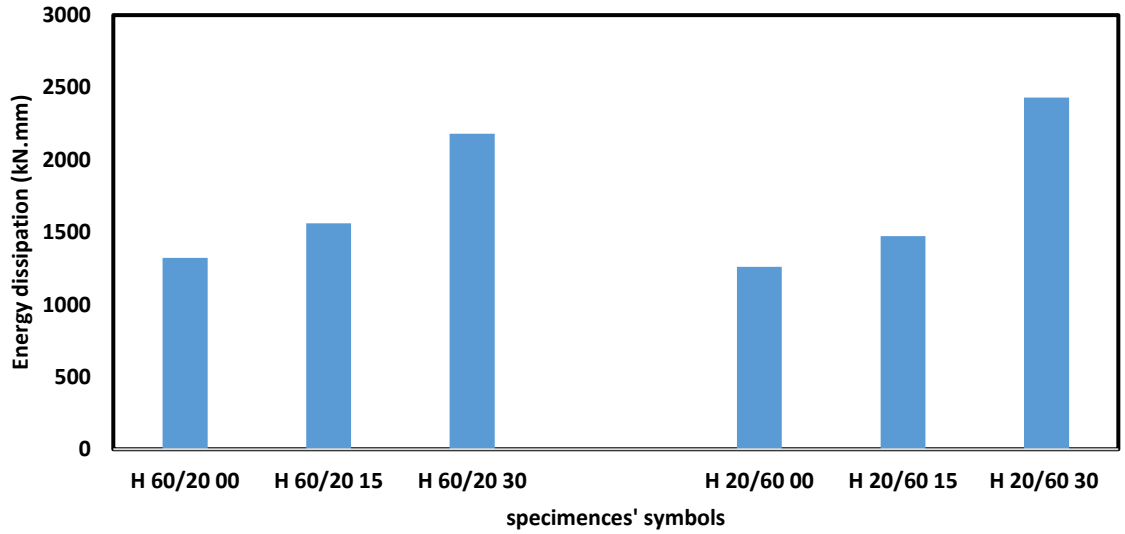

Figure 4.46 The dissipation of energy

CHAPTER FIVE:CONCLUSIONS AND RECOMMENDATIONS

5.1 General

The research deal with the moment redistribution assessment within continuous reinforced concrete beams of hybrid concrete compressive strength, the results and their analysis extrude conclusions are exhibited. Other aspects of reinforced concrete beams of hybrid strength or moment redistribution concept and related recommendations for future works had been introduced.

5.2 Conclusions

1. The hybrid strength modes in RC beams which based on reducing the strength in some regions and increasing it in other regions could be useful likewise steel reinforcement re-assigning and hybrid strength lead to reduce the overall cost of members.
2. For both modes, the moment capacity tends to increase with enhancement rating increasing and the best improving is corresponding to those of hybrid mode II as the comparing rates of Mode I in respect to Mode II are vary between 1.06 to 0.869.
3. The enhancement ratio affects the load – deflect response for both adopted hybrid modes. The specimens of R= 0 do not get difference while the significant divergence indicated in R=30. The same observation is indicated for the mid of span and at the inner quarter of the span, where first Mode I having the rates (1.15, 0.84, 0.91) as comparing with lower limit strength and (1.28, 1.00, 0.95) compared with upper limit strength. While the other Mode II have (1.17,

0.770.88) and (1.30, 0.92, 0.93) compared with lower and upper limit strength respectively.

4. The results depict that, the hybrid specimens of Mode II, get better response than the corresponding specimens of Mode I, in scope of flexural stiffness
5. The flexural ductility is improved as enhancement rating increased with relative more improving in specimens of mode II while the improving rating tends to be matched for higher enhancement rate (30%).
6. The results show that, the load –strain responses that related to specimens of both hybrid modes, tend to diverge as enhancement rating increase. Also, for both modes and in all enhancement ratios (0, 15, and 30%) the load – steel tensile strains are in compatibility state with the corresponding load – concrete compressive strain and the same responses are recorded within middle supports.
7. The results clearly show that, the increasing of enhancement ratio (R) companied with significant plastic rotation capacity improving. The hybrid specimens of Mode II, are extremely better than the corresponding specimens of Mode I, in scope of provided plastic rotation capacity, the comparing rates vary between 0.353 and 0.329.
8. The mechanisms depict that, there is no enhancement mid span section (R=0%), the mechanism confirm that the hybrid section tends to get more rotation capacity as segments of failed specimens tend to get more rotations.
9. The energy dissipation comparing rates between assigned energy dissipation of specimens of hybrids mode II in respect to those of mode I, have slightly variation for various enhancement ratio as the relative rates (0.953, 0.944 and 1.115) for R= 0, 15 and 30 percent, respectively; which are depict that Mode I provide more energy dissipation previous failure for smaller enhancement rating.

5.3 Suggestion for Further Studies

The following suggestions could be considered in the future studies relate to the current proposed reinforced modes:

1. Investigating of moment redistribution in hybrid strength continuous reinforced concrete beams of T- section.
2. Analysis the effect of the overall beam geometry on moment redistribution such as the present of the web opening.
3. Other aspects of hybrid modes according to their strength could be proposed and get moment redistribution analysis.

APPENDEX

Design flexural reinforcement

$$\rho_b = 0.85\beta_1 \left(\frac{f_c`}{f_y}.\frac{600}{600+f_y}\right)$$

$$\rho_{max} = 0.85\beta_1.\left(\frac{f_c`}{f_y}.\frac{0.003}{0.003+\varepsilon_t}\right)$$ where ε_t= 0.004

$$\rho_{min} = \max\left(\frac{1.4}{f_y}, \frac{\sqrt{f_c`}}{4f_y}\right)$$

$$\rho_{min} < \rho < \rho_{max}$$

$$-M = A_s.0.87f_y.d\left(1-\rho\frac{k_2.0.87f_y}{k_1.f_{cu}}\right)$$

$$-M = \frac{wl_n{}^2}{9} \qquad +M = \frac{wl_n{}^2}{14}$$

No.	Designation	at R =0 %							
		Negative				Positive			
		Moment	ρ	As	No. of bars	Moment	ρ	As	No. of bars
1	U 20 00	9.86	0.009	197	7 Φ6mm	6.34	0.005	116	4 Φ6mm
2	U 60 00	11.2	0.009	197	7Φ6 mm	7.2	0.005	124	4Φ6 mm
3	H (20/60) 00	11.2	0.009	197	7Φ 6mm	7.2	0.005	132	4Φ 6mm
4	H (60/20) 00	9.86	0.009	197	7Φ 6mm	6.34	0.005	109	4Φ 6mm

No.	Designation	at R=15%							
		Negative				Positive			
		Moment	ρ	As	No. of bars	Moment	ρ	As	No. of bars
1	U 20 15	8.38	0.007	158	6Φ6mm	7.29	0.006	136	5Φ6mm
2	U 60 15	9.5	0.007	165	6Φ 6mm	8.29	0.006	143	5Φ 6mm
3	H (20/60) 15	9.5	0.007	165	6Φ 6mm	8.29	0.006	155	5Φ 6mm
4	H (60/20) 15	8.38	0.007	160	6Φ 6mm	7.29	0.006	126	5Φ 6mm

No.	Designation	at R=30%							
		Negative				Positive			
		Moment	ρ	As	No. of bars	Moment	ρ	As	No. of bars
1	U 20 30	6.9	0.006	130	5Φ6mm	7.9	0.007	151	6Φ6mm
2	U 60 30	7.84	0.006	135	5Φ 6mm	9	0.007	156	6Φ 6mm
3	H (20/60) 30	7.84	0.006	135	5Φ 6mm	9	0.007	172	6Φ 6mm
4	H (60/20) 30	6.9	0.006	129	5Φ 6mm	7.9	0.007	137	6Φ 6mm

Checking required and provided rotation capacity:

$$\theta_{required} = \frac{L}{6E_c I_{cr}}[2(M_A - M_{FA}) + (M_B - M_{FB})]$$

Where: $I_{cr=} b\frac{x^3}{3} + nA_s(d-x)^2$

$$\theta_{provided} = \frac{\varepsilon_p . L_p}{C}$$

Where: L_p= 2d , $\varepsilon_p = \varepsilon_{cu} - \varepsilon_e$

$C = \frac{a}{0.85}$, $a = \frac{A_s . F_y}{0.85 f_c` . b}$

NO.	Designation	(+/-) Ve	β	ʎ	Θ (provided)	Max. Θ(required) at R=0%	Max. Θ(required) at R= 15%	Max. Θ(required) at R= 30%
1	U 20	- ve	0.85	0.290	0.0094	0.0031	0.0046	0.0066
		+ ve	0.85	0.163	0.0192	0.0085	0.0084	0.0090
2	U 60	- ve	0.71	0.120	0.0270	0.0031	0.0046	0.0066
		+ve	0.71	0.066	0.0510	0.0085	0.0084	0.0090
3	H (20/60)	- ve	0.85	0.163	0.0192	0.0031	0.0046	0.0066
		+ ve	0.71	0.066	0.0510	0.0085	0.0084	0.0090
4	H (60/20)	- ve	0.71	0.120	0.0270	0.0031	0.0046	0.0066
		+ ve	0.85	0.163	0.0192	0.0085	0.0084	0.0090

REFERENCES

[1] Poveda-Bautista, R., Diego-Mas, J. A., & Leon-Medina, D. (2018). Measuring the project management complexity: the case of information technology projects. Complexity, 2018,

[2] Meyer, C. (2009). The greening of the concrete industry. Cement and concrete composites, 31(8), 601-605,

[3] Tolmachov, S., Belichenko, O., & Zakharov, D. (2017). Influence of additives on flexural strength of concrete. In MATEC Web of Conferences (Vol. 116, p. 01019). EDP Sciences,

[4] Whittle, R., & Taylor, H. (2009). Design of Hybrid Concrete Buildings. CCIP-030-ISBN 978-1-904482-55-0,

[5] Iskhakov, I., Ribakov, Y., & Holschemacher, K. (2017). Experimental investigation of continuous two-layer reinforced concrete beams. Structural Concrete, 18(1), 205-215,

[6] Phumlani G. Nkosi. (2012). Theory and analysis of continuous beams. BSC (Mathematical and statistical sciences: Mathematical modelling), BSC Hons (Technology management),

[7] https://www.lijianformwork.com/continuous-beam-formwork/58657742.html,

[8] Li, L., Zheng, W., & Wang, Y. (2019). Review of moment redistribution in statically indeterminate RC members. Engineering Structures, 196, 109306,

[9] Kong, F. K., & Evans, R. H. (2017). Reinforced and prestressed concrete. CRC Press,

[10] Oehlers, D. J., Haskett, M., Ali, M. M., & Griffith, M. C. (2010). Moment redistribution in reinforced concrete beams. Proceedings of the Institution of Civil Engineers-Structures and Buildings, 163(3), 165-176,

References

[11] Barnard, P. R. (1965). The collapse of reinforced concrete beams. Special Publication, 12, 501-520,

[12] Mohammed, A. H. (2020). Torsional Capacity of Hybrid Reinforced Concrete Beams (Doctoral dissertation, University of Technology),

[13] Sada, M. J. (2021). Structural behavior of hybrid reinforced concrete beams of trapezoidal section. *Materials Today: Proceedings*, *42*, 2733-2741.

[14] Bernard, O., Mivelaz, P., & Brühwiler, E. (1998). Investigation Of the Long-Term Behavior of Hybrid Concrete Structures. In 2nd International Ph. D Symposium in Civil Engineering, Budapest (pp. 1-8),

[15] KHEYR, A. A., & Naderpour, H. (2007). Plastic hinge rotation capacity of reinforced concrete beams,

[16] Zhao, X., Wu, Y. F., Leung, A. Y., & Lam, H. F. (2011). Plastic hinge length in reinforced concrete flexural members. Procedia Engineering, 14, 1266-1274.

[17] Hassoun, M. N., & Al-Manaseer, A. (2020). Structural concrete: theory and design. John wiley & sons.

[18] Lin, C. H., & Chien, Y. M. (2000). Effect of section ductility on moment redistribution of continuous concrete beams. Journal of the Chinese Institute of Engineers, 23(2), 131-141,

[19] Maghsoudi, A. A., & Bengar, H. A. (2009). Moment redistribution and ductility of RHSC continuous beams strengthened with CFRP. Turkish Journal of Engineering and Environmental Sciences, 33(1), 45-59,

[20] Akbarzadeh, H., & Maghsoudi, A. A. (2010). Experimental and analytical investigation of reinforced high strength concrete continuous beams strengthened with fiber reinforced polymer. Materials & Design, 31(3), 1130-1147,

References

[21] El-Mogy, M., El-Ragaby, A., & El-Salakawy, E. (2011). Behavior of continuous concrete beams reinforced with FRP Bars. In Advances in FRP Composites in Civil Engineering (pp. 283-286). Springer, Berlin, Heidelberg,

[22] Akiel, M. S., El-Maaddawy, T., & El Refai, A. (2018). Serviceability and moment redistribution of continuous concrete members reinforced with hybrid steel-BFRP bars. Construction and Building Materials, 175, 672-681,

[23] Visintin, P., Ali, M. M., Xie, T., & Sturm, A. B. (2018). Experimental investigation of moment redistribution in ultra-high-performance fibre reinforced concrete beams. Construction and Building Materials, 166, 433-444,

[24] Kheder, G. F., Al Kafaji, J. M., & Dhiab, R. M. (2010). Flexural strength and cracking behavior of hybrid strength concrete beams. Materials and structures, 43(8), 1097-1111,

[25] Abbas, S. R., & Abd, H. J. (2015). Behavior of Hybrid Concrete Beams Containing Two Types of High Strength Concrete (HSC) and Conventional Concrete. International Journal of Science and Research (IJSR), 2319-7064, 6,

[26] Al-Hassani, H. M., Al-Kafaji, J. M., & Ismael, A. L. M. A. (2015). Flexural behavior of hybrid Tee Beams (Containing Reactive Powder Concrete and Normal Strength Concrete). Journal of Engineering and Sustainable Development, 19(2),

[27] Alawsh, N. A., & Mehdi, T. H. (2018). Behavior of Reinforced Concrete Hybrid Trapezoidal Box Girders Using Ordinary and Highly Strength Concrete. Journal of University of Babylon for Engineering Sciences, 26(5), 272-278,

References

[28] Iraqi Standard No. 5 /1984. Physical and chemical requirements for Portland cement,

[29] Iraqi Standard No. 45 /1984. Requirements of the used fine and coarse aggregate in the concrete mixes,

[30] ASTM, C. (1999). 494. Standard Specification for Chemical Admixtures for Concrete. American Society for Testing and Materials,

[31] IQS2091/1999. Carbon steel bars for the reinforcement of concrete. 1-11,

[32] BS 1881, P. 116. (1989). Method for determination of compressive strength of concrete cubes. In British Standards Institution (p. 3),

[33] C496, A. (2006). "Standard Test Method for Splitting Tensile of Cylindrical Concrete Specimens",. American Society for Testing and Materials.

[34] C78, A. (2002). Standard Test Method for Flexural Strength of Concrete. American Society for Testing and Materials,

[35] Sullivan, T. J., Calvi, G. M., & Priestley, M. J. N. (2004). Initial stiffness versus secant stiffness in displacement-based design. 13th World Conference of Earthquake Engineering (WCEE), 2888,

الخلاصة

استخدام مفهوم اعادة توزيع العزوم في تصميم الهياكل الخرسانية غير المحددة ستاتيكياً لتقليل كميات العزوم في المناطق الحرجة وتبسيط التفاصيل من خلال السماح بتقليل نسب العزوم. تهدف الدراسة الحالية الى استخدام مفهوم اعادة توزيع العزوم الى جانب الاستخدام الامثل لمقاومة الخرسانة لتطوير العتبات الخرسانية المسلحة المستمرة باستخدام الخرسانة الهجينة ذات المقاومة العادية وعالية المقاومة بالإضافة الى التحقيق في فعالية الانماط الهجينة عند اعادة توزيع العزوم وبعض المتعلقات ذات الصلة في التصرف الانشائي مثل قابلية التحمل، الصلابة، الليونة، قابلية الدوران بالإضافة الى انماط الفشل.

استعرض هذا البحث دراسة تجريبية تتكون من تطوير واختبار اثني عشر عتبة خرسانية مسلحة مستطيلة المقطع بطول 3000 ملم ومقطع عرضي (200×120) ملم. تم تقسيم العتبات الى أربع مجاميع اثنان من المجاميع عبارة عن عتبات ذات مقاطع متجانسة بمقاومة انضغاط (20 و60) ميكا باسكال على التوالي، والاخرى عبارة عن عتبات ذات مقاطع هجينة (طبقتان) بمقاومة انضغاط (20/60 و60/20) على التوالي. حصلت المجاميع الأخرى على قوة متغيرة لتتوافق مع اعادة التوزيع الفعلي للعزوم تم اعتماد ثلاث نسب لتعزيز المقاطع (R) لمنتصف الفضاء في العتبات والتي تبلغ 0% , 15% و30% وتتوافق مع نسب التقليل للعزوم في منطقة المسند الوسطي.

اوضحت النتائج انه في كلا النمطين; ان اعادة توزيع العزوم تميل الى الزيادة مع زيادة معدل التعزيز وأفضل تعزيز يتوافق مع الوضع الهجين هو النمط IIحيث ان النمط I مقارنة مع النمط IIحيث وجد ان النسب تتراوح بين 1.06 و0.869 علما ان أفضل تحسين مقابل R=30%. كما اثبتت النتائج تأثير نسبة التعزيز على قابلية التحمل في كلا النمطين. كما ان العتبات ذات R=0لا تحصل على فرق بينما الفرق الكبير المشار اليه عند R=30%. نفس التصرف تم تثبيته لمنتصف الفضاء وفي الربع الداخلي من الفضاء. وكما بينت النتائج ان العتبات ذات النمط IIاعطت أفضل القيم من حيث الصلابة اما بالنسبة الى الليونة فتم تعزيزها مع زيادة معدل التحسين النسبي للعتبات في النمط II. بينت النتائج انه اثناء التحسين يميل التصرف الى التطابق للنمطين مع معدل تحسين اعلى (30%) فان زيادة التعزيز تؤدي الى زيادة في قابلية الدوران، علما ان العتبات في النمط IIاعطت أفضل القيم بالنسبة لقابلية الدوران مقارنة مع النمط I حيث تراوحت النسبة بين 0.353 و0.329.بشكل عام يمكن دمج مفهوم إعادة توزيع العزوم مع مفهوم المقاطع الهجينة لقليل تكلفة التصميم الاجمالية دون الغاء الخصائص الهيكلية المطلوبة ويمكن ان تكون انماط التهجين في العتبات الخرسانية المستمرة المسلحة والتي تعتمد على تقليل المقامة في بعض المناطق وزيادتها في مناطق اخرى مفيدا ايضا في اعادة توزيع حديد التسليح.

جمهورية العراق
وزارة التعليم العالي والبحث العلمي
كلية الهندسة/ جامعة ميسان
قسم الهندسة المدنية

تقييم اعادة توزيع العزم في العتبات الخرسانية المسلحة مستمرة الاسناد ذات مقاطع هجينة

من قبل
ضحى كريم حسن

رسالة
مقدمة الى كلية الهندسة في جامعة ميسان
كجزء من متطلبات الحصول على درجة الماجستير في علوم الهندسة المدنية / الانشاءات

نيسان 2022

بأشراف
الاستاذ الدكتور: سعد فهد رسن
الاستاذ المساعد الدكتور: حيدر الخزرجي